Effects of Pre-ovulatory Follicle Physiological Status on Oocyte Metabolic Capacity

A Dissertation Presented for the
Doctor of Philosophy
Degree
The University of Tennessee, Knoxville

Casey C. Read
May 2022

DEDICATION

I dedicate this dissertation to everyone who helped me along the way.
It wouldn't have happened without you.

ACKNOWLEDGEMENTS

First, and most importantly, I would like to take this opportunity to thank my supervisor, Dr. Sarah Moorey. This project has come a long way from our rough sketches on scrap paper. I thoroughly enjoyed gaining the more hands-on cow skillsets, learning OPU, and discovering my ambidextrous palpation talents. I would next like to thank my committee members Drs. Jon Beever, Lannett Edwards, Tom Geary, and Dan Mathew for your input, support, advice, and consult throughout this project. Your efforts helped refine this project and make it what it is today. I would also like to thank my family and friends for their love and support. Notably my wonderful husband Dylan Seago who provided endless support and made sure I ate during the writing process and my parents, siblings, Mary Ali Oliver, Jessica Klabnik, Velislov Stamenov, Allyson Stokes, Emma Horn, Emma Hessock, and Kathleen Wallace for providing encouragement when I needed it. I would also like to thank Capybara Coffee for being the perfect place to work and the source of most of my productivity.

Thanks are also due to the many people who helped with sample collections and processing as well as data analysis – Dr. Justin Rhinehart, Courtney Carter, Dr. Jessica Klabnik, Dr. Rebecca Payton, Dr. Liesel Schneider, Emma Horn, Emma Hessock, Abigayle Pollock, Hunter Liles, Julia Rowinski, Sadi Bhandari, Ashton Kelly, Samantha Roberts, Meredith Hinson, Allyson Stokes, Kennedy Hill, Hector Castro, Shawn Campagna, Courtney Christopher, and Sara Howard. I would not have been able to do everything myself. Thank you also to Plateau AgResearch and Education Center for providing the cattle, facilities and staff needed to work the animals and collect our

samples. Walt Hitch, Jeff Dowlen, Steve Smith, Brent England, Tyler Green, Payton Miller, and Andy Carey – I greatly appreciate you staying late, working weekends, and disrupting your normal schedules so that this project could happen. Additionally, I would like to thank Southeastern Provision, LLC for allowing me to collect samples at their facility and Boyd Dingus for his generous donation of the Estrotect patches® used in the study.

Last, but not least, I would like to thank the USDA NIFA Hatch project 1022068, University of Tennessee AgResearch, and the University of Tennessee Department of Animal Science for their support of this research.

ABSTRACT

Fixed-Time artificial insemination (FTAI) has many benefits, however a subset of cattle inseminated during these protocols rely on the administration of gonadotropin releasing hormone (GnRH) to induce ovulation. Inducing ovulation prior to the animal's endogenous gonadotropin surge results in reduced pregnancy rates, embryo survival, day seven embryo quality, and successful embryo cleavage in beef cows undergoing FTAI. RNA-sequencing of oocytes and associated cumulus cells collected from follicles prematurely exposed to a gonadotropin surge suggested reduced capacity for glucose metabolism in cumulus cells of follicles ≤11.7 mm. Based on this information, we designed a series of studies to investigate the relationship between physiological status of the pre-ovulatory follicle at exposure to an exogenous gonadotropin surge and the metabolic capacity of the oocyte and follicular environment. We synchronized the development of a pre-ovulatory follicle in 319 lactating, Angus beef cattle and collected the follicular contents approximately 20 hours after administration of GnRH to induce the pre-ovulatory gonadotropin surge. Metabolomics analysis of 43 follicular fluid samples identified 18 metabolites with a significant, positive correlation to pre-ovulatory follicle diameter. Individual and pathway enrichment analysis of significantly correlated metabolites suggested that altered glucose and amino acid metabolism likely contribute to reduced developmental competence of oocytes when small pre-ovulatory follicles undergo induced ovulation. To further relate oocyte metabolic capacity to follicle status, we developed and validated procedures to measure both mitochondrial DNA (mtDNA) copy number and intraoocyte ATP in individual oocytes. We next determined the relationship between

follicle physiological status and oocyte metabolic competence and follicular fluid metabolome profiles. Intraoocyte ATP content was significantly related to serum estradiol at administration of gonadotropin releasing hormone to induce ovulation (GnRH2) and time between GnRH2 and follicle aspiration. Serum estradiol concentration at GnRH2 and follicular fluid progesterone concentration were positively correlated with the abundance of 22 and 61 follicular fluid metabolites, respectively. Pathway enrichment analysis of the significant metabolites suggested altered proteinogenesis, citric acid cycle, and pyrimidine metabolism. Collectively, our studies show that premature exposure to an exogenous gonadotropin surge results in reduced metabolic capacity of the oocyte as well as an altered follicular microenvironment.

TABLE OF CONTENTS

LIST OF TABLES

LIST OF FIGURES

INTRODUCTION

Incorporation of a fixed-time artificial insemination (FTAI) protocol into beef cattle production systems improves reproductive management as well as the genetics, weight, and uniformity of the calf crop (Sá Filho et al., 2010; Funston et al., 2012; Cushman et al., 2013). However, a subset of cattle (3-90%) undergoing a FTAI protocol rely on the administration of gonadotropin releasing hormone (GnRH) to induce their ovulation. This subset of cattle has reduced pregnancy rates compared to animals that express estrus prior to FTAI and experience an endogenous pre-ovulatory gonadotropin surge (Perry et al., 2005; Perry et al., 2007; Atkins et al., 2013; Colazo and Mapletoft, 2014; Colazo et al., 2018; Jinks et al. 2013; Richardson et al. 2016). This reduced pregnancy rate could be due, in part, to reduced oocyte developmental competence. Oocyte developmental competence is typically defined as the oocyte's ability to complete maturation, be fertilized, cleave, and develop to the blastocyst stage (Lonergan et al., 2003; Sirard et al., 2006; Boni, 2012). Bovine oocytes from follicles as small as 2-3 mm possess the ability to resume meiosis, but have variations in their developmental potential (Hyttel et al., 1997; Otoi et al., 1997; Hendriksen et al., 2000). Despite completing meiotic maturation, oocytes from follicles 2-6 mm in diameter consistently have decreased cleavage and blastocyst rates than those originating from follicles larger than 6 mm (Fair et al., 1995; Fair et al., 1997; Otoi et al., 1997; Hendriksen et al., 2000; Lonergan et al., 2003; Boni, 2012; Aguila et al., 2020; Sarwar et al., 2020). While most oocytes that have resumed meiosis are capable of interacting with spermatozoa and forming a zygote, the ability of the zygote to reach the blastocyst stage is highly dependent on the degree of cytoplasmic competence and oocyte

metabolic capacitation the oocyte has completed prior to the onset of maturation due to the luteinizing hormone (LH) surge (Hendriksen et al., 2000; Gosden, 2002; Watson, 2007; Jeong et al., 2009; Sirard, 2011; Boni, 2012; Conti and Franciosi, 2018; Aguila et al., 2020).

Metabolic priming consists of the gap junctional transport of metabolic substrates like ATP, pyruvate, and lipids from the cumulus cells to the oocyte as well as an increase in and reorganization of mitochondria within the oocyte's cytoplasm during antral follicle development prior to the LH surge(Smith and Alcivar, 1993; Cao et al., 2007; Dumollard et al., 2007; Jeong et al., 2009; Kidder and Vanderhyden, 2010; Winterhager and Kidder, 2015; Aguila et al., 2020). This process occurs during antral follicle growth prior to the LH surge. The follicular fluid also contributes to the metabolic capacity of the cumulus-oocyte complex (COC) by providing signaling molecules, metabolites, and other nutrients that are required for COC development and metabolic processes (Edwards, 1974; Orsi et al., 2005a; Baka and Malamitsi-Puchner, 2006; Sohel et al., 2013; Dumesic et al., 2015; Ferrazza et al., 2017; Da Broi et al., 2018; Guerreiro et al., 2018). The level of metabolic priming prior to removal from the follicle or exposure to the pre-ovulatory gonadotropin surge in vivo is essential because gap junctions begin to break down and the oocyte and cumulus cells decouple once oocyte maturation commences (Granot and Dekel, 2002; Winterhager and Kidder, 2015; Conti and Franciosi, 2018; Read et al., 2018). This causes metabolite transport from the cumulus cells to the oocyte to stop. Additionally, during oocyte maturation, mitochondrial biogenesis arrests until the blastocyst stage of embryo development (Van Blerkom, 2004; Chappel, 2013; Trebichalská et al., 2020). Because of this, the oocyte and early embryo have to sustain their energy-demanding developmental

processes with the metabolic substrates and mitochondria it has accrued prior to the pre-ovulatory gonadotropin surge.

Progression of the dominant follicle through the pre-ovulatory time period appears to contribute greatly to oocyte developmental competency (Hendriksen et al., 2000; Dieleman et al., 2002; Knijn et al., 2002; Peterson and Lee, 2003; Atkins et al., 2013) and the metabolic capacity of oocytes (Moorey et al., 2021). Utilization of a FTAI protocol synchronizes the development of a pre-ovulatory follicle in a group of cattle. Such procedures, however, result in pre-ovulatory follicles of varied physiological status. Some animals (10-97%) produce a follicle that initiates estrus and a pre-ovulatory gonadotropin surge before the scheduled FTAI (Colazo and Mapltoft, 2014; Colazo et al., 2018; Perry et al., 2005; Jinks et al., 2013; Richardson et al., 2016). Other animals rely on administration of gonadotropin releasing hormone (GnRH) to induce a pre-ovulatory gonadotropin surge and subsequent oocyte maturation before an estrus and an endogenous surge occur. As previously stated, animals that rely on GnRH to induce a gonadotropin surge and ovulation experience lower pregnancy rates than animals that exhibit estrus and stimulate an endogenous surge (Perry et al., 2005; Perry et al., 2007; Colazo and Mapltoft, 2014; Colazo et al., 2018; Jinks et al., 2013; Richardson et al., 2016). The follicles of such animals are denied the opportunity to undergo the final stages of follicle development prior to the endogenous gonadotropin surge experienced by cattle who do display estrous behavior. Such a phenomenon provides a unique opportunity to evaluate the impact of the follicle's status during these final hours leading up to estrus on oocyte developmental competency and fertility.

Further, cattle induced to ovulate a small pre-ovulatory follicle (≤ 11.3 mm) had lower day 27 pregnancy rates and increased early pregnancy loss than cattle induced to ovulate a larger-sized pre-ovulatory follicle (≥ 11.3 mm; Perry et al., 2005). Pre-ovulatory follicle diameter is positively correlated with circulating estradiol concentrations at the time of GnRH injection to induce ovulation (GnRH2; Perry et al., 2005; Jinks et al., 2013). Size of the pre-ovulatory follicle at the time on GnRH2 administration is an indicator of the follicle's physiological status and maturity in animals that have yet to display estrus. Indeed, cattle induced to ovulate a small pre-ovulatory follicle (< 12.5 mm) also had decreased oocyte developmental competence as evidenced by decreased embryo quality and decreased probability of recovering a fertilized embryo 7 days after insemination (Atkins et al., 2013). This prompted further research into the cumulus-oocyte-complexes (COC) induced to ovulate prematurely from small and large pre-ovulatory follicles in females that had not displayed estrus. RNA-sequencing analysis performed on COCs collected approximately 21 hours after the LH surge revealed decreased abundance of genes involved with glycolysis in the cumulus cells of small induced follicles (≤ 11.7 mm) compared to larger induced follicles (≥ 12.7 mm) and decreased mitochondrial gene expression in the oocytes from small induced follicles compared to non-induced follicles (Moorey et al., 2021). This suggests reduced metabolic capacity of the oocytes from follicles induced to ovulate prematurely.

Within the COC, cell-specific metabolic activity contributes to the accumulation of metabolite stores within the oocyte during folliculogenesis. Cumulus cells possess high glycolytic activity while the oocyte and early embryo primarily utilizes oxidative

phosphorylation to sustain development through to the blastocyst stage of embryo development (Biggers et al., 1967; Zeilmaker and Verhamme, 1974; Sutton et al., 2003; Dumollard et al., 2007; Thompson et al., 2007; Sutton-McDowall et al., 2010; Leese, 2012; Paczkowski et al., 2013; Dalton et al., 2014; Roth, 2018; Dalbies-Tran et al., 2020). This metabolic dichotomy is a result of a coupling between the oocyte and cumulus cells prior to the resumption of meiosis in the oocyte. The cumulus cells utilize metabolites such as glucose from the follicular fluid to supply metabolic substrates like ATP, pyruvate, and lipids to the oocyte via gap junctions (Sutton et al., 2003; Kidder and Vanderhyden, 2010; Dumesic et al., 2015). The oocyte uses these metabolites for use in energy production as well as stockpiles them to provide energy for downstream developmental processes of oocyte maturation, fertilization, cleavage, and early embryonic cell divisions (Johnson et al., 2007; Jeong et al., 2009; Sutton-McDowall et al., 2010; Dumesic et al., 2015). Based on this information, we hypothesized that in cattle that are exposed to an induced gonadotropin surge during a FTAI protocol have an oocyte commence maturation prior to the endogenous gonadotropin surge – potentially interrupting the metabolic priming of the oocyte and decreasing the amount of time the oocyte had to accumulate metabolic substrates and increase the number of mitochondria.

By inducing premature ovulation via exposure to an exogenously stimulated gonadotropin surge, these metabolic processes could be altered due to inadequate length of exposure of the COC to the peri-ovulatory follicular microenvironment. Alternatively, modifications in the peri-ovulatory follicular fluid or follicular cell physiology that promote COC metabolism during the final hours leading up to the gonadotropin surge

could be essential for optimal oocyte competence, and the premature stimulation of the pre-ovulatory gonadotropin surge could eliminate the follicle's progression through these essential stages. Decreased availability of the metabolic substrates and organelles necessary to sustain these energy-demanding developmental processes and alterations in the follicular microenvironment could contribute to the reduced embryo cleavage and increased early embryo loss observed in *in vivo* reproductive systems when small follicles are induced to ovulate. Therefore, we hypothesized that pre-ovulatory follicle status at administration of GnRH to induce the pre-ovulatory gonadotropin surge has an impact on the follicular fluid microenvironment and the metabolic capacity of the oocyte. Two studies were performed with objectives to profile the metabolome of follicular fluid and examine the metabolic capacity of oocytes collected from follicles ~20 hours after GnRH administration and determine the correlation between pre-ovulatory follicle status, follicular fluid metabolite concentrations, and oocyte metabolic capacity. We also performed an intermediate study to develop the methodology to quantify both the level of ATP and mitochondrial DNA copy number from an individual oocyte.

CHAPTER I
LITERATURE REVIEW

US Cattle Production and Fixed-Time Artificial Insemination

In a cow-calf herd, the ability of cows and heifers to conceive, birth, and wean a calf each year is essential to the success and profitability of the operation (Mathews 2001; Boyer et al., 2020; Ealy, 2020). Return to cyclicity following calving is a major milestone that must be met for a cow to calve every 365 days and remain productive in the herd (Short et al., 1990; Opsomer and de Kruif, 1999; Cushman et al., 2007; Baruselli et al., 2018). Animals that calve early in the calving season have greater days postpartum to return to cyclicity and become pregnant for the subsequent calving season. Thus, management to increase the percentage of animals calving early in the calving season improves cow longevity and productivity of the herd (Lesmeister et al., 1973; Funston et al., 2012; Cushman et al., 2013; Damiran et al., 2018). To further improve the yield per head, producers can seek to produce a heavier weaning, more uniform calf crop. This can also be accomplished by managing cows to calve earlier in the calving season and by improving the genetic merit of the herd.

The benefits of increasing the percent of animals calving earlier in the calving season are documented in multiple original research and meta-analysis studies (Lesmeister et al., 1973; Lima et al., 2010; Funston et al., 2012; Cushman et al., 2013; Damiran et al., 2018). Among these, Funston et al. 2012 reported that calving period significantly influences progeny performance (Funston et al., 2012). Within heifer calves, those born in the first 21-day calving period had a greater weaning weight, pre-breeding weight, and pre-calving weight as well as increased percent cycling prior to breeding and increased pregnancy rates when compared to those born in the third 21-day period. Their progeny were also born earlier and had increased weaning weights. Cushman et al. (2013) reported

that heifers that calved early in the calving season with their first calf had increased herd longevity and produced increased pounds of weaned calves (Cushman et al., 2013). The steer calves also benefitted from being born earlier in the calving season. They had greater weaning, final, and carcass weights as well as increased marbling, a greater percent grading USDA modest or greater, and increased carcass values. This increased weaning weight of early calved progeny amounted to the production of an extra calf in the dam's lifetime compared to those dams that calve later in the season. Increasing the number of animals that calve earlier in the calving season has the potential to increase the weight of calves weaned and increase the profits of the operation.

Sire genetics also greatly influence herd productivity by influencing calf weaning weights, carcass merit, or other traits economically relevant to the specific marketing strategy of individual operations (Smith, 1976; Ockerman et al., 1984; Cunningham et al., 1987; Crews, 2002; Casas and Cundiff, 2003; Berry et al., 2019; Eriksson et al., 2020; Martín et al., 2020, 2021). Careful selection of natural service sires and semen purchased for artificial insemination (AI) can improve calf genetic potential and performance. Artificial insemination is economically more efficient for improving herd genetics (Lima et al., 2010; Rodgers et al., 2012; Lamb and Mercadante, 2016; Baruselli et al., 2018). Improving herd genetics by purchasing a bull is limited by a producer's budget to purchase high quality genetics and the reduced accuracy of expected progeny differences (EPDs) of most herd sire prospects. Artificial insemination allows producers to purchase semen from bulls with high accuracy and superior genetics without having to purchase the bull itself. While natural service (NS) is the least labor intensive during the onset of the breeding

season, there are additional costs associated with purchasing and maintaining the bull as well as dangers from the temperament. Though the need for natural service sires is not fully eliminated for herds that utilize AI, establishing pregnancy in a percentage of cows via AI reduces the number of bulls required to successfully service the cow herd and thus reduces such costs and concerns (Rodgers et al., 2012).

Fixed-Time artificial insemination (FTAI) is a viable management option as it incorporates the benefits of calving early and improving herd genetics through AI better than natural service alone or performing AI on only animals detected in estrus (Rodgers et al., 2012; Sá Filho et al., 2013; Lamb and Mercadante, 2016; Baruselli et al., 2018). With FTAI, each cow in the herd is inseminated at the start of the breeding season. This gives every cow the opportunity to become pregnant and calve early. As pregnancy rates to FTAI in beef herds is often 40-60%, there is an increase in the percent of cows that become pregnant in the first 45 days of the breeding season when FTAI followed by natural service vs natural service alone was used (Pursley et al., 1997; Bucher et al., 2009; Taponen, 2009; Sá Filho et al., 2010; Sá Filho et al., 2013; Baruselli et al., 2018; Crites et al., 2018). By adopting FTAI as a management practice, producers have the potential to significantly impact their calf productivity and profitability with relatively minimal investment in time and money at the start of the breeding season.

However, despite the many benefits of FTAI, the technology is not perfect. There is a subset of cattle with decreased pregnancy rates to FTAI compared to the rest of the herd. This subset has not expressed estrus and has not had a gonadotropin surge by the time of scheduled insemination and, consequently, relies on the administration of gonadotropin

releasing hormone (GnRH) to induce their ovulation prior to AI. Cattle induced to ovulate had a 14-60% reduction in pregnancy rate compared to animals that displayed estrus prior to breeding (Perry et al., 2005; Kasimanickam et al., 2009; Sá Filho et al., 2010; Nash et al., 2012; Whittier et al., 2013; Bridges et al., 2014; Martin et al., 2014; Richardson et al., 2016; Abel et al., 2017; Colazo et al., 2018; Rodrigues et al., 2018). Further, within the cattle induced to ovulate, cattle induced to ovulate a smaller sized pre-ovulatory follicle ($\leq$ 11.3 mm) had decreased pregnancy rates and increased late embryonic mortality compared to those induced to ovulate a larger pre-ovulatory follicle (> 11.3 mm; Perry et al., 2005). This phenomenon has been observed by multiple research teams in cattle across the United States and in South America (Lamb et al., 2001; Vasconcelos et al., 2001; Perry et al., 2005; Perry et al., 2007; Sá Filho et al., 2010; Cooke et al., 2019). Interestingly, in beef cattle that displayed estrus, pre-ovulatory follicle size at the time of GnRH administration had no effect on pregnancy rate (Perry et al., 2005). This suggests that follicle size is primarily an indicator of the follicle's physiological status in cattle induced to ovulate, and that the physiological status of the follicle at the time of GnRH injection to induce ovulation heavily affects pregnancy outcome. These differences in pregnancy success could be due to inadequate preparation of the maternal environment or decreased oocyte developmental competence (Vasconcelos et al., 2001; Perry et al., 2005; Busch et al., 2008; Atkins et al., 2010a, b; Fields et al., 2012; Atkins et al., 2013; Jinks et al., 2013; Perry et al., 2014; Cooke et al., 2019; Ciernia et al., 2021). Cattle induced to ovulate a smaller pre-ovulatory follicle have lower serum estradiol concentrations at the induction of ovulation and a less rapid rise in serum progesterone during the first 12-14 days after ovulation compared to cattle

induced to ovulate a larger pre-ovulatory follicle or cattle that displayed estrus(Vasconcelos et al., 2001; Perry et al., 2005; Busch et al., 2008; Atkins et al., 2010ab; Jinks et al., 2013), thus an influence of follicle status on the maternal environment is likely. A reciprocal embryo transfer experiment designed to control for alterations in maternal environment highlighted differences in oocyte developmental competence from smaller versus larger pre-ovulatory follicles (Atkins et al., 2013). Cows induced to ovulate a smaller pre-ovulatory follicle had decreased embryo quality as well as decreased probability of recovering a cleaved embryo seven days after FTAI.

Oocyte Developmental Competence and Follicle Physiological Status

While the *in vivo* fertilization rate for assisted reproductive techniques (ARTs) and natural matings in beef cattle is high, accepted to be close to 90%, pregnancy rate per service may range from 40-55% (Spitzer et al., 1978; Diskin and Sreenan, 1980; Smith et al., 1982; Carter et al., 2008; Dickinson et al., 2016; Reese et al., 2020). This decline in fertility is partly attributed to early embryo loss because 7-57% of *in vivo* produced embryos will become degenerate by the morula/blastocyst stage of embryo development (Diskin and Sreenan, 1980; Roche et al., 1981; Smith et al., 1982; Garrett et al., 1988; Breuel et al., 1993; Carter et al., 2008; Reese et al., 2020). These reductions in pregnancy success are mirrored in *in vitro* systems. While fertilization remains high, 70-80%, 30-86% of oocytes entering IVP fail to produce blastocysts (Pavlok et al., 1992; Lonergan et al., 1994; Blondin and Sirard, 1995; Blondin et al., 1996; Hyttel et al., 1997; Otoi et al., 1997; Hagemann et al., 1999; van de Leemput et al., 1999; Lonergan et al., 2001; Dieleman et al., 2002; Iwata et al., 2004; Lequarre et al., 2005; Ferré et al., 2020). Embryo development

from fertilization to the blastocyst stage is largely the responsibility of the oocyte and relies on the acquisition of oocyte developmental competence (Gosden, 2002; Fair, 2003; Sirard et al., 2006; Swain and Pool, 2008; Zhang and Smith, 2015; Conti and Franciosi, 2018). The early embryo loss observed both *in vivo* and *in vitro* is indicative of inadequate oocyte developmental competence. Broadly, oocyte developmental competence is defined as the ability of the oocyte to complete maturation, be fertilized, cleave, and develop to the blastocyst stage (Lonergan et al., 2003; Sirard et al., 2006; Boni, 2012). In order to accomplish these tasks, the oocyte must have completed specific developmental milestones to allow for its acquisition of meiotic and cytoplasmic competence.

2.1 Acquisition of oocyte developmental competence during oocyte and follicle growth

Meiotic competence is the oocyte's ability to undergo germinal vesicle breakdown (GVBD), progress to metaphase II (MII), and complete the extrusion of a polar body (Landim-Alvarenga and Maziero, 2014; Coticchio et al., 2015; Conti and Franciosi, 2018; He et al., 2021). During oogenesis in cattle, meiotically incompetent growth occurs primarily in preantral/early antral (2-3mm) follicles and is typically characterized by oocytes less than ~110μm in diameter (Fair et al., 1995; Hyttel et al., 1997; Otoi et al., 1997; Aerts and Bols, 2010b). Despite being able to resume meiosis beyond this timepoint, the follicular environment maintains a state of meiotic arrest within the oocyte (Gosden, 2002; Fair, 2003; Conti and Franciosi, 2018). During this time, the oocyte enters a period of meiotically competent growth, increasing to its final size of 120-150μm (Fair et al., 1995; Fair et al., 1997; Hyttel et al., 1997; Otoi et al., 1997). Although developmental competence of the oocyte is greatly improved once the oocyte achieves the capacity to

complete meiosis, it continues to improve as antral follicle development progresses to the pre-ovulatory stages (Pavlok et al., 1992; Lonergan et al., 1994; Blondin and Sirard, 1995; Fair et al., 1995; Blondin et al., 1996; Hyttel et al., 1997; Otoi et al., 1997; Hagemann et al., 1999; van de Leemput et al., 1999; Dieleman et al., 2002; Iwata et al., 2004; Atkins et al., 2013).

Throughout the meiotically incompetent and competent growth phases, the oocyte is increasing its cytoplasmic competence. Cytoplasmic competency involves an increase in oocyte size, transcript accumulation, organelle reorganization, and increased energy and nutrient stores made by the oocyte that are important for downstream developmental processes (Fair et al., 1995; Hyttel et al., 1997; Otoi et al., 1997; Swain and Pool, 2008; Graf et al., 2014; Winterhager and Kidder, 2015; Zhang and Smith, 2015; Conti and Franciosi, 2018). Improved cytoplasmic competency leads to further improvements in embryo cleavage and blastocyst rates when COCs are collected from antral follicles of increasing size. A study by Pavlok and others (1992) removed oocytes from abattoir-sourced ovaries and divided them into three groups based on antral follicle diameter: >1-2 mm, > 2-4 mm, and 4-8 mm. Oocytes from follicles > 2 mm had a 20% increase in fertilization (84.5% vs 62%) and blastocyst rate (24.5% vs 0%) and a 40% increase in cleavage rate (66.5% vs 20%) over those removed from follicles < 2 mm (Pavlok et al., 1992). Additional studies further improved developmental competence by including oocytes from larger antral follicles (> 8 mm) in their IVP system (Lonergan et al., 1994; Blondin and Sirard, 1995; Blondin et al., 1996; Hagemann et al., 1999; van de Leemput et al., 1999; Iwata et al., 2004). While Lonergan had similar blastocyst rates to Pavlok et al.

(1992) in oocytes retrieved from 2-6 mm follicles (34%), by obtaining oocytes from all follicles over 6mm they doubled their blastocyst rate to 66% (Lonergan et al., 1994). Studies by Blondin reported a 20-40% increase in developmental rate to the 16+ cell stage in medium/large (> 3 mm) antral follicle groups over the small groups (< 3 mm; Blondin and Sirard, 1995; Blondin et al., 1996). A later study by Iwata and others (2004) also showed an ~20% increase in both cleavage and blastocyst rate of large antral follicles (6-12 mm) over small antral follicles (2-6 mm; Iwata et al., 2004). Hagemann and others further broke down antral follicle size into smaller size ranges: 3-5 mm, 6-8 mm, 9-12 mm, and $\geq$ 13 mm. Oocytes from the largest antral afollicle group had a 26% increase in blastocyst rate compared to the smallest antral follicle group (Hagemann et al., 1999).

Because increased oocyte size is also related to developmental competence, multiple studies have retrieved cumulus-oocyte complexes (COCs) from abattoir follicles of various sizes, grouped oocytes according to intrazonal oocyte diameter, and observed similar results to those based on follicle size (Fair et al., 1995; Hyttel et al., 1997; Otoi et al., 1997). Each of these studies showed that increasing oocyte diameter is related to increased oocyte developmental competence as evidenced by a higher proportion being fertilized, cleaving, and/or developing to the blastocyst stage. However, based on blastocyst rates well below 100% in even the largest follicle or oocyte groups, size alone is not the most accurate predictor of oocyte developmental competence.

As follicle size increases, the average oocyte diameter is also increasing (Fair et al., 1995; Arlotto et al., 1996; Hyttel et al., 1997; Aerts and Bols, 2010b). However, at any given size, two different follicles could have oocytes with vastly different diameters (Fair

et al., 1995; Arlotto et al., 1996; Hendriksen et al., 2000). This suggests that regardless of follicle diameter, these follicles could be at different developmental stages and contain oocytes with different developmental competencies. Studies investigating the dynamics of follicular development within cattle further support that follicles of equal size could be at different physiological stages (Spicer and Echternkamp, 1986; Taylor and Rajamahendran, 1991; Fortune, 1993; Hendriksen et al., 2000; Hendriksen et al., 2003; Atkins et al., 2010a, b; Jinks et al., 2013; de Lima et al., 2020). It can take up to 2 weeks for an atretic follicle to fully regress (Hendriksen et al., 2000). Atretic follicles decreasing in size and healthy follicles increasing in size results in a mix of atretic and healthy follicles at any given follicle size (Kruip and Dieleman, 1982; Spicer and Echternkamp, 1986; Hendriksen et al., 2000; Hendriksen et al., 2003). Additionally, the follicular fluid and serum estradiol levels of cattle with similarly sized follicles can vary greatly, suggestting varied stages of follicular development in similarly sized follicles (Kruip and Dieleman, 1982; Hendriksen et al., 2003; Busch et al., 2008; Atkins et al., 2010a, b; Jinks et al., 2013; Perry et al., 2014). This phenomenon is also demonstrated during the pre-ovulatory time period, as the ability of follicles to initiate an endogenous gonadotropin surge to induce their own ovulation is achieved between ~9 mm and > 17 mm in beef cattle (Fortune, 1993; Perry et al., 2005; Busch et al., 2008; Fields et al., 2012; Perry et al., 2014). Collectively, these studies provide evidence that two follicles at any given size can either be at different physiological stages of development. Therefore, the physiological status of the follicle should be considered prior to utilization of the oocyte to produce an embryo.

2.2 The effects of follicle physiological status on oocyte developmental competence

Within the bovine estrous cycle, there are typically two to three follicular waves with the second or third wave producing the ovulatory follicle (Taylor and Rajamahendran, 1991; Lucy et al., 1992; Fortune, 1993; Hendriksen et al., 2003; Fortune et al., 2004; Jaiswal et al., 2004; Aerts and Bols, 2010a; Miura, 2019). For simplicity, this review will focus on describing the follicular dynamics of an estrous cycle with two follicular waves. The previous cycle's follicle ovulates ~24 hours after estrous onset, designated as day 0 (Skarzynski et al., 2013). Serum estradiol levels decrease to basal levels (~2 pg/ml; Lucy et al., 1992; Alvarez et al., 2000) and serum progesterone levels rise as the corpus luteum (CL) forms. The decrease in circulating estradiol and inhibin from the past ovulatory follicle removes the inhibition on follicle stimulating hormone (FSH) release and FSH levels increase (Hendriksen et al., 2003). The increase in FSH levels recruits a group of 5-24 ~3 mm follicles into the first follicular wave of the new estrous cycle (Ginther et al., 1997; Hendriksen et al., 2003; Aerts and Bols, 2010a). Increased estradiol and inhibin production by the growing cohort of follicles begins to decrease the levels of circulating FSH (Ginther et al., 2000; Ginther et al., 2001; Aerts and Bols, 2010a; Lamb et al., 2010). By ~ day 2-3 of the cycle, the largest follicle reaches ~8 mm and its granulosa cells begin to express LH receptors (Bodensteiner et al., 1996; Aerts and Bols, 2010a; Bisinotto and Santos, 2011). This allows LH to stimulate its growth and further increase its production of estradiol and inhibin while further decreasing circulating FSH levels (Ginther et al., 2001). Despite decreased levels of FSH, the selected follicle continues growth because it has gained LH receptors in its granulosa cells while the subordinate, FSH-dependent

follicles have decreased growth (Ginther et al., 2001; Jaiswal et al., 2004; Aerts and Bols, 2010a). The dominant follicle continues to grow until ~ day 8 of the cycle while the subordinate follicles undergo atresia. The high levels of circulating progesterone (~2-6ng/ml) produced by the CL have a negative feedback on LH pulse frequency, preventing the increase in LH pulse frequency needed for the follicle to continue growing and enter the pre-ovulatory stage of development (Skinner et al., 1998; Alvarez et al., 2000; Perry et al., 2005; Jinks et al., 2013; Hill et al., 2014). The LH-dependent growth of the follicle is inhibited and the dominant follicle undergoes atresia. This causes a drop in the levels of circulating estradiol and inhibin, a rise in FSH, and allows for the second follicular wave to be recruited around days 9-10 (Fortune, 1993; Hendriksen et al., 2003). A new dominant follicle is selected on day 12 (Taylor and Rajamahendran, 1991; Bisinotto and Santos, 2011). Around day 16, the CL undergoes luteolysis, decreasing the levels of circulating progesterone and removing progesterone's inhibition of gonadotropin releasing hormone (GnRH) from the hypothalamus (Taylor and Rajamahendran, 1991; Skarzynski et al., 2013). As the follicle increases in size, it produces increased levels of estradiol due to the removal of progesterone's negative feedback on LH pulsatility (Stumpf et al., 1989; Perry et al., 2014; Jinks et al., 2013; Atkins et al., 2013; Perry et al., 2005). Estradiol continues to have a negative feedback on the tonic center of the hypothalamus, however estradiol does have a positive feedback on the surge center of the hypothalamus (Sinchak and Wagner, 2012; Christian and Moenter, 2010). As a consequence, pulsatile GnRH release from the tonic center and the corresponding LH release from the anterior pituitary is reduced even in the pre-ovulatory time period (Christian and Moenter, 2010). Once

estradiol reaches a threshold level around day 20 (~ 7-9pg/ml), it results in estrous behavior and stimulates the GnRH-induced LH surge (Wettemann et al., 1972; Alvarez et al., 2000; Allrich, 1994). The follicle begins to undergo luteinization and prepare for ovulation. This causes a decrease in production of estradiol by the follicle and a decrease in serum estradiol levels. Approximately 24 hours later, ovulation occurs and the CL increases in size over the next five days (Skarzynski et al., 2013). Serum progesterone levels increase gradually as the CL becomes more developed and the cycle repeats with a new follicular wave.

Each follicular wave can be broken down into FSH-dependent growth of the follicle (days ~1-6 and 9-16, follicle size ~3-8 mm) and LH-dependent follicle growth (days ~7-8 and 17-20, follicle size ~9-preLH surge) phases. The final follicular wave of each estrous cycle results in additional growth of the dominant follicle following luteolysis. In this wave, the dominant follicle reaches the ovulatory phase of follicle development (~day 21, post-LH surge – ovulation). The studies mentioned previously that investigated developmental competence of oocytes collected from follicles of varied sizes inadvertently grouped oocytes from follicles that likely differed in physiological status. However, abattoir-sourced ovaries are from variable, unknown reproductive backgrounds and various stages of atresia. To further decipher impacts of the follicle's known physiological status on oocyte developmental competence, Hagemann and others (1999) produced follicles of known background by synchronizing estrus in a population of cows and collecting the ovaries at slaughter on days 2, 7, 10, and 15 of the estrous cycle (Hagemann, 1999). They collected oocytes from growing, nonatretic follicles 3-5 mm, 6-8 mm, 9-12 mm, and $\geq$ 13 mm and observed a size-dependent increase in blastocyst rate from 45% in the 3-5 mm

group to 70% in the ≥ 13 mm group. The collection of 3-5 mm follicles on day 2 of the estrous cycle likely resulted in the collection of oocytes during FSH-dependent growth phase while the collection of follicles ≥ 13 mm on day 15 of the estrous cycle likely resulted in the collection of oocytes during the LH-dependent growth phase. The improved developmental competence of oocytes collected from this time point provides evidence of the importance of LH-dependent growth on oocyte developmental competence. In the LH-dependent follicular phase, the oocyte undergoes a phase of low growth and increased cytoplasmic reorganization referred to as the oocyte capacitation phase (~120-150μm; Humblot et al., 2005). Despite possessing the ability to resume meiosis and having reached their final size, oocytes in this phase are maintained in a period of meiotic arrest. This allows for ultrastructural changes to occur as well as modifications to be made to RNA and proteins to prevent their degradation (Hyttel et al., 1989; Merton et al., 2003; Gougeon, 2010; Labrecque et al., 2016; Liu et al., 2017; Tang et al., 2019).

Additional studies compare the developmental competence of oocytes collected after the LH surge to oocytes collected during the FSH-dependent and LH-dependent phases. *In vitro* culture studies by van de Leemput and Dieleman (1999) also showed the importance of physiological status of the follicle prior to oocyte removal. The first study compared abattoir-sourced, 2-8 mm follicle (FSH-dependent phase) oocytes that underwent *in vitro* maturation to oocytes removed from super-ovulated cattle 24 hours after the LH surge (full development through post LH surge environment (van de Leemput et al., 1999). Oocytes that were exposed to all of the follicle developmental stages had 20% greater cleavage and blastocyst rates compared to those removed from the physiologically

younger follicles (FSH dependent phase). Gjorret et al. (2003) and Knijn et al. (2002) conducted similar experiments and recorded embryo quality. *In vivo* produced embryos from super-ovulated cattle were better quality as shown by an increase in cell number and a decrease in apoptotic cells compared to *in vitro* produced embryos (Knijn et al., 2002; Gjorret et al., 2003). Dieleman and others (2002) further elucidated the importance of the final stages of antral follicle development, specifically highlighting the importance of the completion of capacitation and exposure to the post LH surge follicular environment. They super-ovulated cattle and removed a group of oocytes from the follicle 2 hours prior to the GnRH-induced LH surge and 24 hours after the LH surge via ovum pick up (OPU). The oocytes removed from the follicle 2 hours prior to the LH surge were matured *in vitro* while those removed after the LH surge were matured *in vivo*. Exposure of the oocyte to the full length of oocyte capacitation and the post LH surge environment is important for downstream developmental competence as oocytes that were allowed to complete oocyte capacitation and mature *in vivo* had a higher blastocyst rate (50% vs 80%). Completion of oocyte capacitation and oocyte maturation *in vivo* is also important for embryo quality as evidenced by an increased embryo cell number (54% vs 96%) and a lower percent of mixoploid embryos (50% vs 21%) in the *in vivo* matured group (Dieleman et al., 2002). Another study by de Loos et al. (1992) revealed that *in vitro* versus *in vivo* final maturation affected cumulus cells as well. Cumulus cells of *in vitro* matured COCs had decreased expansion. Cumulus cell expansion is important for oocyte maturation as well as fertilization. Decreased expansion in *in vitro* matured COCs provides further evidence that

COCs need to be exposed to a complete follicular phase in order to obtain full developmental competence (de Loos et al., 1991).

Studies by Perry and Atkins highlight the importance of pre-ovulatory follicle status and oocyte capacitation on pregnancy outcome or embryo development in beef cows following fixed-time artificial insemination (Perry et al., 2005, Atkins et al., 2013). As previously discussed, cattle that did not display estrus prior to induced ovulation/AI had lower day 27 pregnancy rates compared to those that did (29% vs 90% in cows and 20% vs 63% in heifers; Perry et al., 2005; Perry et al., 2007). Size of the follicle at estrus did not affect pregnancy rate, indicating that physiological status of the follicle was the primary factor in developmental competence. Regardless of size, the follicles had progressed through all the physiological phases of development *in vivo* and should have resulted in ovulation of a maximally developmentally competent oocyte (Dieleman et al., 2002). Oocytes from pre-ovulatory follicles induced to ovulate did not have the opportunity to complete the final hours of LH-dependent oocyte capacitation prior to induction of the gonadotropin surge. Further, the groups that were induced to ovulate were subdivided into small (< 11.3 mm in cows and < 10.7 mm in heifers) and large ($\geq$ 11.3 mm in cows and $\geq$ 12.8 mm in heifers) follicle groups. Those cattle induced to ovulate a smaller pre-ovulatory follicle had a reduced day 27 pregnancy rate following AI compared to animals induced to ovulate a larger pre-ovulatory follicle. These follicle sizes also mark a transition in the degree of progression that the follicle completed prior to premature induction of the pre-ovulatory gonadotropin surge. Small follicles would likely be physiologically younger and the oocyte within would have spent less time in the LH-dependent growth phase. Larger

follicles would contain oocytes that may have likely progressed further through oocyte capacitation before the gonadotropin surge was induced. Taken together, these studies show improved day 27 pregnancy rates as the follicle progresses through more advanced physiological stages.

While improved pregnancy rates of cows that expressed estrus or were induced to ovulate a larger vs smaller pre-ovulatory follicle were undoubtedly related in part to an improved maternal environment (Cooke et al., 2019), multiple studies show that improved oocyte developmental competence is also a contributing factor (van de Leemput et al., 1999; Dieleman et al., 2002; Atkins et al., 2013). Atkins demonstrated that increased follicle size at induced ovulation in cattle that did not display estrus was correlated to increased probability of recovering a fertilized embryo as well as improved day 7 embryo quality. Additionally, Cooke and others (2019) showed that conceptuses collected on day 15 after insemination were almost 3 times longer in cattle that displayed estrus prior to AI compared to those that did not display estrus (Cooke et al., 2019).

To better understand the critical physiological processes that take place during the final hours of oocyte capacitation, Moorey and others (2021) performed an RNA sequencing study that compared the gene expression profiles of oocytes and cumulus cells collected from the follicles of cattle that displayed estrus and those that did not (Moorey et al., 2021). The follicles of the cattle that did not display estrus were further divided into larger ($\geq$ 12.7 mm) and smaller ($\leq$ 11.7 mm) pre-ovulatory follicle groups. Moorey et al. (2021) reported decreased expression of transcripts involved in glycolysis in the cumulus cells of smaller compared to larger pre-ovulatory follicles. Further, oocytes from small

follicles had decreased expression of genes associated with mitochondria and oxidative phosphorylation when compared to the oocytes from cattle that displayed estrus. The oocyte and early embryo rely on cumulus cell glycolysis and oocyte oxidative phosphorylation for energy production (Paczkowski et al., 2013)]. Decreased expression of genes involved in these key pathways suggests a decrease in the metabolic capacity of the oocytes induced to ovulate prematurely from a small follicle.

Metabolic Capacity of the COC and Embryo Development

The oocyte and early embryo primarily rely on oxidative phosphorylation to create the energy necessary to sustain development through to the blastocyst stage of embryo development (Biggers et al., 1967; Tamassia et al., 2004; Sutton-McDowall et al., 2010; Paczkowski et al., 2013; Dalton et al., 2014; Babayev and Seli, 2015; Dalbies-Tran et al., 2020). The ability to meet these energy needs relies on events that happen during antral follicle growth prior to the LH surge and resumption of oocyte meiotic maturation (Zhang et al., 2017). This includes an increase in mitochondrial number within the oocyte as well as an accumulation of metabolic substrates that can be utilized to fuel oxidative phosphorylation. Ultimately, stored metabolic substrates are used to produce ATP via oxidative phosphorylation to meet the energy needs of the oocyte during the resumption of meiosis, fertilization, and cleavage as well as early embryo cell division. Multiple studies reported that ATP levels within the oocyte and embryo are indicative of developmental competence (Quinn and Wales, 1973; Calarco, 1995; Van Blerkom et al., 2000; Stojkovic et al., 2001; Tamassia et al., 2004; Dalton et al., 2014).

Mitochondria are found in high numbers within the oocyte and comprise approximately 30% of the volume of a mature oocyte (Dumollard et al., 2009; May-Panloup et al., 2021). Human and mouse MII stage oocytes have approximately 100,000 mitochondria (Monnot et al., 2013; Zhang et al., 2017). These mitochondria are generated from a small population of ~100 mitochondria present in primordial germ cells (Wai et al., 2008; St John, 2014; Babayev and Seli, 2015; Zhang et al., 2017). Mitochondrial DNA (mtDNA) is present within the mitochondria and encodes for 13 proteins that are components of the electron transport chain (Spikings et al., 2006; Zhang et al., 2017). Within the oocyte, each mitochondrion is reported to possess anywhere from 1 to 15 copies of mtDNA (Pikó and Taylor, 1987; Spikings et al., 2006; May-Panloup et al., 2007; Zhang et al., 2017). In the bovine, mtDNA copy number can range from 13,000 to 3,600,000 copies per oocyte (Dumollard et al., 2007; Jiao et al., 2007; Iwata et al., 2011; Roth, 2018; Hashimoto et al., 2019; Nagano, 2019).

Mitochondrial number and mtDNA copy number both increase throughout oogenesis (Smith and Alcivar, 1993; Hyttel et al., 1997; Tamassia et al., 2004; Chappel, 2013; St John, 2014; Babayev and Seli, 2015). Mitochondrial DNA copy number is frequently used to estimate the quantity of mitochondria within the oocyte (Michaels et al., 1982; Tamassia et al., 2004; Iwata et al., 2011; Archer, 2013; Babayev and Seli, 2015; May-Panloup et al., 2021). Increased mtDNA copy number is associated with highly metabolically active somatic cells like neurons, muscle cells, and oocytes (Archer, 2013; Chappel, 2013). However, the relationship between mtDNA copy number and oocyte developmental competence is debated. Multiple studies have shown oocytes with

increased mtDNA copy number have improved developmental competence while others show no relationship (Van Blerkom et al., 1998; Perez et al., 2000; Reynier et al., 2001; Tamassia et al., 2004; Jiao et al., 2007; May-Panloup et al., 2007; Iwata et al., 2011; Srirattana and St John, 2018). This could be due to differences in study design and measurement of mtDNA copy number.

Within oocytes that have resumed meiosis after exposure to the LH surge, the mitochondria are in a conformation suggestive of low energy production (Hyttel et al., 1986; May-Panloup et al., 2021). They are small, round, and have decreased cristae (Hyttel et al., 1986; Hyttel et al., 1989; Fair et al., 1997; Reader et al., 2017). This suggests that the large mitochondrial mass established within the oocyte prior to maturation is needed to produce the amount of ATP necessary to meet the energy needs of the oocyte (Van Blerkom et al., 1998; Tamassia et al., 2004). Because the number of mitochondria present in the embryo does not increase until after the embryo develops to the blastocyst stage, the early embryo must meet its metabolic needs with the mitochondria it obtained during antral follicle development (Chappel, 2013; St John, 2014; Babayev and Seli, 2015). As the embryo cleaves, the mitochondrial complement is divided amongst the blastomeres and the mitochondria take on a conformation indicative of increased metabolic activity (Motta et al., 2000). This results in a decrease in the mitochondrial mass per cell and an increase in the ATP produced per mitochondrion (Chappel, 2013). Embryos from oocytes with decreased levels of mitochondria have decreased mitochondria per cell and, consequently, decreased metabolic capacity within the blastomeres (Van Blerkom et al., 2000; Van Blerkom, 2004; May-Panloup et al., 2021). Interestingly, transcript abundance for 3

mitochondrial genes (mt*ND1*, mt*ND5*, mt*COX1*) was increased in the oocytes of smaller pre-ovulatory follicles (≤ 11.7 mm) that underwent an induced gonadotropin surge compared to oocytes collected from follicles of cows that had exhibited estrus (Moorey et al., 2021). However, an additional 5 nuclear genes (*ATP6V0D1*, *NDUFA7*, *NDUFA8*, *COX6A1*, *COX5B*) had reduced expression in the oocytes from smaller pre-ovulatory follicles of cattle that did not display estrus versus oocytes from follicles of cattle that did display estrus. Therefore, the impact of pre-ovulatory follicle status on mitochondrial number or function is uncertain.

In addition to needing adequate levels of mitochondria, the oocyte must have obtained stockpiles of the metabolic substrates utilized by the mitochondria to perform oxidative phosphorylation. During oocyte capacitation, which is a critical component of oocyte development occurring during LH-dependent antral follicle growth, the oocyte is increasing the size and number of lipid droplets within the cytoplasm. These lipids are used by the mitochondria to produce energy via beta oxidation (Dunning et al., 2014; Dalbies-Tran et al., 2020). This is evidenced by the clustering of mitochondria around lipid droplets during maturation, the lipid droplets taking on a conformation that indicates their use, and an inhibition of the mitochondrial enzymes important for the oxidation of lipids negatively impacting developmental competence (Hyttel et al., 1986; Sturmey et al., 2009; Paczkowski et al., 2013; Dalbies-Tran et al., 2020). Further, oocyte lipid content has been associated with improved developmental competence (Jeong et al., 2009; Aguila et al., 2020). Premature maturation of the oocyte could interrupt accumulation of lipids and result in decreased energy availability during development.

Additionally, bovine oocytes and early embryos are unable to conduct glycolysis and rely on cumulus cells to provide substrates for oxidative phosphorylation (Biggers et al., 1967; Sutton-McDowall et al., 2010; Paczkowski et al., 2013; Dalbies-Tran et al., 2020). During antral follicle growth, cumulus cell glycolytic activity results in the production of metabolites such as pyruvate, lactate, NADH, and FADH2 (Sutton-McDowall et al., 2010; Winterhager and Kidder, 2015; Richani et al., 2021). These metabolic substrates are transported to the oocyte via gap junctions where they are stockpiled for use during oocyte maturation and embryo development (Swain and Pool, 2008; Sutton-McDowall et al., 2010; Seli et al., 2014; Dumesic et al., 2015; Winterhager and Kidder, 2015; May-Panloup et al., 2021; Richani et al., 2021). The importance of these substrates to the oocyte are evidenced by the oocyte control of cumulus cell glycolysis. BMP15, GDF9, and FGF8 produced by the oocyte increase the expression of glycolytic genes within the cumulus cells (Emori and Sugiura, 2014; Moorey et al., 2021). Moorey et al. (2021) previously reported a decrease in gene expression for key enzymes in the glycolytic pathway (*ALDOC*, *GPI*, *HK2*, *LDHA*, *PFKP*, *TRI1*; FDR<0.01) in the cumulus cells of COCs obtained from small (≤ 11.7 mm) compared to large (≥ 12.7 mm) follicles that received pharmacological injection to induce the gonadotropin surge (Moorey et al., 2021). The lower expression of such genes suggests decreased glycolytic activity in the cumulus cells and decreased metabolic substrate transported to the oocytes of small follicles. A potential decrease in the lipid content and glycolytic metabolite availability in the oocyte removed prematurely could be responsible for the decreased developmental competence of these oocytes.

A combination of the mitochondrial content and metabolic substrate levels within the oocyte result in the metabolic capacity of the oocyte and early embryo to produce ATP. Metabolic capacity of the oocyte is accumulated throughout antral development and relies on exposure to the follicular microenvironment.

3.1 Effects of the follicular fluid microenvironment on oocyte developmental competence

Follicular fluid present during the antral stages of folliculogenesis is a product of serum and follicular cell secretions (Edwards, 1974; Gosden et al., 1988; Clarke et al., 2006; Fahiminiya and Gérard, 2010b; Kidder and Vanderhyden, 2010; Rodgers and Irving-Rodgers, 2010; Hennet and Combelles, 2012; Winterhager and Kidder, 2015; Read et al., 2018). It provides many of the nutrients, metabolic substrates, and signaling molecules required to support the metabolism of the COC and accumulation of stockpiles of metabolic substrates within the oocyte (Edwards, 1974; Gosden et al., 1988; Clarke et al., 2006; Fahiminiya and Gérard, 2010b; Kidder and Vanderhyden, 2010; Rodgers and Irving-Rodgers, 2010; Hennet and Combelles, 2012; Winterhager and Kidder, 2015; Read et al., 2018). Multiple studies have shown that the follicular fluid composition changes throughout antral follicle development and is related to stage of development and stage of the estrous cycle (Orsi et al., 2005a; Moreno et al., 2015). For example, during the LH-dependent and post LH surge phases, steroid hormone profiles change dramatically. During the beginning of the LH dependent phase of a follicular wave, the follicle is exposed to a high progesterone environment. Following luteolysis, and the subsequent decrease in circulating progesterone, the follicular cells increase estradiol production and the follicular

fluid contains increasing levels of estradiol until the pre-ovulatory gonadotropin surge (Fortune and Hansel, 1985; Ginther et al., 2000; De los Reyes et al., 2006; Perry et al., 2014). Once this occurs, the follicular fluid composition decreases in estradiol levels and increases in progesterone. This fluctuation in endocrine profiles is important for the acquisition of oocyte developmental competence.

In addition to preparation of the uterine environment for pregnancy, progesterone is also thought to play an important role in oocyte developmental competence (Bazer et al., 2011; Fair and Lonergan, 2012). This is because the follicle is exposed to systemic progesterone during the majority of antral development, intrafollicular progesterone levels increase after exposure to the pre-ovulatory gonadotropin surge, and cumulus cells express progesterone receptors as well as produce progesterone (Dieleman et al., 1983; Fortune and Hansel, 1985; Alvarez et al., 2000; Lamb et al., 2010; Aparicio et al., 2011; Wiltbank et al., 2011; Fair and Lonergan, 2012; Rispoli et al., 2020). During the LH-dependent growth phase, progesterone levels must decrease in order for the follicle to continue development towards the pre-ovulatory phase (Skinner et al., 1998; Fair and Lonergan, 2012). After the pre-ovulatory gonadotropin surge, progesterone levels within the follicular fluid increase. Increased follicular progesterone levels after the LH surge are associated with increased probability of retrieving an oocyte at the MI or MII stage of meiotic maturation as well as increased blastocyst rate (Seibel et al., 1989; Aardema et al., 2013; Da Broi et al., 2018). Progesterone receptors are present within the COC during this time period. *In vitro* experiments that utilized progesterone receptor antagonists showed a

reduction in cumulus cell expansion, decreased chromosome segregation during meiotic maturation, and decreased blastocyst rates (Luciano et al., 2010; Aparicio et al., 2011).

Estradiol has been reported to promote oocyte developmental competence in multiple studies (Ginther et al., 2000; Ginther et al., 2001; De los Reyes et al., 2006). Estradiol produced by the granulosa cells stimulates the expression of both C-type natriuretic peptide (CNP) and its receptor (NPR2). This system acts to maintain meiotic arrest within the oocyte by increasing the transport of cGMP to the oocyte from the cumulus cells. Increased cGMP inhibits phosphodiesterase 3A (PDE3A) breakdown of cAMP within the oocyte, maintaining high levels of cAMP within the oocyte (Zhang et al., 2010; Liu et al., 2017). The exposure of the COC to estradiol also increases the expression of gap junctional proteins and increases their localization to the plasma membrane (Firestone and Kapadia, 2012). This increase in functional gap junctions increases the ability of the cumulus cells to transport cGMP to the oocyte as well as the metabolic substrates needed to support oocyte and embryo development. Because the oocyte relies on gap junction transport to store pyruvate, lipids, and other metabolic substrates, increased functional gap junctions could contribute to an increase in oocyte stockpiles.

In addition to the changes in hormone levels the oocyte experiences during the LH dependent growth phase, the metabolite, protein, and electrolyte profile of the follicular fluid also changes. Components found within bovine follicular fluid include amino acids, glucose derivatives, and fatty acids that are important for proteinogenesis, energy metabolism, and the regulation of reactive oxygen species (Orsi et al., 2005a; Bender et al., 2010; Renaville et al., 2010; Leroy et al., 2011; Alves et al., 2014; O'Doherty et al.,

2014; Forde et al., 2016a; Guerreiro et al., 2018). Glucose concentrations within the follicular fluid increase throughout antral follicle development before plateauing in pre-ovulatory and post LH surge follicular fluid (Iwata et al., 2004; Orsi et al., 2005a; Bender et al., 2010). *In vivo,* follicular fluid glucose is metabolized by the cumulus cells to support nucleic acid synthesis and the acquisition of stores of metabolic substrates within the oocyte (Biggers et al., 1967; Sutton et al., 2003). Once the pre-ovulatory LH surge occurs, cumulus cells utilize glucose to support their own expansion as well as progression of the oocyte through meiosis (Leroy et al., 2004; Bilodeau-Goeseels, 2006; Leroy et al., 2006; Sutton-McDowall et al., 2010; Leroy et al., 2011; Brown et al., 2017). Increased glucose levels in follicular fluid and maturation media were associated with improved oocyte developmental competence (Rose-Hellekant et al., 1998; Downs and Hudson, 2000; Iwata et al., 2004; Bilodeau-Goeseels, 2006; Leroy et al., 2006). Pyruvate concentration within the follicular fluid also increases with increasing follicle diameter (Orsi et al., 2005a). As cumulus cells convert glucose to pyruvate via glycolysis, they are transporting it through their gap junctions to deposit pyruvate into both the oocyte and the surrounding environment (Uhde et al., 2018a). Increased pyruvate presence within the follicular fluid of larger follicles could be indicative of increased cumulus cell glycolysis during this timepoint. This is further confirmed by the decrease in the glycolytic genes expressed in the cumulus cells from small follicles (Moorey et al., 2021).

In vitro, the presence of pyruvate, glucose, and glutamine in the culture media is essential for progression of the oocyte through MII (Rieger and Loskutoff, 1994; Rose-Hellekant et al., 1998; Downs and Hudson, 2000). Glutamine is thought to act as both a

source of energy as well as provide substrates for nucleic acid synthesis as only oocytes exposed to glutamine were able to achieve MII (Bilodeau-Goeseels, 2006; Hennet and Combelles, 2012). Additionally, decreased levels of glucose in the culture media results in an increase in the amount of time required for the oocyte to reach MII as well as a decrease in blastocyst rate (Iwata et al., 2004). Pyruvate, glucose, and glutamine metabolism by the COC reach a peak around 18 hours after initiation of meiotic maturation (Rieger and Loskutoff, 1994; Roberts et al., 2002). Interestingly, this is the approximate time the oocytes were collected in the study by Moorey et al (2021). In this study, cumulus cells collected ~23 hours after the smaller pre-ovulatory follicles were prematurely exposed to the LH surge had decreased expression of glycolytic genes as well as genes for the glucose transporters *SLC2A1* and *SLC2A10.* The decreased ability to transport metabolic substrates into the cumulus cells as well as a decreased ability to metabolize these substrates could result in a decreased availability of these metabolites during meiotic maturation.

In addition to progression through latter stages of antral follicle growth, the follicular fluid microenvironment can be impacted by extraovarian factors. In ruminants and humans, follicular fluid composition can be impacted by the environment, diet, metabolic status, age, and ovarian stimulation protocol (Fortune and Hansel, 1985; Assey et al., 1994; Ambrose et al., 2006; Leroy et al., 2006; Bender et al., 2010; Von Wald et al., 2010; Wonnacott et al., 2010; Zachut et al., 2010; Leroy et al., 2011; Liu et al., 2012; Alves et al., 2014; O'Doherty et al., 2014; Palini et al., 2014; Moreno et al., 2015; Forde et al., 2016a; Takeo et al., 2017). Changes in the environment an oocyte is exposed to both *in vivo* and *in vitro* have been shown to impact oocyte developmental competence as well as

COC metabolism (Downs and Hudson, 2000; Sutton et al., 2003; Leroy et al., 2011; Krisher, 2013; Matoba et al., 2014; Dumesic et al., 2015). A primary example is the effect of negative energy balance in dairy cattle on follicular fluid composition and oocyte developmental competence (Leroy et al., 2005; Bender et al., 2010; Renaville et al., 2010; Leroy et al., 2011; O'Doherty et al., 2014; Forde et al., 2016a). Lactating dairy cattle have higher concentrations of saturated fatty acids and decreased concentrations of unsaturated fatty acids than heifers and nonlactating cattle (Bender et al., 2010; Forde et al., 2016a). Increased saturated fatty acids in the follicular fluid are associated with impaired meiosis, cleavage, and blastocyst formation while increased unsaturated fatty acids are associated with increased blastocyst rate and decreased pregnancy loss (Leroy et al., 2005; Ambrose et al., 2006; Wonnacott et al., 2010; Matoba et al., 2014). *In vitro,* supplementation with saturated fatty acids induces granulosa cell apoptosis while unsaturated fatty acid supplementation increases the percent of oocytes that achieve MII (Mu et al., 2001; Matoba et al., 2014). There are few studies that investigated the metabolite and nutrient composition of the follicular fluid in beef cattle. However, multiple studies have highlighted how manipulating the estrous cycle can result in altered hormone levels and impact oocyte developmental competence (Fortune and Hansel, 1985; Stock and Fortune, 1993; Assey et al., 1994; Perry et al., 2005; Perry et al., 2007; Bisinotto and Santos, 2011; Perry et al., 2014). Because the follicular fluid changes throughout folliculogenesis and is easily impacted by extraovarian factors, by inducing premature ovulation, the post LH surge follicular fluid microenvironment could be altered in beef cattle. As mentioned in previous sections, an oocyte that is exposed to each intrafollicular microenvironment has

obtained maximal developmental competence as evidenced by increased blastocyst rate and embryo quality compared to oocytes removed from follicles prior to the LH-dependent and post LH surge phases. As oocyte developmental competence is linked to follicular fluid composition, alterations due to premature exposure to an LH surge could have negative impacts on the developmental competence and metabolic capacity of the oocyte.

Taken together, the overarching hypothesis of this dissertation is to investigate the relationship between follicle physiological status at the time of administration of GnRH to induce the LH surge on oocyte metabolic capacity and the ovulatory follicle microenvironment approximately 19 hours after GnRH administration.

CHAPTER II
CORRELATION BETWEEN PRE-OVULATORY FOLLICLE DIAMETER AND FOLLICULAR FLUID METABOLOME PROFILES IN LACTATING BEEF COWS

A version of this chapter was originally published by Casey Read and Sarah Moorey: Casey C. Read, J. Lannett Edwards, F. Neal Schrick, Justin D. Rhinehart, Rebecca R. Payton, Shawn R. Campagna, Hector F. Castro, Jessica L. Klabnik, Emma J. Horn, and Sarah E. Moorey. "Correlation Between Pre-ovulatory Follicle Diameter and Follicular Fluid Metabolome Profiles in Lactating Beef Cows." *Metabolites* 11 (2021): 623.

Conceptualization, Sarah Moorey; Data curation, Casey Read, Shawn Campagna, Hector Castro and Sarah Moorey; Formal analysis, Casey Read and Sarah Moorey; Investigation, Casey Read, F. Schrick, Justin Rhinehart, Rebecca Payton, Jessica Klabnik, Emma Horn and Sarah Moorey; Methodology, J. Edwards, F. Schrick and Sarah Moorey; Project administration, Sarah Moorey; Resources, Shawn Campagna, Hector Castro and Sarah Moorey; Software, Casey Read and Sarah Moorey; Supervision, Sarah Moorey; Visualization, Casey Read and Sarah Moorey; Writing – original draft, Casey Read, Emma Horn and Sarah Moorey; Writing – review & editing, J. Edwards, F. Schrick, Justin Rhinehart, Rebecca Payton, Shawn Campagna, Hector Castro and Jessica Klabnik.

Funding: This research was supported by the USDA NIFA Hatch project 1022068, the University of Tennessee AgResearch, and the University of Tennessee Department of Animal Science.

Acknowledgments: The authors would like to thank Dr. Liesel Schneider for her statistical analyses consulting, Courtney Christopher and Sara Howard for their assistance with the UHPLC-HRMS metabolomics processing, Emma Hessock for her assistance in researching enriched pathways, Boyd Dingus for the donation of the Estrotect ® patches, and Walt Hitch and the staff of the Plateau AgResearch and Education Center for providing the cattle and their assistance in processing the cattle for this study.

Abstract

Induced ovulation of small pre-ovulatory follicles reduced pregnancy rates, embryo survival, day seven embryo quality, and successful embryo cleavage in beef cows undergoing fixed-time artificial insemination. RNA-sequencing of oocytes and associated cumulus cells collected from pre-ovulatory follicles 23 hours after gonadotropin releasing hormone (GnRH) administration to induce the pre-ovulatory gonadotropin surge suggested reduced capacity for glucose metabolism in cumulus cells of follicles ≤ 11.7 mm. We hypothesized that the follicular fluid metabolome influences metabolic capacity

of the cumulus-oocyte complex and contributes to reduced embryo cleavage and quality grade observed following induced ovulation of small follicles. Therefore, we performed a study to determine the correlation between pre-ovulatory follicle diameter and follicular fluid metabolome profiles in lactating beef cows (Angus, n=130). We synchronized the development of a pre-ovulatory follicle and collected the follicular contents approximately 20 hours after GnRH administration. We then performed UHPLC-HRMS metabolomic studies on 43 follicular fluid samples and identified 38 metabolites within pre-ovulatory follicles of increasing size. We detected 18 metabolites with a significant, positive correlation to follicle diameter. Individual and pathway enrichment analysis of significantly correlated metabolites suggest that altered glucose and amino acid metabolism likely contribute to reduced developmental competence of oocytes when small pre-ovulatory follicles undergo induced ovulation.

Introduction

Decreased pre-ovulatory follicle diameter at the time of pharmacological induction of ovulation was associated with lower pregnancy rates and/or reduced embryo survival in beef cattle undergoing fixed-time artificial insemination (FTAI; Lamb et al., 2001; Perry et al., 2005; Perry et al., 2007; Sá Filho et al., 2010). Such reductions in fertility were likely the result of poor preparation of the maternal environment for pregnancy establishment and the ovulation of an oocyte with reduced developmental competency (Perry et al., 2005; Atkins et al., 2013; Jinks et al., 2013; Ciernia et al., 2021). When beef cows were induced to ovulate a pre-ovulatory follicle < 12.5 mm (smaller) versus a follicle $\geq$ 12.5 mm (larger) in diameter, embryo quality grade and the probability of recovering a fertilized embryo

seven days after FTAI were decreased (Atkins et al., 2013). RNA-sequencing of pools of four oocytes or associated cumulus cells recovered ~23 hours after administration of gonadotropin releasing hormone (GnRH) to stimulate the pre-ovulatory gonadotropin surge in smaller (≤ 11.7 mm) versus larger (≥ 12.7 mm) pre-ovulatory suggested decreased metabolic capacity of cumulus cells from smaller pre-ovulatory follicles (Moorey et al., 2021).

Cumulus cells possess high glycolytic activity and are responsible for producing and transporting metabolites such as pyruvate, lactate, NADH, and FADH2 to the oocyte via gap junctions (Winterhager and Kidder, 2015). These metabolites are then utilized as substrates or electron carriers to maintain production of adenosine triphosphate (ATP) via oxidative phosphorylation in the maturing oocyte and pre-blastocyst stage embryo (Babayev and Seli, 2015; Coticchio et al., 2015; Brown et al., 2017). The oocyte and early embryo rely on stores of pyruvate, ATP, and other metabolites to support the metabolic requirements of oocyte maturation, fertilization, and sustained development through the blastocyst stage (Biggers et al., 1967; Cetica et al., 2002; Johnson et al., 2007; Chappel, 2013). During the antral stages of follicle development, the follicular fluid provides many of the nutrients, metabolic compounds, and signaling molecules that are essential for the accumulation of stockpiles of metabolic substrates within the oocyte (Winterhager and Kidder, 2015; Read et al., 2018). Follicular fluid, which is derived from serum and the secretions of intrafollicular cells, both influences and is the result of varied metabolic activities within the follicular cells (Edwards, 1974; Gosden et al., 1988; Clarke et al., 2006; Kidder and Vanderhyden, 2010; Rodgers and Irving-Rodgers, 2010; Hennet and

Combelles, 2012). Therefore, exploration of the follicular fluid milieu provides insight into follicular cell function. The follicular fluid metabolome is dependent on the stage of antral follicle development, the developmental stage of the oocyte, and stage of the estrous cycle (Orsi et al., 2005a; Moreno et al., 2015). Follicular fluid metabolome profiles have been linked to fertility in multiple species, and multiple follicular fluid components have been identified as biomarkers of oocyte developmental competence (Sinclair et al., 2008; Bender et al., 2010; Kafi et al., 2017).

Though studies of the follicular fluid metabolome have been performed in humans and dairy cows, little focus has been placed on the impact of follicle diameter at GnRH administration to induce ovulation on the follicular fluid and resulting cellular functions of the granulosa cells or cumulus-oocyte complex in beef cows. Studies that investigate the relationship between pre-ovulatory follicle size and the follicular fluid milieu are essential to further understanding reduced oocyte developmental competence and subsequent fertility when beef cows are induced to ovulate a small pre-ovulatory follicle. We hypothesized that size of the pre-ovulatory follicle prior to the LH surge impacted the follicular fluid's metabolome and metabolic capacity of the cumulus-oocyte complex that contribute to reduced embryo cleavage and quality grade observed following induced ovulation of small pre-ovulatory follicles. Therefore, we designed a study with the objective to profile the metabolome of follicular fluid collected from pre-ovulatory follicles ~20 hours after GnRH administration to induce the pre-ovulatory gonadotropin surge and determine the correlation between pre-ovulatory follicle diameter at GnRH administration and follicular fluid metabolite concentrations. We utilized ultra-high - performance liquid

chromatography – high resolution mass spectrometry (UHPLC-HRMS) to identify metabolites within pre-ovulatory follicles of increasing size and determined metabolites with a significant correlation to follicle diameter.

Materials and Methods

Animal handling and synchronization of pre-ovulatory follicle development

All animal protocols and procedures were approved by the University of Tennessee Knoxville Institutional Animal Care and Use Committee. Development of pre-ovulatory follicles were synchronized in postpartum, suckled beef cattle (Angus; n=130) according to procedures outlined in Figure 1. Estrous cycles were pre-synchronized by administration of gonadotropin-releasing hormone (GnRH; i.m.; 100 μg; Cystorelin; Boehringer Ingelheim; Ingelheim am Rhein, Germany) and placement of a controlled internal drug release (CIDR; intravaginal; 1.38 g progesterone; Eazi-Breed CIDR®; Zoetis Animal Health, Kalamazoo, MI, USA). After seven days, the CIDR was removed and cows were administered prostaglandin F2α (PGF; i.m.; 25mg; Lutalyse ® HighCon; Zoetis Animal Health, Kalamazoo, MI, USA). Approximately 66 hours later, cows were administered a second dosage of GnRH (i.m.; 100 μg; Cystorelin). Cows were then divided into 3 groups to facilitate transvaginal aspiration with 42-44 cows per group.

Eight to ten days after pre-synchronization, cows were administered GnRH (GnRH1; i.m.; 100 μg; Cystorelin) on day -9 to start a new follicular wave. On day -2, PGF (i.m.; 25mg Lutalyse ® HighCon) was administered to lyse corpora lutea. On day 0, cows received a second dosage of GnRH (GnRH2; i.m.; 100 μg; Cystorelin) to induce a pre-ovulatory gonadotropin surge.

Estrous detection patches (Estrotect®; Rockway Inc; Spring Valley, WI, USA) were placed on all cows at the time of PGF administration during pre-synchronization and on day -9. Patches were visually assessed 66 hours after pre-synchronization PGF administration to determine estrous expression during pre-synchronization and on days -2 and 0 of synchronization to detect any animals that displayed estrus between GnRH1 and PGF (removed from study because of failed synchronization, n=0) or between PGF and GnRH2 (endogenous gonadotropin surge, not included in study, n=2). Patches were scored on a scale of 0-4 with 0 being missing, and 1-4 equating to <25% rubbed (patch=1), 25-50% rubbed (patch=2), 50-75% rubbed (patch=3), and >75% rubbed (patch=4). Estrous expression was recorded if patch score equaled 3 or 4.

On days -9, -2, 0, and 1, ovaries of all cattle were examined by an experienced technician using trans-rectal ultrasonography with a Samsung HM70A ultrasound and CF4-9 convex probe. All follicles > 7 mm in diameter and all corpora lutea were recorded. Follicle size was calculated for all recorded follicles by averaging the measures of the largest diameter and the diameter perpendicular to it. Body weights of all animals were collected and body condition score [Whitman, 1975; scale of 1, emaciated-9, obese] was assigned on day -9.

Transvaginal aspiration for collection of follicular fluid from the pre-ovulatory follicle

On day 1, approximately 20 hours after GnRH2 administration, each cow's largest follicle underwent transvaginal aspiration by 1 of 4 experienced technicians to collect the

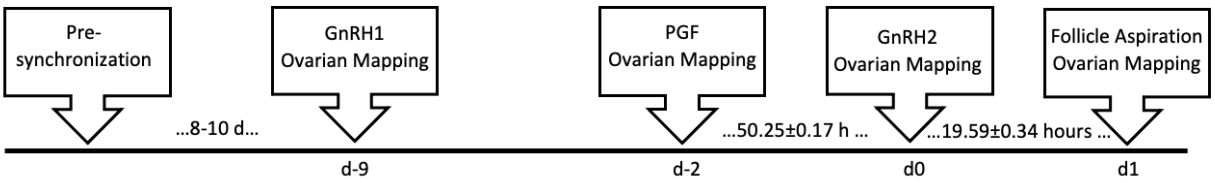

Figure 1. Timeline for synchronization of pre-ovulatory follicle development. GnRH1, gonadotropin releasing hormone administration to turn over a new follicular wave at the onset of synchronization; PGF, prostaglandin F2α; GnRH2, gonadotropin releasing hormone administration to induce the pre-ovulatory gonadotropin surge

pre-ovulatory follicle contents (Rispoli et al., 2020). Prior to aspiration, all cows received a spinal block via administration of lidocaine (2% lidocaine, 5ml). The perineal area of each cow was then cleaned of all contaminants and an ultrasound guided aspiration device attached to a Samsung HM70A ultrasound and CF4-9 convex probe was inserted into the anterior vagina. The ultrasound device consisted of an 18-gauge needle and a series of tubing to facilitate removal of follicular contents. The ovary containing the pre-ovulatory follicle was located and positioned for follicle aspiration before the needle was gently pushed through the vaginal wall and guided through the ovarian cortex into the antrum of the pre-ovulatory follicle. Follicular fluid was withdrawn into a clean 12 ml syringe before the syringe was removed, replaced, and the follicle lavaged with PVA TL-HEPES media multiple times to collect remaining follicular cells.

Follicular fluid processing

Follicular fluid was deposited into a 4-well petri plate and searched to find the cumulus-oocyte-complex which was removed and snap frozen for a subsequent study. The follicular fluid was then collected into 1.7ml tubes and centrifuged at 4^{o}C for 5 minutes at 500 x g to remove the remaining cellular debris. The follicular fluid supernatant was distributed amongst 2 ml cryovials and snap frozen in liquid nitrogen for storage at -80 ^{o}C until further processing.

UHPLC-HRMS metabolomics

Forty-three follicular fluid samples were selected for metabolomics processing. Follicular fluid samples were thawed on ice, and 60µl aliquots of each sample were placed

into individual 2 ml tubes. Each sample was analyzed by ultra-high performance liquid chromatography – high resolution mass spectrometry (UHPLC-HRMS) at the University of Tennessee Biological and Small Molecule Mass Spectrometry Core (RRID: SCR_021368). Briefly, metabolites were extracted from the follicular fluid using a 20:40:40 water/methanol/acetonitrile solution with 0.1M formic acid (Lu et al., 2010; Greene et al., 2020). The metabolomes of each sample were separated on a Synergy Hydro RP (2.5 µm, 100 mm x 2.0 mm column; Phenomenex, Torrance, CA) at 25 °C. The solvents for the elution were: phase A: 97:3 methanol/water with 11 mM tributylamine and 15 mM acetic acid and phase B: 100% methanol. The solvent gradient from 0 to 5 min was 100% A: 0% B, from 5 to 13 min was 80% A: 20% B, from 13 to 15.5 min was 45% A: 55% B, from 15.5 to19 min was 5% A: 95% B, and from 19 to 25 min was 100% A: 0% B with a flow rate of 200 μL/min. Detection of the metabolome components was accomplished using an Exactive Plus Orbitrap mass spectrometer (Thermo Fisher Scientific, Waltham, MA) fitted with an electrospray ionization (ESI) probe operated in negative mode. The scan range was 72-1000 *m/z*, the resolution was set to 140,000, and the acquisition gain control target to 3e6.

Primary data analysis

Files were generated by the HRMS in the Xcalibur (RAW) format and were converted to the open-source mzML format (Martens et al., 2011) via the open-source msconvert software, which is part of the ProteoWizard package (Chambers et al., 2012). MAVEN (mzroll) software, Princeton University (Melamud et al., 2010; Clasquin et al., 2012), which uses a grouping algorithm for non-linear retention time alignment, was used

to pick peaks, integrate intensities, and visualize the data and extracted ion chromatograms. Pre-processed data from MAVEN was used to conduct all further biological and statistical analyses.

Statistical analyses

All analytical procedures were performed using R software (R Core Team, 2020), and the code is available online (https://github.com/CaseyRead/Read_etal_2021_metabolome). Analysis of variance was used to determine any effects of cow age and BCS on pre-ovulatory follicle diameter at GnRH administration to induce the pre-ovulatory gonadotropin surge (GnRH2), and a linear model was used to determine any effects of cow weight, days postpartum at aspiration, days between PGF and GnRH2, and hours between GnRH2 and aspiration on pre-ovulatory follicle diameter at GnRH2.

A heatmap was constructed to visualize differences in metabolite peak area among metabolites and follicle diameters. Data for each metabolite was tested for normality by performing a Shapiro Wilk test and by plotting the residuals for visual evaluation of normality. Each metabolite was determined to have an approximately normal distribution. A linear model was used to determine the relationship between pre-ovulatory follicle size and follicular fluid metabolite peak area values in the 38 metabolites identified in our samples. Metabolites were considered significantly correlated to pre-ovulatory follicle diameter at GnRH2 administration if FDR < 0.05 was observed. Metaboanalyst 5.0 (Pang et al., 2021) was used to perform KEGG pathway enrichment analysis of the 18 metabolites that were significantly correlated to follicle diameter at GnRH2. Enrichment of pathways was determined to be significant if the FDR was < 0.05.

Results and Discussion

Animal Data

We utilized follicular fluid that was collected from the pre-ovulatory follicle of 43 lactating beef cows for this study. Follicle size at GnRH administration to induce the pre-ovulatory gonadotropin surge ranged from 9.2-17.7 mm (12.62 $\pm$ 0.28 mm). This measure is consistent with pre-ovulatory follicle diameters observed in multiple studies across varied locations and beef breeds (Geary et al., 2001; Lamb et al., 2001; Perry et al., 2005; MacNeil et al., 2006; Atkins et al., 2013; Moorey et al., 2021). To examine the influence of cow phenotype or study timeline on follicle diameter, we utilized analysis of variance or linear regression to quantify relationships between cow descriptive characteristics or study timeline and pre-ovulatory follicle size at GnRH2 administration. There was no relationship between pre-ovulatory follicle diameter at GnRH2 administration and cow age (p=0.93), body condition score (BCS; scale of 1 to 9 in which 1 = emaciated and 9 = obese; p=0.84), weight (p=0.54), days postpartum at aspiration (p=0.51), hours between prostaglandin F2α (PGF) and GnRH2 administration (p=0.72), or hours between GnRH2 administration and pre-ovulatory follicle aspiration (p=0.44; Figure 2).

Average cow age (5.75±0.34 years) was consistent with previous reports of mean beef cow longevity of approximately four to eight years, depending on production and geographical location (Cushman et al., 2013; Damiran et al., 2018). Average body condition score (6.02±0.26) and weight (623.3±17.1 kg) of animals included in this study were as expected in beef cattle operations; however, the upper BCS range in our cohort extended to beyond the BCS range commonly observed in beef production scenarios

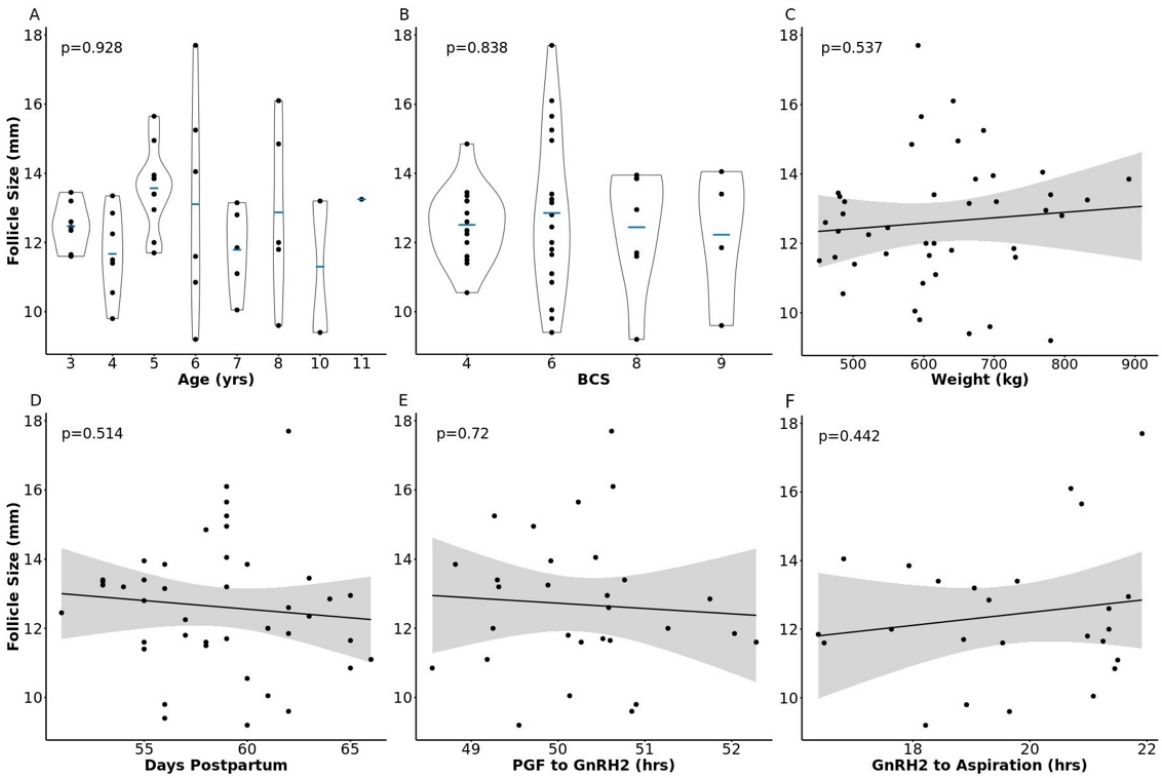

Figure 2. Relationship between pre-ovulatory follicle diameter and cow phenotype or timeline parameters. Panels A-F depict the relationship between follicle size at gonadotropin releasing hormone administration to induce a pre-ovulatory gonadotropin surge (GnRH2) and cow age, body condition score (BCS), weight, days postpartum, hours from prostaglandin F2α administration (PGF) to GnRH2 administration, and hours from GnRH2 administration to follicle aspiration, respectively.

(Bonacker et al., 2020). Cows were 58.7±0.56 days postpartum at the time of follicle aspiration. Though 62.9±2.1 days was reported as the mean postpartum anestrous period of Angus-sired cows (Cushman et al., 2007), all animals in the current study were exposed to a seven-day progestin treatment (Eazi-Breed CIDR®) during pre-synchronization procedures. The majority (84%) of the animals in this study had a corpus luteum present on the ovaries at the onset of synchronization, and 47% had displayed estrus by 66 hours post PGF administration and CIDR removal in the pre-synchronization protocol. Neither parameter influenced pre-ovulatory follicle diameter at GnRH2 administration (p=0.23 and p=0.53, respectively). Time between PGF and GnRH2 administration (50.25±0.17 hours) or between GnRH2 administration and aspiration (19.59±0.34 hours) were similar to previous studies by our lab and collaborators that determined the impact of pre-ovulatory follicle diameter on beef cow pregnancy rates and cumulus-oocyte complex transcriptome profiles, respectively (Perry et al., 2005; Moorey et al., 2021). Samples collected at this timepoint represent intrafollicular conditions post gonadotropin surge (Komar et al., 2001), when somatic follicular cells have begun luteinization, cumulus cells have expanded, and the oocyte's nuclear maturation has progressed through metaphase one (MI) and has reached or is nearing metaphase two (MII; Hyttel et al., 1986; de Loos et al., 1991; Hyttel et al., 1997; Richards et al., 1998). The metabolome of follicular fluid collected at this timepoint should reveal critical cellular processes taking place in the granulosa cells and cumulus-oocyte complex during the final stages of oocyte maturation, while highlighting potential processes that are altered when smaller pre-ovulatory follicles are prematurely exposed to a pharmacologically-induced gonadotropin surge.

Metabolome profiles of follicular fluid collected from pre-ovulatory follicles of lactating beef cows

To our knowledge, this is the first study that investigates size-related differences within the follicular fluid metabolome of pre-ovulatory follicles in beef cattle during the peri-ovulatory period of follicular development. The follicular fluid is primarily derived from the circulation and its composition is influenced by both the serum and products excreted by the intrafollicular cells (Fahiminiya and Gérard, 2010a), and the abundance of many metabolic substrates present in the follicular fluid is closely correlated to metabolic activity of the follicular cells (Sinclair et al., 2008). Thirty-eight metabolites were identified in the follicular fluid of bovine pre-ovulatory follicles following UHPLC-HRMS and metabolite identification with metabolic analysis visualization engine (MAVEN; Figure 3). Metabolites identified in the follicular fluid were predominantly amino acids and their derivatives. We also identified a number of glucose derivatives and tricarboxylic acid (TCA) cycle intermediates or derivatives as well as fatty acids, the steroid ester cholesterol sulfate and the nucleoside uridine. The majority of the metabolites identified in this study have been previously identified in the follicular fluid of cattle, humans, pigs, sheep, or horses (Chang et al., 1976; Grimek et al., 1984; Gérard et al., 2002; Orsi et al., 2005b; Nandi et al., 2007; Piñero-Sagredo et al., 2010; Tabatabaei et al., 2011; Bertoldo et al., 2013; Xia et al., 2014; Nagy et al., 2015; Zhao et al., 2015; Forde et al., 2016b; Jóźwik et al., 2017; Blaschka et al., 2018; Guo et al., 2018; Bernabé et al., 2019; Song et al., 2019a; Song et al., 2019b; Bódis et al., 2020; Luti et al., 2020; Hou et al., 2021; Mo et al., 2021; Zhang et al., 2021). To our knowledge, the metabolites N-acetyl-beta-alanine, *O*-acetyl-L-

serine, 2-oxo-4-methylthiobutanoate, 3-methylphenylacetic acid, phenyllactic acid, N-acetylornithine, tricarbalylic acid, 2-dehydro-D-gluconate, and D-gluconate are more novel components of the mammalian follicular fluid metabolome.

The impact of increasing pre-ovulatory follicle diameter on the follicular fluid metabolome

Levels of eighteen metabolites within the follicular fluid 19.59±0.34 hours after GnRH2 were impacted by pre-ovulatory follicle diameter at GnRH2 administration. To this end, as follicle size at the time of GnRH2 administration increased, so did the concentration of each of the 18 metabolites (false discovery rate (FDR) < 0.05; Figure 4). Pathway analysis of metabolites present 19.59±0.34 hour after GnRH2 that were significantly correlated with follicle diameter at GnRH2 identified the enrichment of multiple Kyoto Encyclopedia of Genes and Genomes (KEGG) pathways including 'alanine, aspartate and glutamate metabolism' (FDR=0.009), 'arginine biosynthesis' (FDR=0.011), 'aminoacyl-tRNA biosynthesis' (FDR=0.019), and 'D-glutamine and D- glutamate metabolism' (FDR=0.020; Table 1). Significantly enriched pathways and literature review of all metabolites whose abundance was correlated with pre-ovulatory follicle diameter highlighted key processes related to metabolism, transcription, and translation. Follicular fluid pyruvate concentration significantly increased with increasing follicle diameter at GnRH2 administration (FDR=0.032; Figure 4J). The intrafollicular cumulus cells that envelop the oocyte have a high capacity to convert glucose to pyruvate via glycolysis, and glucose consumption by cumulus cells increases during the first 18 hours of oocyte maturation (Rieger and Loskutoff, 1994; Sutton-McDowall et al., 2004; Harris et al., 2007; Thompson,

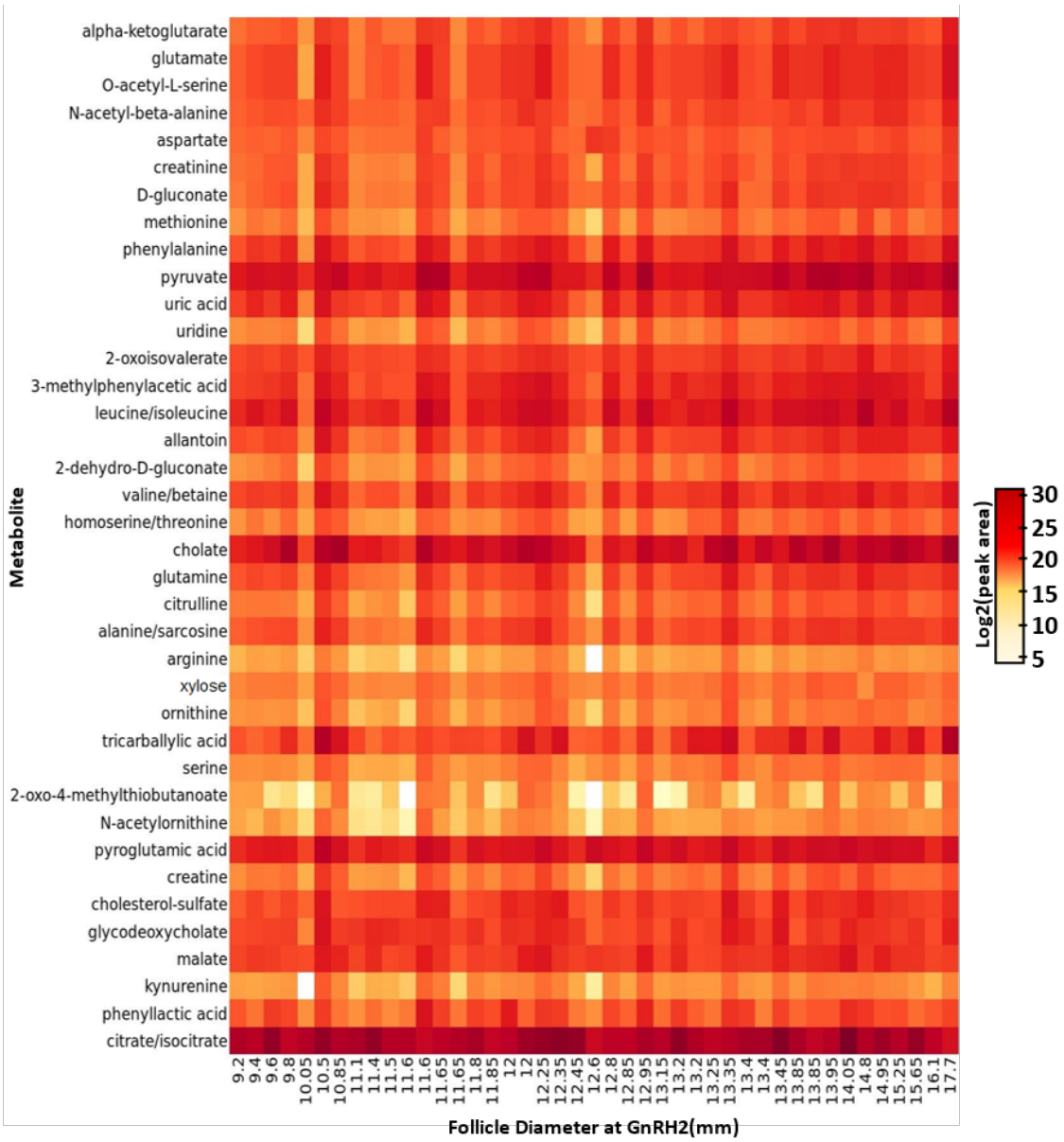

Figure 3. Heatmap of 38 metabolites detected in pre-ovulatory follicular fluid. Metabolites are listed as row titles and the pre-ovulatory follicle diameter at the time of gonadotropin releasing hormone administration to induce a pre-ovulatory gonadotropin surge (GnRH2) corresponding to each follicular fluid sample is listed under each column. Log2(peak area) of each metabolite within each sample is designated by increasing color intensity. The color intensity scale depicts differences in peak area across all metabolites and demonstrates metabolites present in higher (darker color) and lower (lighter color) concentration in the follicular fluid.

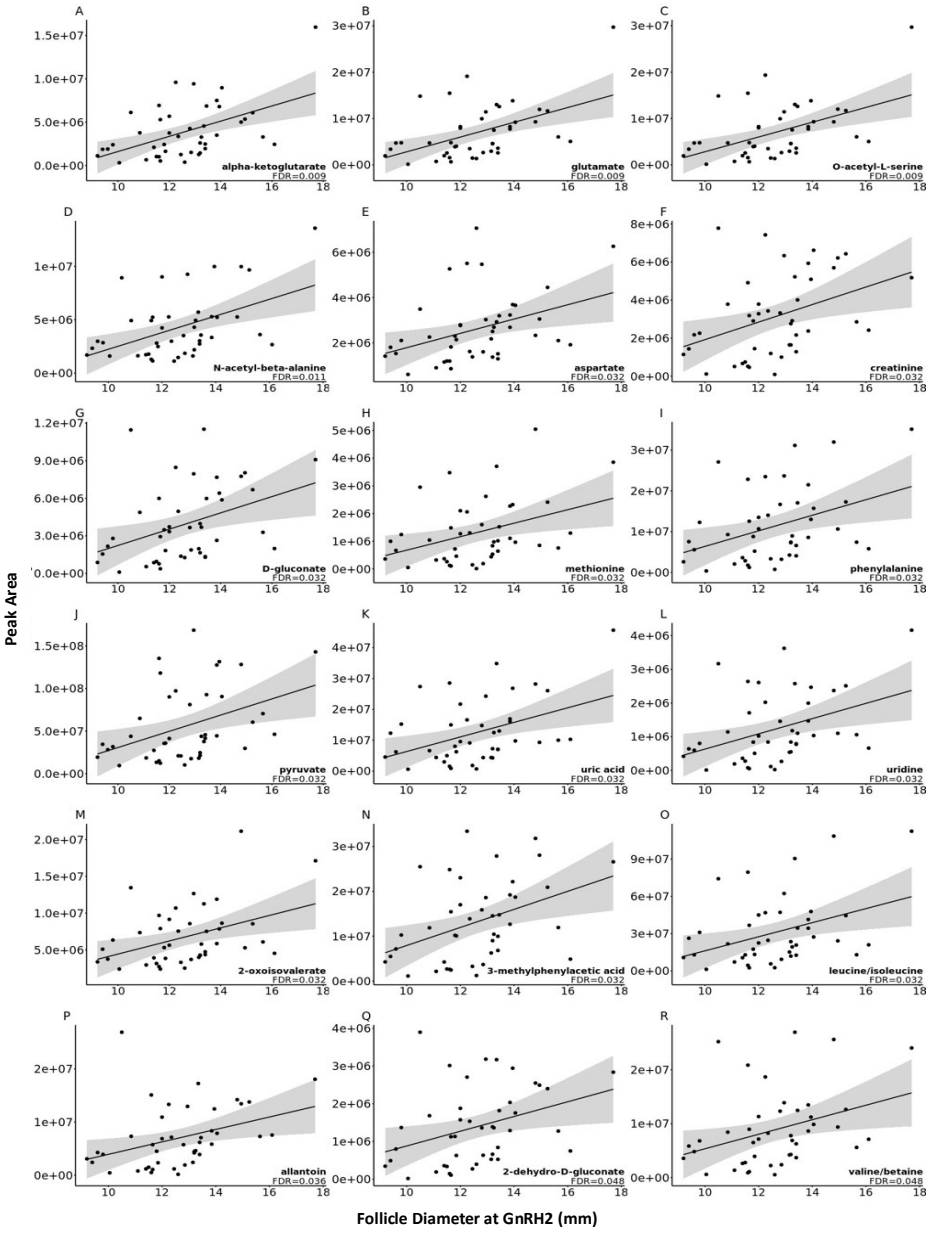

Figure 4. Scatter plots of the correlation between metabolite peak area and follicle diameter at the time of gonadotropin releasing hormone (GnRH2) administration to induce the pre-ovulatory gonadotropin surge for 18 metabolites that were significantly correlated with increasing follicle diameter at GnRH2 (FDR<0.05).

2014). We recently discovered that cumulus cells from small pre-ovulatory follicles had reduced transcript abundance for hexokinase and phosphofructokinase enzymes, which suggests decreased glycolytic capacity for pyruvate production in the cumulus cells of smaller pre-ovulatory follicles (Moorey et al., 2021). Cumulus cell-produced pyruvate was effectively transferred to both the enclosed oocyte and surrounding medium during *in vitro* studies, with increased pyruvate concentration detected in the medium as maturation progressed (Uhde et al., 2018b).

Therefore, it is logical that increased concentration of follicular fluid pyruvate in the current study may be the result of increased pyruvate production by the cumulus cells of larger follicles. The oocyte has a poor capacity to metabolize glucose and relies on pyruvate transferred from the cumulus cells and surrounding follicular environment to drive oxidative phosphorylation and ATP production for energy demanding processes of maturation, fertilization, cleavage, and early embryonic development (Biggers et al., 1967; Cetica et al., 2002; Warzych and Lipinska, 2020).

Interestingly, D-Gluconate, and 2-Dehydro-D-gluconate concentration were increased in the follicular fluid of larger follicles (FDR<0.05; Figure 4G, 4Q, respectively). Gluconate is an alternate carbon source for pyruvate production that can also be converted to 2-Dehydro-D-gluconate. Increased concentrations of D-Gluconate and 2-Dehydro-D-gluconate suggest reduced utilization of gluconate for cumulus cell metabolism in larger pre-ovulatory follicles.

The KEGG pathways 'D-glutamine and D-glutamate metabolism' and 'alanine, aspartate, and glutamate metabolism' were significantly enriched with follicular fluid

Table 1. KEGG pathways significantly enriched with metabolites that were significantly correlated with increasing pre-ovulatory follicle diameter.

Pathway	**Pathway Name**	**Match Status[1]**	**FDR[2]**	**Differentially Abundant Metabolites in Pathway[3]**
bta00250	alanine, aspartate and glutamate metabolism	4/28	0.009	Alpha-Ketoglutarate (C00026) Aspartate (C00049) Glutamate (C00025) Pyruvate (C00022)
bta00220	arginine biosynthesis	3/14	0.011	Alpha-Ketoglutarate (C00026) Aspartate (C00049) Glutamate (C00025)
bta00970	aminoacyl-tRNA biosynthesis	4/48	0.019	Aspartate (C00049) Glutamate (C00025) Methionine (C00073) Phenylalanine (C00079)
bta00471	D-glutamine and D-glutamate metabolism	2/5	0.020	Alpha-Ketoglutarate (C00026) Glutamate (C00025)

[1] Number of differentially abundant metabolites in pathway/total number of metabolites in pathway

[2] FDR = False Discovery Rate

[3] Displayed as Name (KEGG identifier number); KEGG = Kyoto Encyclopedia of Genes and Genomes

metabolites whose abundance increased with increasing pre-ovulatory follicle size (FDR<0.03; Table 1). Pathway metabolites alpha-ketoglutarate, glutamate, and aspartate concentrations were increased in the follicular fluid of larger pre-ovulatory follicles (FDR < 0.05; Figure 4A, 4B, 3E, respectively). While the proportion of follicular fluid aspartate concentration compared to total amino acid concentration was higher in 6-8 mm bovine follicles that encased a cumulus-oocyte complex of improved morphology grade, there was no relationship between follicular fluid aspartate concentration and successful cleavage or development to the blastocyst stage (Sinclair et al., 2008). In humans, however, increased follicular fluid concentration of D-aspartate was associated with improved oocyte morphology and increased fertilization rates (D'Aniello et al., 2007). Previous studies in cattle have demonstrated the importance of follicular fluid glutamine and glutamate for oocyte energy production and developmental competence. Bovine cumulus-oocyte complexes possess the ability to metabolize glutamine by the enzyme glutaminase (Bilodeau-Goeseels, 2006), and we detected mRNA expression for glutaminase in bovine cumulus cells collected from pre-ovulatory follicles of similar stage and size to the current study (Moorey et al., 2021). In cattle, when oocytes collected from follicles 6-8 mm in size were submitted to *in vitro* embryo production, cumulus-oocyte complex morphological quality grade improved as the proportion of follicular fluid glutamate increased. Additionally, follicular fluid glutamate levels were higher when fertilized oocytes successfully cleaved and developed to the blastocyst stage versus failed to cleave (Sinclair et al., 2008).

Addition of glutamine, pyruvate, and glucose to maturation media increased oocyte nuclear maturation in cattle. Compared to M16 salts media, the addition of glutamine to media significantly increased the percentage of cumulus-enclosed oocytes reaching MII, whereas the addition of glucose, pyruvate, or lactate reduced the percentage of cumulus-enclosed oocytes remaining in the germinal vesicle stage and increased the percentage progressing to MI after 21 hours of culture (Bilodeau-Goeseels, 2006). Interestingly, the metabolism of glucose and glutamine was impacted by maturation timepoint during *in vitro* bovine oocyte maturation, with glucose and glutamine metabolism in cumulus-oocyte complexes at their highest at 18 hours of maturation (Rieger and Loskutoff, 1994). This timepoint is similar to the stage at which samples were collected for the current study and highlights the importance of glucose and glutamine metabolism for energy production during the latter stages of oocyte nuclear maturation.

Increased concentration of alpha-ketoglutarate, glutamate, and aspartate in follicular fluid of larger follicles may be due to increased metabolic activity of the TCA cycle and active transport of these metabolites to the oocyte or follicular fluid. Alpha-ketoglutarate and oxaloacetate are TCA cycle intermediates that can be interconverted with amino acids glutamate and aspartate, respectively (Rathod and Fellman, 1985; Liu et al., 2018). Cumulus cells actively transfer glutamate to the oocyte (Colonna and Mangia, 1983), and increased levels of cumulus cell derived alpha-ketoglutarate, glutamate, and aspartate from the TCA cycle could realistically also be transported to the surrounding follicular fluid.

As pyruvate is produced, converted to acetyl CoA, and the TCA cycle is utilized, ATP, NADH, and FADH2 are produced. These metabolic products are critical for oxidative phosphorylation, which is the primary energetic pathway in the oocyte (Thompson et al., 2007). Increased concentration of pyruvate, D-gluconate, alpha-ketoglutarate, glutamate, and aspartate in the follicular fluid of larger pre-ovulatory follicles lead us to conclude that aberrant glucose metabolism likely exists in the cumulus cells of smaller pre-ovulatory follicles (Figure 5). Reduced glucose metabolism in smaller follicles would lead to a reduction of energetically important stores of ATP, pyruvate, or metabolic intermediates in the oocyte. Decreased metabolic capacity in the cumulus cells of smaller pre-ovulatory follicles would support previous observations of reduced probability of recovering a high quality or cleaved embryo (reported as fertilization success) when cattle are induced to ovulate a smaller pre-ovulatory follicle < 12.5 mm (Atkins et al., 2013).

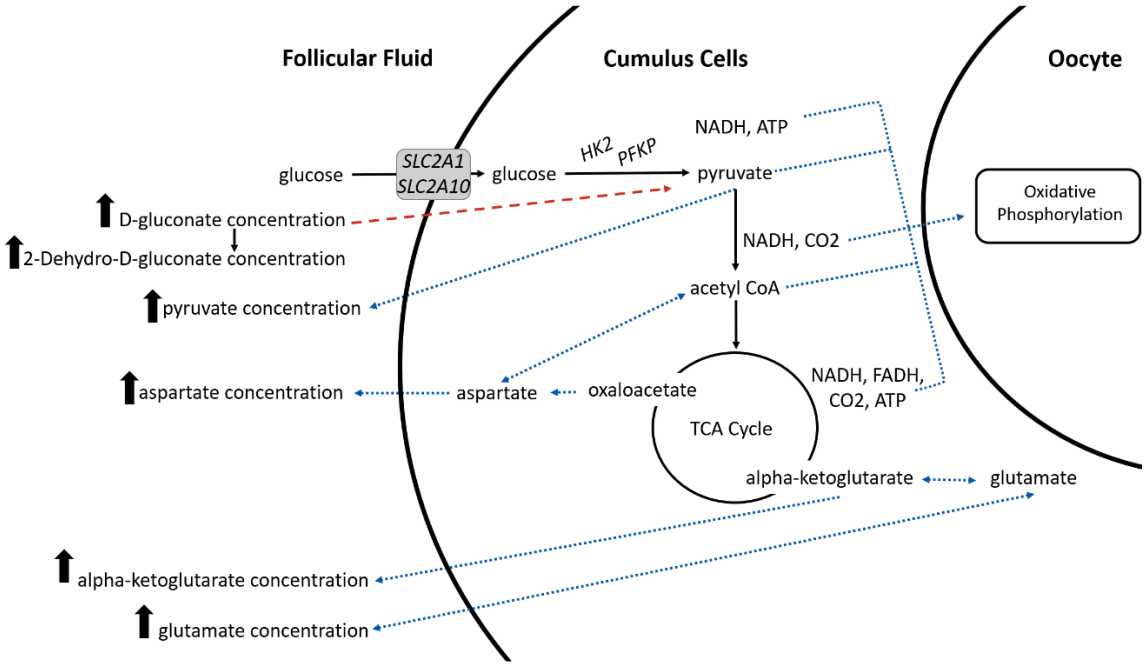

Figure 5. Proposed model of altered glucose metabolism in cumulus cells of smaller pre-ovulatory follicles. Increased concentration of pyruvate, aspartate, alpha-ketoglutarate, and D-glutamate in the follicular fluid of larger pre-ovulatory follicles is likely the result of increased glucose consumption by the cumulus cells and more efficient glucose, pyruvate, and tricarboxylic acid (TCA) cycle metabolism in the cumulus cells of larger follicles (represented by solid black arrows). Our previous results of increased transcript abundance for glucose transporters (*SLC2A1, SLC2A10*) and glycolytic enzymes (*HK2, PFKP*) in cumulus cells of large versus small pre-ovulatory follicles support the proposed model. Increased production of pyruvate and downstream metabolic products allows increased metabolite abundances to be transferred back into the follicular fluid and to the oocyte to support energy production needed for oocyte maturation, fertilization, cleavage, and early embryo development (represented by blue dotted arrows). Increased concentration of D-gluconate and its downstream product 2-Dehydro-D-gluconate in the follicular fluid of larger follicles is likely due to reduced import of D-gluconate into the cumulus cells (represented by dashed red arrow) because of preferential import of glucose.

The KEGG pathway ‘arginine biosynthesis’ was also enriched with follicular fluid metabolites whose abundance increased as follicle diameter at GnRH2 administration increased (FDR=0.011; Table 1). Increased concentrations of alpha-ketoglutarate, glutamate, and aspartate are consistent with increased glucose metabolism and production of the TCA cycle intermediates or their derivatives (discussed above). Glutamate and aspartate also eventually promote arginine biosynthesis by entering the urea cycle and undergoing conversions that produce the amino acid arginine. Arginine itself was lowly detected in pre-ovulatory follicular fluid samples of the current study, and arginine concentration was not influenced by follicle diameter (Figure 3; FDR=0.12). Therefore, we do not hypothesize a biologically relevant impact of enrichment of the ‘arginine biosynthesis’ pathway beyond its relationship to the TCA cycle and improved metabolism in the cumulus cells of larger pre-ovulatory follicles.

The importance of follicular fluid amino acids for oocyte developmental competency expands beyond metabolic support. Amino acids are also important for proteinogenesis, and during maturation, oocytes and cumulus cells undergo morphological changes that involve increased protein synthesis (Edson et al., 2009). Enrichment of amino acids in the pathway ‘aminoacyl-tRNA biosynthesis’ (FDR=0.019; Table 1) indicates that these amino acids are more readily available to be incorporated into protein. Within the follicle and cumulus-oocyte-complex, there are many important signaling molecules, receptors, and enzymes that are made up of amino acids (Revelli et al., 2009). Deficits in the availability of key amino acids could impact the formation of these molecules and subsequently alter signaling and metabolic pathways as well as developmental events.

Essential amino acids phenylalanine, methionine, leucine/isoleucine, and potentially valine as well as the nonessential amino acids glutamate and aspartate increase as follicle diameter increases. In the bovine, increased total amino acid concentration within the follicular fluid of 6-8 mm follicles was associated with increased oocyte cleavage and development to the blastocyst stage (Sinclair et al., 2008). *In vitro,* supplementation of cumulus-oocyte-complexes with amino acids supports the acquisition of oocyte developmental competence, and cumulus-oocyte complex utilization and/or excretion of amino acids has been demonstrated to increase during maturation (Uhde et al., 2018c). We hypothesize that increased availability of amino acids in the follicular fluid of larger follicles leads to greater capacity for proteinogenesis and improved developmental competence.

On the contrary, an *in vitro* study of bovine cumulus-oocyte complexes collected from 6-8 mm follicles, demonstrated that increased proportion of the follicular fluid amino acids histidine, leucine, isoleucine, lysine, methionine, phenylalanine, proline, tyrosine, and valine was negatively associated with cumulus-oocyte-complex morphological assessment and/or oocyte competency for cleavage and/or blastocyst development. In the current study, we detected the presence of methionine, phenylalanine, leucine/isoleucine, and valine/betaine in pre-ovulatory follicular fluid (Figure 3). There was, however, a significant, positive relationship between follicle diameter at GnRH2 administration and the concentration of each amino acid (FDR<0.05; Figure 4H, 4I, 4O, 4R, respectively). Though we did not measure oocyte developmental competency in the current study, oocytes from pre-ovulatory follicles $\geq$ 12.5 mm were previously determined to exhibit increased capacity for ferilization and the formation of a high-quality embryo compared to

oocytes from follicles < 12.5 mm (Atkins et al., 2013). We cannot fully explain the discrepancy between our results and that of the *in vitro* study, but the variation of follicular fluid source and follicle size/stage of development between the two experiments were likely contributors.

Not only do amino acids make up the peptide subunits that are used to form proteins, but they also play a role in DNA methylation and initiation of mRNA synthesis. During oocyte development, it is acquiring stockpiles of RNA transcripts and changes in DNA methylation regulate which genes are being actively transcribed. Additionally, during maturation, the chromatin within the oocyte condenses to facilitate the resumption of meiosis (Sendžikaitė and Kelsey, 2019). Methionine plays a key role in DNA methylation by forming S-adenosyl methionine (SAM; Zhang, 2018; Sendžikaitė and Kelsey, 2019). This molecule plays a key role in the methylation of CpG islands (Sendžikaitė and Kelsey, 2019). Multiple dietary studies have reported that increased methionine intake results in increased SAM and hypermethylation (Zhang, 2018). The increased methionine present in the follicular fluid of larger follicles (FDR=0.032; Figure 4H) could be indicative of increased DNA methylation within the oocytes of larger follicles.

In addition to its contributions to metabolism and proteinogenesis of follicular cells, the follicular fluid also provides an oxidatively balanced environment for the somatic follicular cells and oocyte. Alpha-ketoglutarate acts as an antioxidant agent, and uric acid is a scavenger of free radicals that is primarily oxidized to allantoin (Kand'ár et al., 2006; Liu et al., 2018). Alpha-ketoglutarate, uric acid, and allantoin were significantly increased in the follicular fluid of larger pre-ovulatory follicles (FDR<0.04; Figure 4A, 4K and 4P,

respectively). Such results suggest increased capacity for reduction-oxidation reactions in the follicular fluid, however we cannot speculate if such phenomena lead to improved oocyte developmental competence in larger follicles. Increased concentration of uric acid in the follicular fluid has been previously associated with increasing body mass index in women and poor cumulus-oocyte complex morphology in buffalo cows, indicating that elevated levels of uric acid may be the result of oxidative stress (Cassano et al., 1999; Bou Nemer et al., 2019). However, the follicular fluid of obese women also possessed higher levels of hormones related to glucose metabolism, and increased abundance of uric acid could be a combative response to potential oxidative stress due to increased metabolic activity of the follicular cells.

Conclusions

In conclusion, we identified a total of 38 metabolites in the follicular fluid of bovine pre-ovulatory follicles. Eighteen metabolites were positively related to increasing follicle diameter at the time of GnRH administration to induce the pre-ovulatory gonadotropin surge. Pathway and individual analysis of these metabolites revealed that pathways and substrates involved in glucose metabolism, energy production, and proteinogenesis are present in higher levels in the follicular fluid of larger follicles. The follicular fluid microenvironment plays a key role in oocyte acquisition of developmental competence by providing the cumulus-oocyte complex with nutrients and metabolic substrates. Decreased availability of metabolites and proteinogenic components to cumulus-oocyte-complexes from smaller pre-ovulatory follicles likely contributes to the reduced oocyte developmental

competence and lower pregnancy rates observed when beef cows are induced to ovulate a small pre-ovulatory follicle.

CHAPTER III
CONCURRENT MEASUREMENT OF MITOCHONDRIAL DNA COPY NUMBER AND ATP CONCENTRATION IN SINGLE BOVINE OOCYTES

A version of this chapter was originally published by Casey Read and Sarah Moorey: Casey C. Read, Sadikshya Bhandari, and Sarah E. Moorey. “Concurrent Measurement of Mitochondrial DNA Copy Number and ATP Concentration in Single Bovine Oocytes.” *Methods and Protocols* 4 (2021): 88-97.

Conceptualization, Sarah Moorey; Data curation, Casey Read, Sadikshya Bhandari, and Sarah Moorey; Formal Analysis, Investigation, Methodology, Software, and Visualization, Casey Read and Sarah Moorey; Project administration, resources, and supervision, Sarah Moorey, writing – original draft, review, and editing, Casey Read and Sarah Moorey, writing – editing, Sadikshya Bhandari.

Funding: This research was supported by the USDA NIFA Hatch project 1022068, the University of Tennessee AgResearch, and the University of Tennessee Department of Animal Science.

Acknowledgments: The authors would like to thank Liesel Schneider for her statistical analysis consulting, Lannett Edwards and Becca Payton for their contributions to planning of the experiment and for sharing information from ATP assays performed in the Edwards lab, Southeastern Provisions LLC for providing the ovaries used in this study, and Emma Hessock and Samantha Roberts for assisting with the collection of the samples used.

Abstract

To sustain energy-demanding developmental processes, the oocyte must accumulate adequate stores of metabolic substrates and mitochondrial numbers prior to the initiation of maturation. In order to obtain measures of the metabolic capacity of an oocyte, researchers would have to utilize pools of multiple oocytes. These measures would have decreased sensitivity due to being averages of the population. Further difficulty arises when researchers are limited in the number of oocytes they can collect due to increased cost, difficulty, or both. Incorporation of this protocol will allow researchers to get more information from a limited sample number as well as obtain intraoocyte values they can directly relate to each other. We developed and validated procedures to measure both mitochondrial DNA (mtDNA) copy number and ATP quantity in single oocytes.

Validation of our procedures revealed that we could successfully divide oocyte lysates into quarters and measure consistent results from each of the aliquots for both ATP and mtDNA copy number. Coefficient of variation between the values retrieved for mtDNA copy number and ATP quantity quadruplicates were 4.72±0.98 and 1.61±1.19, respectively. We then utilized our methodology to concurrently measure mtDNA copy number and ATP quantity in germinal vesicle (GV) and metaphase two (MII) stage oocytes. Our methods revealed a significant increase in ATP levels (GV=628.02199.53 pg, MII=1326.24±199.86 pg, $P < 0.001$) and mtDNA copy number (GV=490,799.4±544,745.9 copies, MII=1,087,126.9±902,202.8 copies, $p=0.035$) in MII compared to GV stage oocytes. This finding is consistent with published literature and provides further validation of the accuracy of our methods. The ability to produce consistent readings and expected results from aliquots of the lysate from a single oocyte reveals the sensitivity and feasibility of using this method.

Introduction

The accumulation of adequate stores of metabolic substrates as well as an increase in mitochondrial number within the oocyte are important components of the acquisition of developmental competence. Increases in mitochondrial number and the creation of metabolic substrate stockpiles within the oocyte occur throughout antral follicle development (Stojkovic et al., 2001; Chiaratti et al., 2010; Kidder and Vanderhyden, 2010; Iwata et al., 2011; Mao et al., 2012; Scantland et al., 2014; St John, 2014; Contreras-Solís et al., 2021; May-Panloup et al., 2021). The oocyte and early embryo have low levels of glycolytic activity and rely on mitochondrial oxidative phosphorylation to produce the ATP

necessary to sustain development to the blastocyst stage of embryo development (Biggers et al., 1967; Sutton-McDowall et al., 2010; Paczkowski et al., 2013; Dalbies-Tran et al., 2020). Substrates and co-factors such as pyruvate, acetyl CoA, NADH, CO_2, and FADH are produced from glycolytic activity of the cumulus cells and transferred to the oocyte via gap junctions to support oxidative phosphorylation (Sutton-McDowall et al., 2010; Winterhager and Kidder, 2015; Richani et al., 2021). This transfer of metabolic substrates occurs throughout antral stages of development until the onset of oocyte maturation leads to gap junction breakdown. The oocyte must support energy demanding developmental processes like fertilization and embryonic cell division with the mitochondria and metabolic substrates accumulated prior to oocyte maturation.

Previous studies have linked intraoocyte ATP levels, mtDNA copy number, and mitochondrial function to oocyte developmental competence (Dumollard et al., 2007; Van Blerkom, 2011; Roth, 2018; Hashimoto et al., 2019; Nagano, 2019; Payton et al., 2018). Within bovine oocytes, reported ATP concentrations range from 0.25 to 35 pmol and reported mtDNA levels range from 13,000 to 3,600,000 copies per oocyte. Due to low quantities of starting materials in single oocytes, many studies utilized pooled oocytes for analyses, and no papers have measured multiple metabolic parameters within a single oocyte. Single cell analysis is a valuable tool to better understand and evaluate intraoocyte relationships among metabolic components and mitochondria functionality. While pooling oocytes allows researchers to account for high variability in abattoir-derived oocytes, single oocyte analyses are necessary for *in vivo* studies where sample numbers are often limiting.

Therefore, we developed a protocol with the objective to divide the lysate of a single oocyte into quarters and measure ATP and mtDNA copy number in duplicate, quarter oocyte equivalents. After successful validation of the protocol for both ATP and mtDNA measurements, we performed a second study with the objective to compare ATP quantity and mtDNA copy number between germinal vesicle (GV) and metaphase two (MII) stage oocytes as an additional validation to demonstrate that the protocol would yield similar results to previously published studies of pooled oocytes.

Materials and Methods

Collection of cumulus-oocyte-complexes

Abattoir-sourced, mixed breed, bovine (Bos taurus) ovaries were obtained for the manual aspiration of follicles and collection of cumulus-oocyte-complexes (COCs). Briefly, COCs were manually aspirated from 3-8 mm follicles using a 12 mL syringe and 18-gauge needle. The aspirate was then transferred to a petri dish and searched for COCs. Once located, COCs were placed into oocyte collection media (OCM; M199 with Hanks' salts, 2% (v/v) FBS, 2 mmol/l L-glutamine, 50 U/ml penicillin, and 50 µg/ml streptomycin) until searching was completed. Only those COCs with a homogenous cytoplasm and at least 5 layers of cumulus cells were selected for further use. For the validation of procedures, selected COCs were stripped of their cumulus cells by vortexing for 3-5 minutes in 1x trypsin, washed through PBS, and immediately snap frozen in 2µl of PBS for storage at -80°C until used for assays. For the comparison of GV and MII stage oocytes, COCs were randomly divided and half (n=15) were collected at the GV stage as described above. The remaining COCs were washed in oocyte maturation media (OMM; M199 with

Earle's salts, 10% (v/v) FBS, 2 mmol/l L-glutamine, 0.2 mmol/l sodium pyruvate, and 50 mg/ml gentamycin) before undergoing maturation for 22-24 hours at 38.5°C in 5% CO_2 and humidified air. The matured COCs, which represent MII oocytes (n=15), were then collected, denuded, and stored in the same manner as the GV stage oocytes.

TaqMan Primer and Probe Design

Primers were designed using NCBI BLAST according to the bovine mitochondrial genome (Accession Number: NC_006853.1; Table 2). The selected primer pair created a 183 base pair product from base pairs 11569 to 11751 of the bovine mitochondrial genome. The probe sequence was located between the forward and reverse primers and ranged from base pairs 11621 to 11645. A gradient polymerase chain reaction (PCR) ranging from 50 to 60° C was performed to determine optimal annealing temperature ranges of the primers.

Validation

Oocyte Lysis and Division

Germinal vesicle stage oocytes were used to optimize and develop the protocol. Following optimization, we validated the protocol's ability to provide consistent values for ATP and mtDNA copy number assays in quarter oocyte equivalents. Tubes containing single oocytes were thawed and centrifuged at 12,000 x g for 30 seconds at 4°C. For ATP quantification (n = 5), 8µl 5 mM Tris-HCl was added to each sample and all samples were heated at 95°C for 10 minutes. Thirty microliters of nuclease free water were added to each sample to achieve a final volume of 40µl. This volume was then divided into four, 10µl aliquots for the ATP assay. For mtDNA copy number quantification (n = 6), 8µl Tris-HCl

were added to each sample and samples were heated at 95°C for 10 minutes. Twenty-six microliters of proteinase K (Zymo Research; Irvine, CA) were added to each sample to reach a final concentration of 200ug/ml. Samples were heated at 55°C for 30 minutes followed by heating at 95°C for 10 minutes for proteinase K deactivation. The lysate was then divided into four, 9µl aliquots for use in qPCR analysis of mitochondrial DNA copy number.

ATP Quantification Validation

Samples were processed using the ATP Determination Kit (Life Technologies; Carlsbad, CA) according to the manufacturer's directions. Each lysate was thoroughly mixed by pipetting, and 10µl was added to individual wells of a white, 96 well plate (Costar ®, 96 well, flat bottomed, white polystyrene assay plate, Corning Incorporated, Corning, NY) and combined with 90µl of assay mix. Luminescence was recorded using the Synergy H1 Microplate Reader (Biotek; Winooski, VT).

mtDNA Copy Number Quantification Validation

Samples were processed using custom TaqMan primers and probe (Table 2). Each lysate was mixed thoroughly by pipetting and 9µl was combined with 1µl of the custom TaqMan primer/probe mix and 10µl Fast Advanced Master Mix (ThermoFisher Scientific, Waltham, MA) in a MicroAmp® Fast 96-well Reaction Plate (0.1mL, ThermoFisher Scientific, Waltham, MA). The PCR settings were as follows: 2 minutes at 94°C followed by 40 cycles of 10 seconds at 94°C, 15 seconds at 57°C, and 12 seconds at 72°C (QuantStudio3, ThermoFisher Scientific, Waltham, MA).

Table 2. Relevant information for primers and probe designed to the bovine mitochondrial genome.

Name	Sequence	Product Length	Tm
mtDNA Primer Forward	CCTACAAACGCTCCTTCCAC	183	59
mtDNA Primer Reverse	AGAGAATATAGGGCGGTGATTACT	183	59
TaqMan Probe	TTGTTGGGGGTAGAGCTAAGTTGGT	---	64

Germinal Vesicle and Metaphase II Comparison

Oocyte Lysis and Division

Tubes containing single oocytes were centrifuged at 12,000 x g for 30 seconds at 4°C. Then, 8 µl 5 mM Tris – HCl was added to each sample and all samples were heated at 95°C for 10 minutes. Oocyte lysate was mixed thoroughly by pipetting and 5 µl of oocyte lysate was removed for ATP analysis (Figure 6). Thirteen microliters of proteinase K were added to the tubes with the remaining 5 µl of oocyte lysate to create a final concentration of 200 µg/ml proteinase K. Tubes containing oocyte lysate + proteinase K were heated at 55°C for 30 minutes. Proteinase K was deactivated by re-heating at 95°C for 10 minutes. After deactivation, the lysate was used for qPCR analysis of mitochondrial DNA copy number (Figure 6).

ATP Quantification

The initial 5 µl of oocyte lysate (collected before proteinase K addition) was diluted with nuclease free water to a total volume of 20 µl which was then divided into two, 10 µl aliquots to perform ATP quantification in duplicate (Figure 6). Standards were generated via dilution of the kit-included 5 mM ATP substrate (0.5 µM, 0.05 µM, 0.025 µM, 0.005 µM, 0.0025 µM). Samples and standards were processed using the ATP determination kit (Life Technologies; Carlsbad, CA) as described above. Luminescence values of standards were used to generate a standard curve. The standard curve was used to quantify ATP concentration in each one quarter oocyte equivalent based on the average value of the duplicates assayed for each sample. Oocyte ATP values were then converted to weight using the molarity calculator by GraphPad with the following settings: concentration =

micromolar, ATP formula weight = 507.18, volume = 10µl. The result was then multiplied by four because the 10µl samples used for the ATP concentration assay represented one fourth of an oocyte.

mtDNA Standard Preparation

A group of five oocytes with a homogenous cytoplasm and 3-5 layers of cumulus cells were denuded and snap frozen in 2 µl of PBS. They were then lysed as previously described. The oocyte lysate was then combined with 12.5 µl of Accustart II PCR SuperMix (2X; Quantabio, Beverly, MA), 0.5 µl of 5 µm forward primer, and 0.5 µl of 5 µm reverse primer (Table 2) for a final volume of 25 µl. Cycling conditions of 2 minutes at 94°C followed by 40 cycles of 10 seconds at 94°C, 15 seconds at 57°C, and 12 seconds at 72°C were used. The PCR product was further processed through electrophoresis on a 1.5% agarose gel. The resulting band was located at ~ 183 base pairs, indicating that it was the correct PCR product. The band was then excised from the gel, and the PCR product was purified from the gel using the Zymoclean™ Gel DNA Recovery kit (Zymo Research, Irvine, CA). DNA concentration of the final eluate was determined using the Qubit™ dsDNA High Sensitivity Assay Kit (ThermoFisher Scientific, Waltham, MA), and purity was determined using 260/280 ratios measured on a NanoDrop spectrophotometer. Number of mitochondrial DNA copies per microliter was calculated from the DNA concentration of the eluate and the molecular weight of the PCR product. The eluate was first diluted 1:1000 before being further diluted to create a standard curve ranging from 10 copies to 1,000,000 copies of the mitochondrial DNA segment per 9µl. The amplification

efficiency of the standard curve was calculated using the qPCR efficiency calculator from ThermoFisher.

mtDNA Copy Number Quantification

The 18 µl portion of oocyte lysate and inactivated proteinase K were divided into two, 9 µl aliquots and quantitative PCR (qPCR) was performed in duplicate using our custom TaqMan primers and probe (Table 2). The standards of known mtDNA copy number (described above) were included during each assay. Nine microliters of sample or standard was combined with 1µl of the custom TaqMan primer/probe mix and 10µl Fast Advanced Master Mix (ThermoFisher Scientific, Waltham, MA) in a MicroAmp® Fast 96-well Reaction Plate (0.1mL, ThermoFisher Scientific, Waltham, MA). The PCR settings were as follows: 2 minutes at 94°C followed by 40 cycles of 10 seconds at 94°C, 15 seconds at 57°C, and 12 seconds at 72°C (QuantStudio3, ThermoFisher Scientific, Waltham, MA). Average cycle threshold (CT) values were calculated and compared to those obtained from the standard curve to determine mtDNA copy numbers.

Statistics and Analyses

All statistical analyses were performed in R software (R Core Team, 2020). The code is available online (https://github.com/CaseyRead/Read_etal_2021_MethdPrtc). For validation of our procedures, coefficient of variation (CV) was calculated for the quadruplicate ATP (fluorescence) or mtDNA copy number (CT) values obtained for each individual oocyte analyzed. The data for ATP and mtDNA values was tested for normality by performing a Shapiro Wilk test and by plotting the residuals for visual evaluation of normality. The values for ATP were determined to have an approximately normal

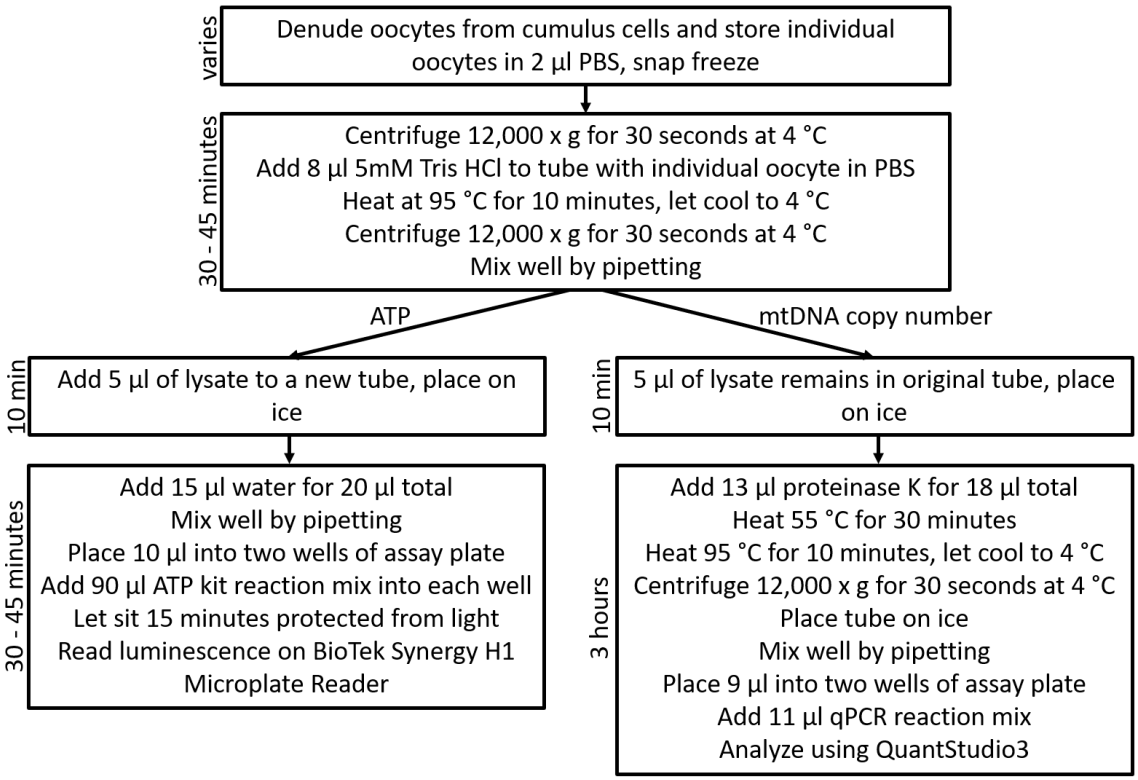

Figure 6. Workflow for oocyte lysis and quantification of ATP levels and mtDNA copy number within a single oocyte.

distribution while the mtDNA values were natural log transformed. Analysis of variance was performed to determine the differences in ATP and ln(mtDNA) between GV and MII oocytes. Linear regression was performed to determine the relationship between ATP and ln(mtDNA). Results were considered significant if $P < 0.05$. All values are presented as mean $\pm$ SD.

Results and Discussion

Standards Quality

The 260/280 ratio for the PCR product used to make the standards was 1.78. A 260/280 ratio of approximately 1.8 is generally accepted as "pure" for DNA, so we confidently used this PCR product to generate the standards for mtDNA copy number (Wang et al., 2011). The amplification efficiency of the qPCR assay was calculated to be 100.25%. The desired range for amplification efficiency is 90-110% (Svec et al., 2015). The R^2 values for the standard curves for each assay were ≥ 0.99. Desired R^2 values fall in the range of 0.95-1.0 with the goal to be as close to one as possible (Hazra and Gogtay, 2016). Based on the values for our standard curves falling within the optimal ranges, we are confident that our standard curves were accurate measures of the mtDNA copy number and ATP concentration within the oocyte.

Validation of Procedures for Quantification of ATP and mtDNA Copy Number in Quarter Oocyte Equivalents

We validated that the lysate from a single oocyte could be divided into quarters with minimal variation among the ATP or mtDNA CT values for each quarter oocyte

equivalent. Intra-assay CV values for ATP and mtDNA were 4.72 ± 0.98% and 1.61 ± 1.19%, respectively. Because the CV values from our methodology were below 5%, we have concluded that there is minimal variation between oocyte lysate portions. This allows us to be confident that the measures obtained via use of this protocol in future studies are valid for comparisons of both ATP and mtDNA copy number in single oocytes.

ATP and mtDNA Copy Number in GV versus MII Oocytes

Of the 30 total oocytes utilized for this study, data from 4 oocytes were removed from the dataset prior to analysis due to values outside of the standard curve. Interassay coefficient of variation was 6.61 ± 5.89 and 2.04 ± 1.48 for the ATP and mtDNA copy number assays, respectively.

Metaphase II stage oocytes had significantly higher quantities of ATP than GV stage oocytes (GV=628.02 ± 199.53 pg, MII=1326.24 ± 199.86 pg, $P < 0.001$, Figure 7A). The increased levels of ATP in MII oocytes is consistent with previously published studies of bovine oocytes (Stojkovic et al., 2001; Iwata et al., 2011; Scantland et al., 2014). This further validates the accuracy of our protocol and the sensitivity of our protocol to distinguish ATP quantities between different developmental stages of oocytes. However, our values for the concentration of ATP within the oocyte were higher than those previously reported in literature (Stojkovic et al., 2001; Tamassia et al., 2004; Jiao et al., 2007; Iwata et al., 2011; Scantland et al., 2014; Dadarwal et al., 2017; Payton et al., 2018; Hashimoto et al., 2019). This difference could be due to differences in assay sensitivity, oocyte dilution factors, and/or additional sources of variation in sample processing. Due to

differences in assay methods and dilutions, and to allow for interstudy comparison, we suggest presenting the amount of ATP present within the oocyte as a weight measure.

Mitochondrial DNA copy number was significantly different between GV and MII stage oocytes (GV=490,799.4±544,745.9, 1,087,126.9±902,202.8, p=0.035, Figure 7B). Multiple studies have shown that, in the bovine, MII stage oocytes have significantly more copies of mtDNA than GV stage oocytes (Jiao et al., 2007; Iwata et al., 2011). Additionally, the values retrieved for our assessment of mtDNA copy number were in the same range as those previously reported for bovine oocytes (Tamassia et al., 2004; Jiao et al., 2007; Chiaratti et al., 2010; Iwata et al., 2011; Hashimoto et al., 2019). This experiment also validated the capability of our methods to measure a large range in mtDNA copy numbers (12,478 to 3,141,658 copies).

Mitochondrial DNA copy number and ATP content were not significantly correlated in our samples (p=0.18, Figure 7C). Iwata et al 2011 evaluated ATP levels and mtDNA copy number from separate pools of oocytes collected from cows of increasing age and reported a positive correlation between ATP concentration and age, but a negative correlation between mtDNA copy number and age (Iwata et al., 2011). Such results suggest a negative correlation between ATP concentration and mtDNA copy number. This was the only paper we identified that compared mtDNA copy number to ATP level within the bovine oocyte. One potential reason for our different outcomes is that Iwata et al. 2011 utilized different pools of oocytes for analysis and our measures were from the same oocyte which allowed us to more accurately relate ATP levels to the corresponding mtDNA copy number from the same oocyte. Studies involving other cell types have shown no

relationship between ATP content and mtDNA copy number as well as both positive and negative correlations between the two values (May-Panloup et al., 2007; Jeng et al., 2008; Van Blerkom, 2011). The highly variable relationship between ATP level and mtDNA copy number suggests that there are multiple variables within the cell that are affecting ATP levels and highlights the importance of collecting multiple metabolic measurements when possible to fully elucidate the cause of altered oocyte metabolism.

Conclusions

Due to small sample volumes, many oocyte focused studies rely on pooled oocyte samples to have adequate substrate to perform analyses. As technology has advanced, single cell oocyte analysis is possible (Kimble et al., 2018). Because ATP concentration and mitochondrial numbers within oocytes are important for downstream developmental competence, it is integral that protocols be developed to further investigate these parameters within single oocytes. This would eliminate the need to pool oocytes and retrieve average values for an oocyte population. By retrieving values for individual oocytes, one can relate ATP and mtDNA copy number values, use fewer samples for analysis, and more accurately depict intraoocyte variations in these values.

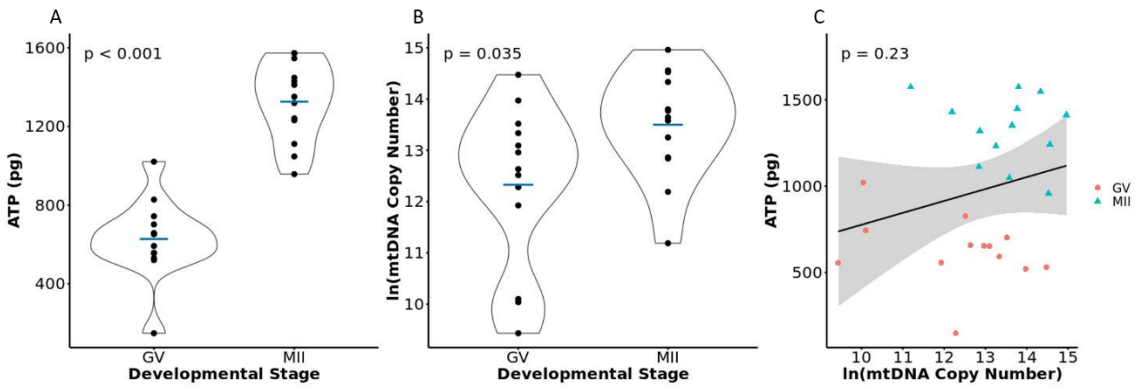

Figure 7. (A) Violin plot depicting the differences in ATP quantity within single GV stage and MII stage oocytes. (B) Violin plot depicting the natural log of the differences in mtDNA copy number between single GV stage and MII stage oocytes. (C) Scatterplot depicting the relationship between the ATP quantity and natural log of the mtDNA copy number within individual oocytes.

CHAPTER IV
PRE-OVULATORY SERUM ESTRADIOL CONCENTRATION IS POSITIVELY CORRELATED WITH OOCYTE ATP AND FOLLICULAR FLUID METABOLITE ABUNDANCE

A version of this chapter will be published by Casey Read and Sarah Moorey:
Casey C. Read, J. Lannett Edwards, F. Neal Schrick, Justin D. Rhinehart, Rebecca R. Payton, Shawn R. Campagna, Hector F. Castro, Jessica L. Klabnik, and Sarah E. Moorey. "Pre-ovulatory serum estradiol concentration is positively correlated with oocyte ATP and follicular fluid metabolite abundance."

Conceptualization, Sarah Moorey; Data curation, Casey Read, Shawn Campagna, Hector Castro and Sarah Moorey; Formal analysis, Casey Read and Sarah Moorey; Investigation, Casey Read, F. Schrick, Justin Rhinehart, Rebecca Payton, Jessica Klabnik, and Sarah Moorey; Methodology, J. Edwards, F. Schrick and Sarah Moorey; Project administration, Sarah Moorey; Resources, Shawn Campagna, Hector Castro and Sarah Moorey; Software, Casey Read and Sarah Moorey; Supervision, Sarah Moorey; Visualization, Casey Read and Sarah Moorey; Writing – original draft, Casey Read and Sarah Moorey; Writing – review & editing, J. Edwards, F. Schrick, Justin Rhinehart, Rebecca Payton, Shawn Campagna, Hector Castro and Jessica Klabnik.

Funding: This research was supported by the USDA NIFA Hatch project 1022068, the University of Tennessee AgResearch, and the University of Tennessee Department of Animal Science.

Acknowledgments: The authors would like to thank Dr. Liesel Schneider for her statistical analyses consulting, Courtney Christopher and Sara Howard for their assistance with the UHPLC-HRMS metabolomics processing, Boyd Dingus for the donation of the Estrotect ® patches, and Walt Hitch and the staff of the Plateau AgResearch and Education Center for providing the cattle and their assistance in processing the cattle for this study. . The authors would also like to thank Emma Horn, Emma Hessock, Julia Rowinski, Hunter Liles, Samantha Roberts, Meredith Hinson, Sadie Bhandari, Abigayle Pollock, and Kennedy Hill for their assistance with sample collection and processing.

Abstract

Cattle induced to ovulate a small, physiologically immature pre-ovulatory follicle had reduced oocyte developmental competence that resulted in decreased embryo cleavage and day 7 embryo quality compared to animals induced to ovulate a more advanced follicle. RNA-sequencing performed on oocytes and their corresponding cumulus cells 23 hours after gonadotropin releasing hormone (GnRH) administration to induce the pre-ovulatory gonadotropin surge suggested reduced capacity for glucose metabolism and oxidative

phosphorylation in the cumulus cells and oocytes from follicles ≤ 11.7 mm, respectively. We hypothesized that induced ovulation of a small, physiologically immature pre-ovulatory follicle results in a suboptimal follicular microenvironment and reduced oocyte metabolic capacity. We performed a study with the objective to determine the impact of pre-ovulatory follicle diameter and serum estradiol concentration at GnRH administration on oocyte metabolic competence and follicular fluid metabolome profiles. We synchronized the development of a pre-ovulatory follicle and collected the follicle contents via transvaginal aspiration ~20 hours after GnRH administration in lactating beef cows (n = 319). We determined ATP levels and mitochondrial DNA (mtDNA) copy number in 110 oocytes and performed ultra-high-performance liquid chromatography – high resolution mass spectrometry metabolomic studies on 45 follicular fluid samples. Intraoocyte ATP and the amount of ATP produced per mtDNA copy number were significantly associated with serum estradiol concentration at GnRH and time from GnRH administration to follicle aspiration ($P < 0.05$). Mitochondrial DNA copy number was not significantly related to follicle diameter at GnRH, serum estradiol concentration at GnRH, or any potential covariates ($P > 0.10$). We detected 90 metabolites in the aspirated follicular fluid. We identified 22 metabolites significantly associated with serum estradiol concentration at GnRH and 63 metabolites associated with follicular fluid progesterone concentration at the time of follicle aspiration. Pathway enrichment analysis of significant metabolites suggested altered proteinogenesis, citric acid cycle, and pyrimidine metabolism in follicles of reduced estrogenic capacity pre-gonadotropin surge or reduced progesterone production by the time of follicle aspiration.

Introduction

Utilization of fixed time artificial insemination (FTAI) positively impacts reproductive management and genetic merit of the beef herd (Lima et al., 2010; Sá Filho et al., 2010; Funston et al., 2012; Rodgers et al., 2012; Cushman et al., 2013; Lamb and Mercadante, 2016; Baruselli et al., 2018). Such protocols, however, result in a subset of cattle that have not displayed estrus prior to insemination and rely on the administration of gonadotropin releasing hormone (GnRH) to induce ovulation. Expression of estrus is essential for optimal pregnancy outcomes, and induced ovulation of small, physiologically less advanced pre-ovulatory follicles is associated with decreased pregnancy rates and increased early pregnancy loss in beef cattle (Lamb et al., 2001; Perry et al., 2005; Perry et al., 2007). Reduced fertility is likely the result of ovulation of an oocyte with reduced developmental competence and poor preparation of the maternal environment to support a pregnancy (Perry et al., 2005; Sá Filho et al., 2010; Atkins et al., 2013; Jinks et al., 2013; Ciernia et al., 2021). Cattle induced to ovulate prematurely after pharmacological induction of ovulation had lower serum estradiol concentrations before GnRH administration and reduced progesterone production by the corpus luteum (CL) after ovulation compared to animals that displayed estrus (Busch et al., 2008; Richardson et al., 2016; Cooke et al., 2019). Additionally, cattle pharmacologically induced to ovulate a small (< 12.5mm) versus large (≥ 12.5mm) pre-ovulatory follicle had impaired oocyte developmental competence that resulted in decreased probability of producing a cleaved embryo and decreased embryo quality grade 7 days after insemination (Atkins et al., 2013). In the same study, serum estradiol concentration at the time of GnRH administration to induce

ovulation was also positively associated with probability of recovering a cleaved or high-quality embryo. Multiple *in vitro* studies have demonstrated that removal of the oocyte from the follicle, and thus inducing oocyte maturation, prior to the endogenous gonadotropin surge results in decreased oocyte developmental competence as evidenced by decreased cleavage rates, blastocyst rates, and embryo quality (Pavlok et al., 1992; Lonergan et al., 1994; Blondin and Sirard, 1995; Fair et al., 1995; Blondin et al., 1996; Hyttel et al., 1997; Otoi et al., 1997; Hagemann et al., 1999; van de Leemput et al., 1999; Dieleman et al., 2002; Iwata et al., 2004). Collectively, these studies support the hypothesis that decreased oocyte developmental competence contributes to the reduced fertility in cattle induced to ovulate a small, physiologically immature pre-ovulatory follicle.

Though oocytes obtain meiotic competence much earlier than the pre-ovulatory follicle stage of development, follicles greater than ~9 mm contain oocytes that are completing the capacitation phase of oogenesis (Hyttel et al., 1997; Mermillod et al., 1999; Conti and Franciosi, 2018). Throughout this phase, the oocyte is maintained in a state of meiotic arrest while it undergoes ultrastructural changes, modifies its RNA and proteins to prevent degradation, increases its organelle number, alters the distribution of organelles, and finishes accumulating nutrient and metabolic substrate stockpiles important to sustain development (Hyttel et al., 1986; Hyttel et al., 1989; Hyttel et al., 1997; Mermillod et al., 1999; Merton et al., 2003; Swain and Pool, 2008; Gougeon, 2010; Zhang and Smith, 2015; Labrecque et al., 2016; Liu et al., 2017; Reader et al., 2017; Conti and Franciosi, 2018). Metabolism in the oocyte and early embryo relies on energetic substrates such as pyruvate, lactate, NADH, and $FADH_2$ that are derived from cumulus cell glycolytic activity and

transferred to the oocyte via gap junctions during antral follicle development (Sutton-McDowall et al., 2010; Winterhager and Kidder, 2015; Richani et al., 2021). The oocyte creates stockpiles of these substrates that are utilized by its mitochondria to produce ATP necessary to sustain development through the energy-demanding processes of oocyte maturation, fertilization, and embryo development to the blastocyst stage (Johnson et al., 2007; Swain and Pool, 2008; Chappel, 2013; Zhang and Smith, 2015). In addition to metabolic coupling with the cumulus cells, the follicular microenvironment plays a key role in the ability of the oocyte to achieve metabolic competency. The follicular fluid of antral follicles provides many of the nutrients, metabolic compounds, and signaling molecules that are essential for the cumulus cells to perform glycolysis and for the oocyte to increase its mitochondrial number and perform oxidative phosphorylation (Jeong et al., 2009; Hennet and Combelles, 2012; Mao et al., 2012; Dunning et al., 2014; Da Broi et al., 2018; Aguila et al., 2020).

The pre-ovulatory gonadotropin surge induces oocyte maturation, and the subsequent breakdown of gap junctional transfer of metabolic compounds to the oocyte (Granot and Dekel, 2002; Conti et al., 2012; Conti and Franciosi, 2018). By inducing the pre-ovulatory gonadotropin surge before estrus and the onset of an endogenous gonadotropin surge, the capacitation timeline of the oocyte is interrupted. As such, we have previously detected transcriptome profiles indicative of altered oxidative phosphorylation or mitochondrial function in oocytes and altered glycolytic activity in cumulus cells collected from small pre-ovulatory follicles ~23 hours following gonadotropin releasing hormone administration to induce the pre-ovulatory gonadotropin surge (Moorey et al.,

2021). We recently also detected a positive correlation between pre-ovulatory follicle diameter and abundance of metabolites involved in glucose metabolism in follicular fluid collected ~20 hours following an induced gonadotropin surge of pre-ovulatory follicles of increasing size (Read et al., 2021b). Such observations may be due to incomplete progression of the follicle's physiological maturity before the induced pre-ovulatory gonadotropin surge and thus an altered follicular microenvironment and inadequate opportunity for the oocyte to complete capacitation. Therefore, we hypothesized that the follicle's developmental progression toward estrus and exposure to an endogenous pre-ovulatory gonadotropin surge leads to necessary alterations in the follicular microenvironment that are essential for optimal metabolic capacity of the cumulus-oocyte complex and induced ovulation of small, physiologically immature pre-ovulatory follicles results in a suboptimal follicular microenvironment and reduced oocyte metabolic capacity. To test this hypothesis, we utilized pre-ovulatory follicle diameter and serum estradiol concentration as indicators of follicle physiological maturity at the time of GnRH administration to induce the pre-ovulatory gonadotropin surge. We then performed a study with the objective to determine relationships between pre-ovulatory follicle diameter and serum estradiol concentration, follicular fluid metabolome profiles, oocyte mitochondrial DNA copy number, and oocyte ATP concentration.

Materials and Methods

Animal handling and synchronization of pre-ovulatory follicle development

All animal protocols and procedures were approved by the University of Tennessee Knoxville Institutional Animal Care and Use Committee. Pre-ovulatory follicle

development was synchronized in postpartum, suckled beef cattle (Angus; n = 319) according to procedures outlined in Figure 1. The study contained two replicates conducted over two years (year 1: n = 162, year 2: n = 157). Estrous cycles were pre-synchronized by administration of gonadotropin-releasing hormone (GnRH; Cystorelin, Boehriner Ingelheim, Ingelheim am Rhein, Germany) and placement of a controlled internal drug release (CIDR; Eazi-Breed CIDR, Zoetis Animal Health, Kalamazoo, MI, USA). After seven days, the CIDR was removed and cows were administered prostaglandin F2α (PGF; Lutalyse HighCon, Zoetis Animal Health). Approximately 66 hours later, cows were administered a second dosage of GnRH. Cows were then divided into 4 groups to facilitate transvaginal aspiration with 21 to 44 animals per group. Eight to eleven days after pre-synchronization, cows were administered GnRH on day -9 to start a new follicular wave. On day -2, PGF was administered to lyse corpora lutea. On day 0, cows received a second dosage of GnRH (GnRH2) to induce a pre-ovulatory gonadotropin surge. On day 1, approximately 19 hours after GnRH2 administration, each cow's largest follicle underwent transvaginal aspiration by one of four experienced technicians to collect the pre-ovulatory follicle contents (Moorey et al., 2021; Read et al., 2021b).

Transvaginal aspiration of the pre-ovulatory follicle

We performed transvaginal aspiration to collect oocyte and follicular fluid samples ~19 hours after GnRH2 administration to induce the pre-ovulatory gonadotropin surge. We aimed to determine the functional significance of variations in pre-ovulatory follicle maturity at the time of GnRH2 administration on follicular fluid metabolome profiles and

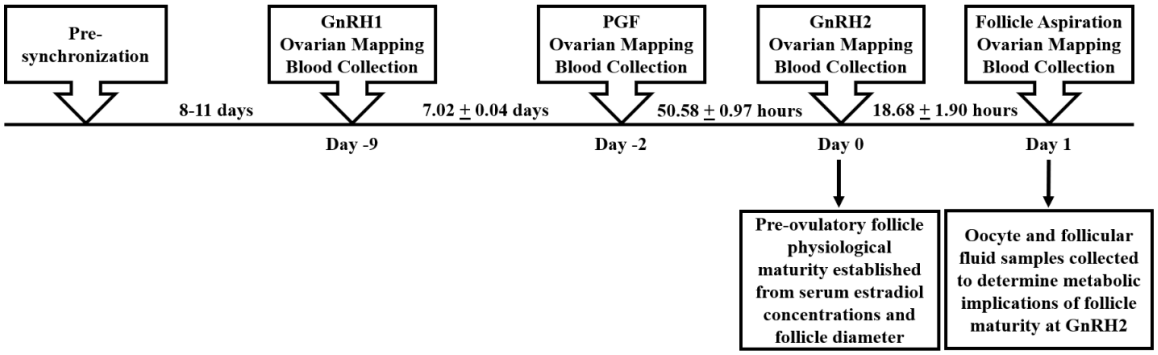

Figure 8. Timeline for synchronization of pre-ovulatory follicle development and sample collection. We collected oocyte and follicular fluid samples ~19 hours after GnRH administration to induce the pre-ovulatory gonadotropin surge to determine the functional significance of varied pre-ovulatory follicle maturity at the time of GnRH administration on the follicular fluid metabolome and oocyte metabolic capacity. GnRH1, gonadotropin releasing hormone administration to turn over a new follicular wave at the onset of synchronization; PGF, prostaglandin F2α; GnRH2, gonadotropin releasing hormone administration to induce the pre-ovulatory gonadotropin surge. Values depicted as mean ± SD.

oocyte metabolic capacity after progression toward oocyte maturation. Prior to aspiration, all cows received a spinal block via administration of lidocaine (2% lidocaine, 5 ml) into the spinal cord at the first intercoccygeal space of the tailhead. The perineal area of each cow was then cleaned of all contaminants and an ultrasound guided aspiration device attached to a Samsung HM70A ultrasound and CF4-9 convex probe was inserted into the anterior vagina. The ultrasound device consisted of an 18-gauge needle and a series of tubing to facilitate removal of follicular contents. The ovary containing the pre-ovulatory follicle was located and positioned for follicle aspiration before the needle was gently pushed through the vaginal wall and guided through the ovarian cortex into the antrum of the pre-ovulatory follicle. Follicular fluid was withdrawn into a clean 12 ml syringe before the syringe was removed, replaced, and the follicle lavaged with PVA TL-HEPES (114.0 mM NaCl, 3.2 mM KCl, 2.0 mM NaHCO3, 0.34 mM NaH2PO4, 0.50 μM MgCl2*6H2O, 10.0 mM HEPES, 2.0 mM CaCl2*H2O, 2.3 μM PVA, and 12 mM sorbitol) multiple times to collect remaining follicular cells.

Detection of estrus, ovarian mapping, and determination of cow weight and body condition score

Patches for the detection of estrus (Estrotect; Rockway Inc; Spring Valley, WI, USA) were placed on the tailhead of all cows at the time of PGF administration during pre-synchronization and on day -9 of synchronization. Patches were visually assessed 66 hours after pre-synchronization PGF administration to determine expression of estrus during pre-synchronization and on days -2 and 0 of synchronization to detect any animals that displayed estrus between GnRH1 and PGF (n=0) or between PGF and follicle aspiration

(removed from the study, n=5). Patches were scored on a scale of 0-4 with 0 being a missing patch, and 1-4 equating to < 25% rubbed (patch=1), 25-50% rubbed (patch=2), 50-75% rubbed (patch=3), and > 75% rubbed (patch=4). Estrus was recorded if patch score equaled 3 or 4.

On days -9, -2, 0, and 1, ovaries of all cattle were examined by an experienced technician using trans-rectal ultrasonography with a Samsung HM70A ultrasound and CF4-9 convex probe. All follicles > 7 mm in diameter and all corpora lutea were recorded. Follicle size was calculated for all recorded follicles by averaging the measures of the largest diameter and the diameter perpendicular to it. Body weights of all animals were collected and body condition score ((Whitman, 1975; scale of 1, emaciated-9, obese) was assigned on day 1.

Blood collection and processing

Blood samples were collected on days -9, -2, 0, and 1. Approximately 10ml of blood was collected via the tail vein using vacutainers for serum collection and 18-gauge, 1-inch long needles (Becton, Dickinson and Company; Franklin Lakes, NJ, USA). Blood was allowed to clot for at least 1 hour before being refrigerated at 4 ºC for approximately 24 hours. Samples were then centrifuged at 1200 x g for 25 min at 4 ºC and the serum supernatant was collected into borosilicate glass tubes and stored at -20 ºC until processing for estradiol and progesterone hormone assays (VWR, Radnor, PA, USA). Samples collected in year one were stored for 19 months and samples collected in year two were stored for 7 months prior to processing.

Processing of follicular fluid and oocyte samples

Follicular fluid and PVA TL-HEPES media flushes collected during follicle aspiration were deposited into individual wells of a 4-well petri plate and searched to find the cumulus-oocyte-complex (COC). Once located, the COC was placed into a four-well plate containing 1 ml of 1x trypsin (Thermo Fisher Scientific, Waltham, MA, USA). The oocyte was denuded by gently pipetting the COC within the trypsin using a Cook Flexipet Adjustable Handle pipette with a 130 µm Cook Flexipet pipette tip (Cook Group, Bloomington, IN, USA). The oocyte underwent 3 consecutive washes in phosphate buffered saline (PBS) before being snap frozen in a 2 ml cryovial (Neptune Scientific, San Diego, CA, USA) containing 2 µl PBS. The follicular fluid was then collected into 1.7 ml tubes (VWR, Radnor, PA, USA) and centrifuged at 4 ^{o}C for 5 min at 500 x g to remove the remaining cellular debris. The follicular fluid supernatant was distributed between a borosilicate glass tube and 2 ml cryovials. Follicular fluid samples in glass tubes were stored at -20 ^{o}C, and samples stored in cryovials were snap frozen in liquid nitrogen for storage at -80 ^{o}C until further processing.

Oocyte ATP and mtDNA copy number quantification

Quantification of oocyte ATP levels and mtDNA copy number were performed according to a protocol previously optimized by our lab (n = 110; Read et al., 2021a). Briefly, oocytes were lysed by adding 8 µl of 5 mM Tris HCl to each tube and heating for 10 min at 95 ^{o}C. The lysate was then divided in half with 5 µl used to quantify intra-oocyte ATP levels and the remaining 5 µl used to quantify mtDNA copy number. Quantification of ATP levels was performed in duplicate using the ATP Determination Kit according to

the manufacturer's directions (Life Technologies; Carlsbad, CA, USA). The portion of the lysate for mtDNA copy number analysis was combined with proteinase K (final concentration of 200 µg/ml; Zymo Research, Irvine, CA, USA) and heated at 55 ºC to expose the mtDNA. A custom TaqMan assay was designed to determine the mtDNA copy number of each oocyte (Thermo Fisher Scientific, Waltham, MA, USA; Read et al., 2021a). TaqMan primer and probes were combined with the oocyte lysate and Fast Advanced Master Mix (Thermo Fisher Scientific) and analyzed in duplicate using a QuantStudio3 (Thermo Fisher Scientific). The PCR settings were as follows: 2 min at 94°C followed by 40 cycles of 10 seconds at 94 °C, 15 seconds at 57 °C, and 12 seconds at 72 °C. Average sample values for each assay were compared to the values from a known standard curve (ATP: 0.5 µM, 0.05 µM, 0.025 µM, 0.005 µM, 0.0025 µM; mtDNA: 10, 100, 1000, 10000, 100000, 1000000 copies) and used to calculate the levels of ATP and mtDNA copy number within each oocyte. Intra-assay and inter-assay CV values averaged 0.65% and 4.39% for mtDNA copy number and 13.29% and 15.16% for intraoocyte ATP.

UHPLC-HRMS metabolomics

Follicular fluid samples corresponding to each collected oocyte (n = 45) from year two were selected for metabolomics processing. Cryovial-stored, follicular fluid samples were thawed on ice, and 50 µl aliquots of each sample were placed into individual 2 ml tubes. Each sample was analyzed by ultra-high-performance liquid chromatography – high resolution mass spectrometry (UHPLC-HRMS) at the University of Tennessee Biological and Small Molecule Mass Spectrometry Core (RRID: SCR_021368). Briefly, metabolites were extracted from the follicular fluid using a 20:40:40 water/methanol/acetonitrile

(v/v/v) solution with 0.10 M formic acid (Martens et al., 2011; Greene et al., 2020). The metabolomes of each sample were separated on a Synergy Hydro RP (2.5 μm, 100 mm x 2.0 mm column (Phenomenex, Torrance, CA, USA) at 25 ^{o}C. The solvents for the elution were: phase A: 97:3 methanol/water (v/v) with 11mM tributylamine and 15mM acetic acid and phase B: 100% methanol. The solvent gradient from 0 to 5 min was 100% A: 0% B, from 5 to 13 min was 80% A: 20% B, from 13 to 15.5 min was 45% A: 55% B, from 15.5 to19 min was 5% A: 95% B, and from 19 to 25 min was 100% A: 0% B with a flow rate of 200 μL/min. Detection of the metabolome components was accomplished using an Exactive Plus Orbitrap mass spectrometer (Thermo Fisher Scientific, Waltham, MA) fitted with an electrospray ionization (ESI) probe operated in negative mode. The scan range was 72-1000 *m/z*, the resolution was set to 140,000, and the acquisition gain control target to 3e6. Files were generated by the HRMS in the Xcalibur (RAW) format and were converted to the open-source mzML format via the open-source msconvert software, which is part of the ProteoWizard package (Chambers et al., 2012; Clasquin et al., 2012). MAVEN (mzroll) software, Princeton University (Melamud et al., 2010), which uses a grouping algorithm for non-linear retention time alignment, was used to pick peaks, integrate intensities, and visualize the data and extracted ion chromatograms. Pre-processed data from MAVEN was used to conduct all further biological and statistical analyses.

Quantification of estradiol and progesterone concentrations in serum and follicular fluid

Serum collected on days -2, 0, and 1 (PGF, GnRH2, and FA timepoints, respectively) that corresponded to each collected oocyte (n = 110) underwent estradiol

radioimmunoassay as previously described (Kirby et al., 1997). Intra-assay and inter-assay CV values averaged 3.49% and 10.74%.

Serum collected on days -9, -2, 0, and 1 (GnRH1, PGF, GnRH2, and FA timepoints, respectively) that corresponded to each collected oocyte (n = 110) as well as the follicular fluid stored in the glass tubes (n = 106) were analyzed for progesterone concentration using the ImmuChem progesterone double antibody radioimmunoassay kit (MP Biomedicals; Pohler et al., 2016; Rispoli et al., 2019) per manufacturer's instructions. Due to limitations in sample volume, three serum samples from the GnRH1 timepoint and four follicular fluid samples were not analyzed. Follicular fluid samples were diluted 1:5 to 1:20 to ensure it was within the assay's range of detection. Intra-assay and inter-assay CV values averaged 5.97% and 5.66% for serum samples and 4.54% and 3.52% for follicular fluid samples. The follicular fluid stored in glass tubes corresponding to the collected oocytes (n = 106) was also analyzed for estradiol concentration using the DetectX1 serum 17β-estradiol multi-species enzyme immunoassay (Arbor Assays, Ann Arbor, MI, USA) per manufacturer's instructions. Samples were diluted from 1:20 to 1:2500 to ensure they were within the detectable range of the assay. Intra-assay and inter-assay CV values were 6.67% and 8.58%.

Statistical analyses

Before statistical analyses were performed, steroid hormone profiles in serum, follicle dynamics, and/or follicular fluid estradiol: progesterone ratios were utilized to identify cattle that underwent luteolysis following PGF administration, developed a growing pre-ovulatory follicle, and responded to the induced pre-ovulatory gonadotropin

surge. Successful luteolysis was defined as serum progesterone < 1 ng/ml at the GnRH2 and FA timepoints (Tenhagen et al., 2000; Rispoli et al., 2019; Madureira et al., 2021). Development of a growing pre-ovulatory follicle was classified as an increase in serum estradiol concentration and follicle diameter between PGF and GnRH2 (Alvarez et al., 2000; Fortune et al., 2004; Perry et al., 2014). Response to the administration of GnRH2 was verified by a decrease in serum estradiol between GnRH2 and FA and a follicular fluid estradiol:progesterone ratio < 3 (Fortune and Hansel, 1985). Thirty oocytes were removed from analyses due to their corresponding hormonal profiles not meeting these criteria. All analytical procedures were performed using R software (R Core Team, 2020), and the corresponding code is available online (https://github.com/CaseyRead/Read_etal_2022_JAS). Oocytes with ATP and mtDNA values inside the standard curve and ideal hormonal profiles were used for analysis (n = 52). All values are presented as mean $\pm$ SD.

A mixed effects linear model with the random effect of year was used to perform intraoocyte ATP, mtDNA copy number, and ATP per mtDNA copy number analyses and identify cow trait or synchronization timeline parameter covariates. Linear regression (cow weight, cow age in days, days postpartum at aspiration, hours between PGF and GnRH2, follicular fluid progesterone, follicular fluid estradiol, and hours between GnRH2 and aspiration) or analysis of variance (serum progesterone $\geq$ 1 vs <1 ng/ml at the start of synchronization, BCS) were used to determine any effects of potential covariates on pre-ovulatory follicle diameter and serum estradiol at GnRH2 or oocyte ATP, oocyte mtDNA copy number, and oocyte ATP produced per mtDNA copy number. After initial analyses of each covariate, variables that were significantly related to ATP, mtDNA copy number,

or ATP/mtDNA copy number were included in the respective models along with follicle diameter and serum estradiol at GnRH2. We then utilized a top down, stepwise approach to remove covariates that lost significance ($P > 0.10$) in the full model and reach a final model for ATP, mtDNA copy number, or ATP/mtDNA copy number analyses. For ATP and ATP/mitochondrial DNA copy number analyses, the final model contained our independent variables of interest (follicle diameter and serum estradiol at GnRH2) as well as time from GnRH2 to follicle aspiration. For the mitochondrial DNA copy number analysis, the final model only contained pre-ovulatory follicle diameter and serum estradiol concentration at GnRH2.

Linear regression and analysis of variance were also performed where appropriate to determine the effects of cow trait and/or synchronization timeline parameters on the 90 individual follicular fluid metabolites. A similar top down, stepwise approach was taken to determine the best model for each individual metabolite. Each cow trait and timeline parameter was included in the full model and any covariates with $P > 0.05$ were removed. Once the final model was obtained for each metabolite, false discovery rate (FDR) was calculated for the p-values of pre-ovulatory follicle diameter, serum estradiol concentration at GnRH2, and each covariate. Metabolites were considered significantly correlated to each predictive variable if FDR < 0.10 was observed. Metaboanalyst 5.0 (Pang et al., 2021) was used to perform KEGG pathway enrichment analysis of metabolites whose abundance was correlated with variables of interest or covariates. Enrichment of pathways was determined to be significant if FDR was < 0.10.

The effects of individual follicular fluid metabolite on intraoocyte ATP level were determined using linear regression with the covariates of serum estradiol at GnRH2 and hours from GnRH2 to follicle aspiration included in the model. After false discovery rate was calculated, no follicular fluid metabolites were found to be significant to intraoocyte ATP (FDR > 0.10).

Results and Discussion

Overview of Animal Data

All samples were collected from suckled, postpartum beef cows managed as part of the productive herd at one of the University of Tennessee AgResearch and Education Centers. Age (2068.3 + 648.02 days, 5.2 + 2.3 years), BCS (5.96 + 1.10), and weight (617.40 + 103.19 kg) of the 52 cattle included in our analyses were similar to previously reported values for beef cattle operations (Cushman et al., 2007; Cushman et al., 2013; Damiran et al., 2018; Bonacker et al., 2020). To maintain the yearly breeding season schedule, animals were 58.36 + 4.12 days postpartum at the time of pre-ovulatory follicle aspiration. There was no effect of days postpartum or serum progesterone concentration at onset of synchronization on pre-ovulatory follicle diameter, serum estradiol concentration, oocyte ATP, oocyte ATP per mtDNA copy number, or oocyte mtDNA copy number ($P >$ 0.10). Largest follicle diameter at GnRH administration to induce a pre-ovulatory gonadotropin surge (GnRH2) was 12.33 + 1.53 mm and serum estradiol concentration at the time of GnRH2 administration was 7.23 + 3.69 pg/ml. These measures are consistent with previously published studies investigating pre-ovulatory follicle diameter or estradiol production (Geary et al., 2001; Lamb et al., 2001; Perry et al., 2005; MacNeil et al., 2006;

Perry et al., 2007; Atkins et al., 2013; Moorey et al., 2021; Read et al., 2021b). Serum estradiol and follicle diameter at GnRH2 were not significantly associated with cow phenotypic traits of age, BCS, weight, and days postpartum or synchronization timeline parameters of time between GnRH1 and PGF, PGF and GnRH2, or GnRH2 and FA ($P > 0.05$).

Oocytes and follicular fluid samples utilized in this study were collected via transvaginal follicle aspiration of the pre-ovulatory follicle 19.02 $\pm$ 1.90 hours after administration of GnRH2. At this time, the induced luteinizing hormone (LH) surge should have stimulated the follicle's progression towards ovulation resulting in alterations in the pre-ovulatory follicular environment. At this timepoint after GnRH administration, the somatic follicular cells have begun luteinization and are increasing their production of progesterone, cumulus cells are expanding, and the oocyte has achieved metaphase I (MI) and has reached or is progressing towards metaphase II (MII) (Hyttel et al., 1986; de Loos et al., 1991; Hyttel et al., 1997; Richards et al., 1998; Iwata et al., 2011; Pulley et al., 2015). The mitochondria within oocytes of this maturation stage would have increased their production of ATP in order to support progression through meiotic maturation (Fair et al., 1997; Jeong et al., 2009; Dalbies-Tran et al., 2020). Measuring the metabolic capacity of the oocyte at this time point should reveal differences in the acquisition of metabolic competence of oocytes within follicles of varied physiological maturity when exposed to an induced pre-ovulatory gonadotropin surge. Alterations in the metabolome of follicular fluid samples collected at this time after premature induction of the gonadotropin surge could highlight both lasting implications of the follicle's physiological status at the time of

the surge as well as impacts of the follicle's pre-surge developmental status on metabolic processes occurring in cumulus-oocyte complex and granulosa cells.

The impact of follicle physiological status on oocyte metabolic capacity

Amount of ATP (pg) and mtDNA copy number were used to quantify the metabolic capacity of individual oocytes. Intraoocyte ATP ranged from 55.31-1111.30 pg (532.29 $\pm$ 279.15 pg) and mtDNA copy number ranged from 25355-1070864 copies (535696 $\pm$ 419745.3 copies). ATP values were higher than those previously reported by others, however this could be due to differences in assay sensitivity, dilution factors, and/or other sample processing variations (Stojkovic et al., 2001; Tamassia et al., 2004; Jiao et al., 2007; Iwata et al., 2011; Scantland et al., 2014; Dadarwal et al., 2017; Payton et al., 2018; Hashimoto et al., 2019). The mtDNA copy number values obtained in this study were consistent with previously published literature (Tamassia et al., 2004; Jiao et al., 2007; Chiaratti et al., 2010; Iwata et al., 2011; Hashimoto et al., 2019).

Initial correlation analyses determined time between GnRH2 and follicle aspiration should be included in oocyte ATP modelling and weight should be included in mtDNA copy number modelling (Table 3). Intraoocyte ATP at approximately 19 hours after GnRH2 administration was significantly related to serum estradiol concentration at GnRH2 ($P = 0.014$; Figure 2A) and time between GnRH2 and follicle aspiration ($P = 0.004$; Figure 2B). Follicle diameter at GnRH2, however, was not significantly related to oocyte ATP level approximately 19 hours after GnRH administration ($P = 0.085$). Though samples collected from year two had higher levels of both intraoocyte ATP and serum estradiol ($P < 0.001$)), similar trends for the relationship between oocyte ATP level and serum estradiol

concentration or time from GnRH2 to follicle aspiration were observed in each year (Figure 2C, Figure 2D). Mitochondrial DNA copy number was not significantly related to follicle diameter at GnRH2, serum estradiol concentration at GnRH2, or any potential covariates ($P > 0.10$). The lack of relationship between mtDNA copy number and physiological status of the follicle and/or intraoocyte ATP is not surprising. There is variation in published literature on the relationship of mtDNA copy number and oocyte developmental competence (Reynier et al., 2001; Tamassia et al., 2004; May-Panloup et al., 2007; Wai et al., 2010; Iwata et al., 2011; Hashimoto et al., 2019). A study by van Blerkom et al in 2004 suggested that mtDNA copy number could be linked to oocyte developmental competence if metabolic capacity of the oocyte was accounted for. Therefore, we performed an additional analysis to determine if there was an impact of follicle physiological status on the amount of intraoocyte ATP present per mtDNA copy number. The amount of ATP produced per mtDNA copy number was significantly related to serum estradiol concentration at GnRH2 ($P = 0.015$; Figure 3A, Figure 3C) and time from GnRH2 to follicle aspiration ($P = 0.039$; Figure 3B, Figure 3D).

Increased level of oocyte ATP has been associated with increased developmental competence of the oocyte (Quinn and Wales, 1973; Calarco, 1995; Stojkovic et al., 2001; Tamassia et al., 2004; Dalton et al., 2014). Therefore, the positive relationship between serum estradiol concentration at GnRH2 and both oocyte ATP level and oocyte ATP production per mitochondria likely contributes to the positive relationship between serum estradiol concentration at GnRH2 and day seven embryo cleavage and quality grades previously observed by Atkins (Atkins et al., 2013). As the dominant follicle progresses

Table 3: P values for the initial correlations performed to identify covariates to be used in oocyte ATP (pg) and oocyte mtDNA copy number analyses.

Independent Variable	Oocyte ATP (pg)	TP Correlation	Oocyte mtDNA Copy Number	mtDNA Copy Number Correlation
Follicle Diameter at GnRH2 (mm)*	0.11	0.017	0.12	0.051
Cow Age*	0.38	0.008	0.73	0.0035
Days Postpartum at FA*	0.17	0.013	0.73	0.0025
Weight*	0.46	0.001	0.04	0.062
Serum Estradiol at PG (pg/ml)*	0.76	0.014	0.13	0.0003
Serum Estradiol at GnRH2 (pg/ml)*	0.26	0.011	0.91	0.04
Serum Estradiol at FA (pg/ml)*	0.3	0.02	0.2	0.031
Serum Progesterone at PG (ng/ml)*	0.43	0.0044	0.18	0.039
Serum Progesterone at GnRH2 (ng/ml)*	0.91	0.0001	0.84	0.0009
Serum Progesterone at FA (ng/ml)*	0.7	0.0011	0.11	0.055
Follicular Fluid Progesterone (ng/ml)*	0.09	0.020	0.27	0.028
Follicular Fluid Estradiol (ng/ml)*	0.3	0.0078	0.94	0.0001
Follicular Fluid Estradiol:Progesterone Ratio*	0.74	0.0009	0.53	0.0093
Days from GnRH1 to PG*	0.87	0.0002	0.31	0.024
Hours from PG to GnRH2*	0.33	0.011	0.1	0.074
Hours from GnRH2 to FA*	0.003	0.067	0.39	0.022
Pyruvate**	0.41	-0.014	0.65	-0.043
Alanine/Sarcosine**	0.14	0.06	0.83	-0.053
Serine**	0.09	0.093	0.89	-0.055
Creatinine**	0.32	0.0014	0.57	-0.036
Valine/Betaine**	0.3	0.0062	0.89	-0.054
Homoserine/Threonine**	0.22	0.027	0.77	-0.05
Pyroglutamic Acid**	0.22	0.028	0.92	-0.055
N-Acetyl-β-Alanine**	0.2	0.032	0.73	-0.048
Creatine**	0.04	0.14	0.97	-0.056
Leucine/Isoleucine**	0.24	0.02	0.72	-0.048
Ornithine**	0.1	0.084	0.69	-0.046
Aspartate**	0.47	-0.021	0.08	0.11
Malate**	0.24	0.019	0.73	-0.048
α-Ketoglutarate**	0.31	0.0027	0.97	-0.056

Table 3 continued

Independent Variable	Oocyte ATP (pg)	ATP Correlation	Oocyte mtDNA Copy Number	mtDNA Copy Number Correlation
Glutamine**	0.1	0.081	0.84	-0.0539
Glutamate**	0.15	0.052	0.69	-0.0533
2-Oxo-4-Methylthiobutanoate**	0.91	-0.047	0.13	0.1677
Methionine**	0.53	-0.028	0.89	-0.0522
Xylose**	0.17	0.043	0.82	-0.0475
3-Methylphenylacetic Acid**	0.39	-0.011	0.68	0.0034
Allantoin**	0.08	0.096	0.69	-0.0467
Phenylalanine**	0.32	0.0021	0.77	-0.0477
Phenyllactic Acid**	0.38	-0.0086	0.81	-0.0554
Uric Acid**	0.06	0.12	0.8	-0.0484
N-Acetylornithine**	0.15	0.052	0.85	-0.0545
Arginine**	0.09	0.092	0.68	0.0044
Citrulline**	0.09	0.089	0.71	-0.0027
Tricarballylic Acid**	0.84	-0.045	0.36	-0.0549
Citrate/Isocitrate**	0.5	-0.025	0.69	-0.0455
2-Dehydro-D-Gluconate**	0.15	0.052	0.92	-0.0536
D-Gluconate**	0.09	0.091	0.98	-0.0544
Kynurenine**	0.26	0.016	0.93	-0.0064
Uridine**	0.26	0.015	0.78	-0.047
Cholate**	0.49	-0.023	0.63	-0.0525
Glycodeoxycholate**	0.42	-0.015	0.77	-0.0542
Cholesterol Sulfate**	0.49	-0.024	0.84	-0.0548
Glycine**	0.34	-0.0021	0.64	0.0607
Lactate**	0.67	-0.038	0.29	0.0388
Proline**	0.1	0.084	0.98	-0.0555
Guanidoacetic Acid**	0.12	0.067	0.19	-0.0456
Succinate/Methylmalonate**	0.52	-0.027	0.77	-0.0067
3-Hydroxyisovalerate**	0.12	0.068	0.96	-0.0245
Taurine**	0.33	-0.0011	0.12	0.0279
Citraconate**	0.13	0.064	0.12	-0.0518
Hydroxyproline**	0.04	0.16	0.79	0.1158

Table 3 continued

Independent Variable	Oocyte ATP (pg)	ATP Correlation	Oocyte mtDNA Copy Number	mtDNA Copy Number Correlation
Asparagine**	0.12	0.068	0.87	-0.054
Homocysteine**	0.45	-0.019	0.85	-0.053
Phosphorylethanolamine**	0.6	-0.034	0.04	0.17
Lysine**	0.3	0.006	0.81	-0.05
Hydroxyphenylacetate**	0.42	-0.015	0.71	-0.048
Xylitol**	0.75	-0.042	0.32	0.0034
2-3-Dihydroxybenzoate**	0.69	-0.039	0.7	-0.047
Histidine**	0.43	-0.017	0.72	-0.048
Orotate**	0.59	-0.033	0.96	-0.055
Methionine Sulfoxide**	0.07	0.11	0.73	-0.048
Quinolinate**	0.68	-0.039	0.9	-0.055
Phosphoenolpyruvate**	0.83	-0.045	0.31	0.0044
Sulfolactate**	0.33	0.0004	0.34	-0.0027
SN-Glycerol-3-Phosphate**	0.65	-0.037	0.92	-0.055
Aconitate**	0.6	-0.034	0.68	-0.046
N-Carbamoyl-L-Aspartate**	0.16	0.048	0.86	-0.054
Allantoate**	0.36	-0.0063	0.89	-0.054
Myo-Inositol**	0.45	-0.019	0.36	-0.0064
Tyrosine**	0.3	0.006	0.71	-0.047
Acetyllysine**	0.12	0.067	0.82	-0.053
Homocitrulline**	0.03	0.17	0.88	-0.054
Tryptophan**	0.87	-0.046	0.91	-0.055
Xanthurenic Acid**	0.28	0.011	0.15	0.061
Jasmonate**	0.38	-0.0082	0.2	0.039
Cystathionine**	0.51	-0.026	0.97	-0.056
Deoxycytidine**	0.22	0.027	0.68	-0.046
Deoxyuridine**	0.9	-0.047	0.36	-0.0067
Ribose Phosphate**	0.17	0.044	0.47	-0.025
Cystine**	0.27	0.013	0.23	0.028
Cytidine**	0.19	0.038	0.8	-0.052
Biotin**	0.82	-0.045	0.08	0.12

Table 3 continued

Independent Variable	Oocyte ATP (pg)	ATP Correlation	Oocyte mtDNA Copy Number	mtDNA Copy Number Correlation
Thiamine**	0.18	0.042	0.92	-0.055
6-Phospho-D-Gluconate**	0.09	0.086	0.36	-0.0068
1-Methyladenosine**	0.11	0.077	0.79	-0.051
Ophthalmate**	0.14	0.06	0.19	0.045
S-Methyl-5-Thioadenosine**	0.3	0.0056	0.82	-0.052
N-Acetylglucosamine-1-6-Phosphate**	0.41	-0.014	0.47	-0.024
Trehalose/Sucrose**	0.52	-0.027	0.82	-0.053
GMP**	0.2	0.035	0.44	-0.021
Octulose Bisphosphate**	0.86	-0.046	0.87	-0.054
Taurodeoxycholate**	0.13	0.065	0.93	-0.055
Cysteine**	0.2	0.032	0.76	-0.05
Uracil**	0.11	0.078	0.19	0.045
Aminocaproic Acid**	0.24	0.02	0.72	-0.048
Trehalose-6-Phosphate**	0.18	0.04	0.32	0.0019
BCS***	0.87	---	0.33	---
BCS 5 x BCS 4****	0.97	---	1.0	---
BCS 6 x BCS 4****	0.9	---	0.86	---
BCS 7 x BCS 4****	0.98	---	0.99	---
BCS 8 x BCS 4****	0.85	---	0.36	---
BCS 6 x BCS 5****	1.0	---	0.82	---
BCS 7 x BCS 5****	1.0	---	0.99	---
BCS 8 x BCS 5****	0.97	---	0.30	---
BCS 7 x BCS 6****	1.0	---	0.98	---
BCS 8 x BCS 6****	1.0	---	0.71	---
BCS 8 x BCS 7****	0.97	---	0.50	---

* Analysis performed using linear regression including year as a random effect
** Analysis performed using linear regression on data from year two only
*** Analysis performed using ANOVA including year as a random effect
**** Pairwise comparisons performed on BCS ANOVA using Tukey post-hoc test

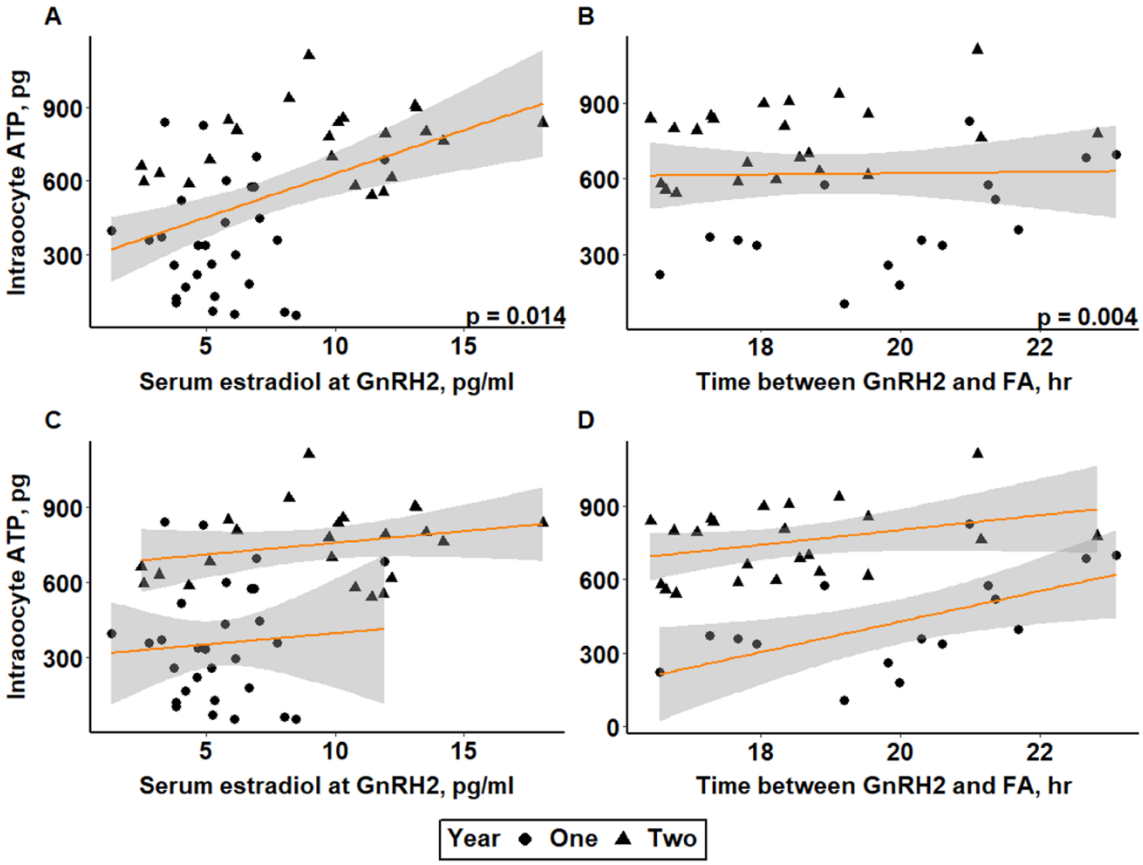

Figure 9. (A, C) Relationship between serum estradiol concentration at GnRH2 and intraoocyte ATP (pg). (B, D) Relationship between time from GnRH2 to FA and intraoocyte ATP (pg). Panels A and B depict the line of best fit for both years of the study, and panels C and D depict the line of best fit for each year individually. GnRH2 = gonadotropin releasing hormone administration to induce the pre-ovulatory gonadotropin surge, FA= pre-ovulatory follicle aspiration.

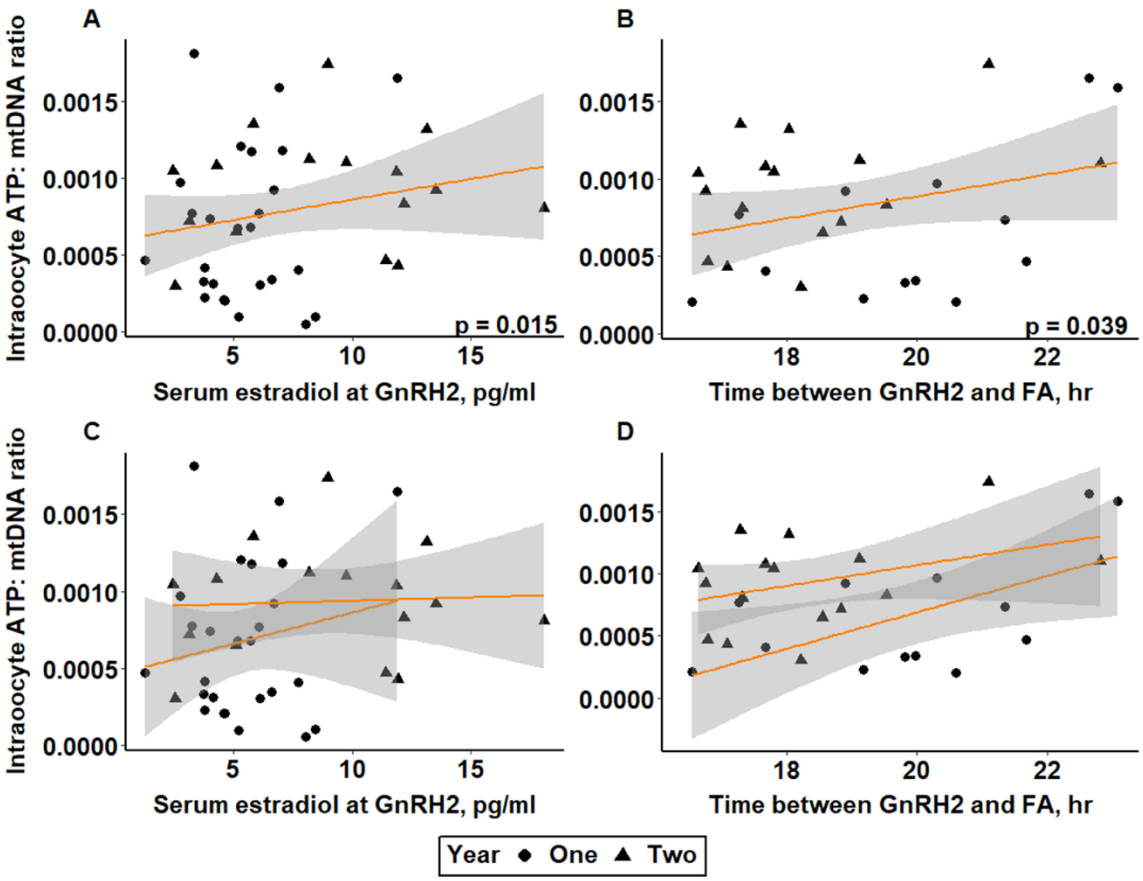

Figure 10. (A, C) Relationship between serum estradiol concentration at GnRH2 and intraoocyte ATP per mtDNA copy number ratio. (B, D) Relationship between time from GnRH2 to FA and intraoocyte ATP per mtDNA copy number ratio. Panels A and B depict the line of best fit for both years of the study, and panels C and D depict the line of best fit for each year individually. GnRH2 = gonadotropin releasing hormone administration to induce the pre-ovulatory gonadotropin surge, FA= pre-ovulatory follicle aspiration, mtDNA = mitochondrial DNA copy number.

through proestrus, it grows in diameter and produces increasing levels of estradiol (Alvarez et al., 2000; Fortune et al., 2004; Perry et al., 2005; Perry et al., 2014). Though both pre-ovulatory follicle diameter and serum estradiol concentration have been previously associated with embryo cleavage, embryo quality, and pregnancy success in animals that did not exhibit estrus, data from animals that did exhibit estrus and experience an endogenous gonadotropin surge determined that pre-ovulatory follicle diameter did not influence pregnancy outcome in estrual cows (Perry et al., 2005; Atkins et al., 2013). Therefore, pre-ovulatory follicle diameter is primarily an indicator of the follicle's physiological maturity and its proximity to reaching estradiol production required to stimulate estrus and an endogenous gonadotropin surge. As such, there is variation in serum estradiol concentration across pre-ovulatory follicle diameters among cows requiring exogenous GnRH to induce ovulation (Jinks et al., 2013), which indicates that follicle maturity is likely equally variable across such follicles. The results of the present study support the notion that serum estradiol concentration is more closely tied to follicle maturity prior to the induced gonadotropin surge than follicle diameter and may have a stronger correlation with oocyte metabolic capacity. The positive relationship between intraoocyte ATP (pg) at ~19 hours post GnRH2 and serum estradiol concentration at the time of GnRH2 likely indicates that the oocyte was allowed to progress further through capacitation prior to induction of the LH surge and oocyte maturation. The oocyte would have an improved ability to produce ATP due to an increased opportunity to accumulate the stores of metabolic substrates like pyruvate, lactate, and lipids through gap junctional transfer from the cumulus cells prior to maturation and the disruption of such transfer (Fair

et al., 1997; Swain and Pool, 2008; Zhang and Smith, 2015; Reader et al., 2017; Conti and Franciosi, 2018). These metabolic substrates are required by the oocyte or early embryo's mitochondria to produce ATP during oocyte maturation and embryo development to the blastocyst stage (Biggers et al., 1967; Chappel, 2013; Ge et al., 2013; Dalton et al., 2014; Aguila et al., 2020). Aside from indicating advanced follicle maturity prior to the induced gonadotropin surge, increased estradiol concentration at GnRH2 may also have a more direct effect on COC metabolism as exposure of the COC to estrogen increases the expression of gap junctional proteins and increases their localization to the plasma membrane (Firestone and Kapadia, 2012). This increase in functional gap junctions enhances the ability of the cumulus cells to transport cGMP to the oocyte as well as the metabolic substrates needed to support oocyte and embryo development. Because the oocyte relies on gap junction transport to store pyruvate, lipids, and other metabolic substrates, increased functional gap junctions during proestrus could allow for more effective transport of these materials and thus greater ATP levels in oocytes collected from pre-ovulatory follicles of increased estradiol production.

As the oocyte progresses from the germinal vesicle (GV) stage to MII, the activity of its mitochondria increases to produce the ATP necessary to sustain progression through meiotic maturation (Fair et al., 1997; Jeong et al., 2009; Chappel, 2013; Dalton et al., 2014; Aguila et al., 2020). The positive relationship between time from GnRH2 to follicle aspiration and ATP level or ATP per mtDNA copy number observed in the present study reflects this increase in mitochondrial activity during oocyte maturation. Because the pre-ovulatory gonadotropin surge, and thus the onset of oocyte maturation, is induced

approximately 2 hours after GnRH is administered (Giordano et al., 2012), the positive correlation between time from GnRH2 to follicle aspiration is also related to the stage of meiotic resumption of the oocyte. Oocytes in the current study were collected from 16.42 to 23.08 hours after GnRH2 administration and, thus, would have reached approximately 15-21 hours of oocyte maturation. *In vitro* studies have indicated that bovine oocytes reach MI at approximately 10-15 hours of maturation and MII at approximately 18-24 hours of maturation (Sirard et al., 1989; Fair et al., 1995; Hyttel et al., 1997). Therefore, the oocytes utilized in this study should all have completed MI and have reached or are nearing MII. Multiple studies have demonstrated that intraoocyte ATP increases as oocytes progress from GV to MII (Jiao et al., 2007; Iwata et al., 2011; Read et al., 2021a). Therefore, increased time between the administration of GnRH2 and follicle aspiration would result in an oocyte closer to MII with increased levels of intraoocyte ATP.

As the oocyte progresses from the germinal vesicle (GV) stage to MII, the activity of its mitochondria increases to produce the ATP necessary to sustain progression through meiotic maturation (Fair et al., 1997; Jeong et al., 2009; Chappel, 2013; Dalton et al., 2014; Aguila et al., 2020). The positive correlation between time from GnRH2 to follicle aspiration and ATP level or ATP per mtDNA copy number observed in the present study reflects this increase in mitochondrial activity during oocyte maturation. Because the pre-ovulatory gonadotropin surge, and thus the onset of oocyte maturation, is induced approximately 2 hours after GnRH is administered (Giordano et al., 2012), the positive correlation between time from GnRH2 to follicle aspiration is also related to the stage of meiotic resumption of the oocyte. Oocytes in the current study were collected from 16.42

to 23.08 hours after GnRH2 administration and, thus, would have reached approximately 15-21 hours of oocyte maturation. In vitro studies have indicated that bovine oocytes reach MI at approximately 10-15 hours of maturation and MII at approximately 18-24 hours of maturation (Sirard et al., 1989; Fair et al., 1995; Hyttel et al., 1997). Therefore, the oocytes utilized in this study should all have completed MI and have reached or are nearing MII. Multiple studies have demonstrated that intraoocyte ATP increases as oocytes progress from GV to MII (Jiao et al., 2007; Iwata et al., 2011; Read et al., 2021a). Therefore, increased time between the administration of GnRH2 and follicle aspiration would result in an oocyte closer to MII with increased levels of intraoocyte ATP.

The impact of follicle physiological status on follicular fluid metabolites

We previously determined that pre-ovulatory follicle diameter at GnRH2 was positively correlated with abundance of follicular fluid metabolites potentially involved in glucose metabolism, proteinogenesis, DNA methylation, and oxidative balance (Read et al., 2021b). In the current study, we aimed to determine repeatability of such a relationship and determine if abundance of follicular fluid metabolites was related to intraoocyte ATP levels. We detected 90 metabolites in the follicular fluid of the aspirated pre-ovulatory follicles (Table 4). Serum estradiol concentration at GnRH2 was positively associated with the abundance of 22 follicular fluid metabolites (FDR < 0.10; Figure 4, Table 4). There was no relationship between follicle diameter at GnRH2 and abundance of any metabolites (FDR > 0.90; Table 4). However, four of the metabolites positively related to serum estradiol at GnRH2 were previously determined to be positively correlated with follicle diameter at GnRH2 (2-dehydro-d-gluconate, 3-methylphenylacetic acid, α-ketoglutarate,

and pyruvate). Follicular fluid progesterone concentration at the time of follicle aspiration was significantly associated with the abundance of 62 metabolites (FDR < 0.10; Figure 4, Table 4). A positive relationship between follicular fluid progesterone concentration and metabolite abundance was identified in each significant metabolite with the exception of N-carbamoyl-l-aspartate and aspartate. Animal weight was negatively related to the abundance of 60 metabolites and positively related to 1 metabolite, phosphoenolpyruvate (FDR < 0.10; Figure 4, Table 4). Covariates of BCS, hours from GnRH2 to follicle aspiration, follicular fluid estradiol, and/or days postpartum also contributed significantly to the abundance of 12 follicular fluid metabolites (FDR < 0.10; Table 4).

The KEGG pathways 'Aminoacyl tRNA biosynthesis' and the 'Citrate cycle' were significantly enriched with metabolites positively related to serum estradiol concentration at GnRH2 (FDR < 0.10; Figure 5, Table 5). Interestingly, metabolites significantly associated with follicular fluid progesterone concentration at follicle aspiration and with cow weight also were enriched within KEGG pathways 'Aminoacyl tRNA biosynthesis', and 'Citrate cycle' as well as 'Arginine biosynthesis', 'Arginine and proline metabolism', 'Alanine, aspartate, and glutamate metabolism', 'D-glutamine and D-glutamate metabolism', 'Glyoxylate and dicarboxylate metabolism', 'Cysteine and methionine metabolism', 'Phenylalanine, tyrosine, and tryptophan biosynthesis' and 'Pyrimidine metabolism' (FDR<0.10; Figure 5, Tables 6 and 7). The KEGG pathways 'Glycine, serine, and threonine metabolism' and 'Phenylalanine metabolism' were also enriched with metabolites significantly correlated with follicular fluid progesterone concentration at follicle aspiration (FDR < 0.10; Figure 5, Table 6).

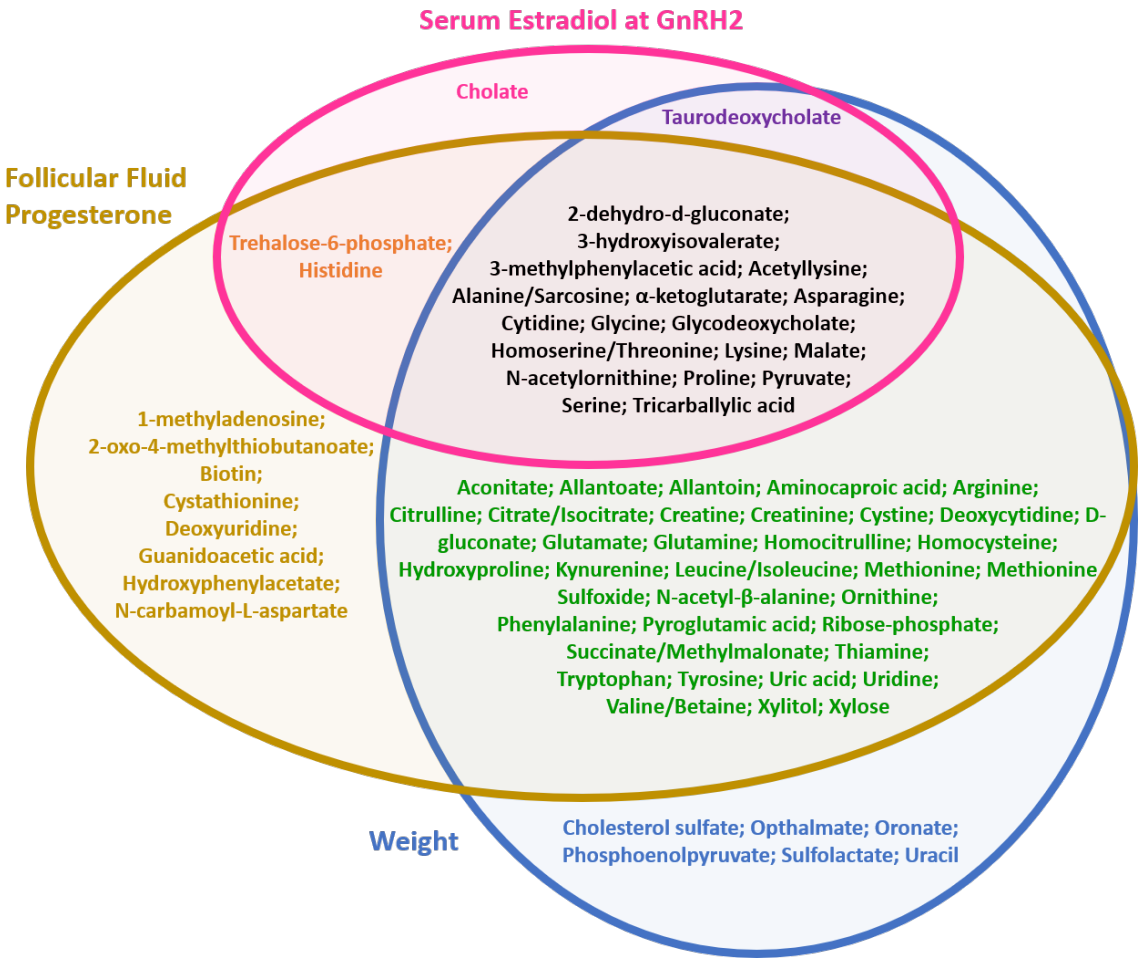

Figure 11. Venn diagram listing the follicular fluid metabolites whose abundance in follicular fluid collected ~19 hours after GnRH2 administration was significantly related to serum estradiol concentration at GnRH2 (pg/ml), follicular fluid progesterone concentration at follicle aspiration (ng/ml), and cow weight (kg). GnRH2 = gonadotropin releasing hormone administration to induce the pre-ovulatory gonadotropin surge.

Table 4: False discovery rate values for the correlation between follicular fluid metabolites and serum estradiol at GnRH2[1], pre-ovulatory follicle diameter at GnRH2, or final model covariates.

Metabolite	KEGG ID[1]	False Discovery Rate							
		Serum E2[2] at GnRH2[3] (pg/ml)	Follicle diameter at GnRH2 (mm)	FF[4] P4[5] at FA[6] (ng/ml)	Weight (kg)	Hours GnRH2 to FA	BCS[7]	FF E2 at FA (ng/ml)	Days Postpartum
Taurodeoxycholate	C05463	0.034	0.998	NA [5]	0.002	NA	NA	NA	NA
Glycine	C00037	0.036	0.998	0.001	0.003	NA	NA	NA	NA
3-Hydroxyisovalerate	C20827	0.038	0.998	0.002	0.017	0.046	NA	0.035	NA
2-Dehydro-D-Gluconate	C03342	0.045	0.998	0.005	0.004	NA	NA	NA	NA
3-Methylphenylacetic Acid	12121[9]	0.045	0.998	0.006	0.007	NA	NA	NA	NA
Acetyllysine	C12989	0.045	0.998	0.001	0.003	NA	NA	NA	NA
Cholate	C00695	0.045	0.998	NA	NA	NA	0.037	NA	NA
Glycodeoxycholate	C05464	0.045	0.998	0.046	0.013	NA	NA	NA	NA
Histidine	C00135	0.045	0.998	0.002	0.129	NA	NA	NA	NA
Malate	C00149	0.045	0.998	0.005	0.014	NA	NA	NA	NA
Trehalose-6-Phosphate	C00689	0.045	0.998	0.001	NA	NA	NA	0.035	NA
Alanine/Sarcosine	C00041; C00213	0.054	0.998	0.001	0.002	NA	NA	NA	NA
A-Ketoglutarate	C00026	0.054	0.998	0.003	0.012	NA	NA	NA	NA
Tricarballylic Acid	C19806	0.054	0.998	0.015	0.013	NA	NA	NA	NA
Pyruvate	C00022	0.060	0.998	0.006	0.007	NA	NA	NA	NA
Asparagine	C00152	0.060	0.998	0.001	0.004	NA	NA	NA	NA
Cytidine	C00475	0.060	0.998	0.003	0.004	NA	NA	NA	NA
Proline	C00148	0.069	0.998	0.002	0.003	NA	NA	NA	NA
Homoserine/Threonine	C00263; C00188	0.075	0.998	0.002	0.003	NA	NA	NA	NA
Lysine	C00047	0.094	0.998	0.001	0.008	NA	NA	NA	NA
N-Acetylornithine	C00437	0.094	0.998	0.002	0.002	NA	NA	NA	NA
Serine	C00716	0.094	0.998	0.002	0.003	NA	NA	NA	NA
Ribose Phosphate	C00117	0.101	0.998	0.005	0.013	NA	NA	NA	NA
Allantoate	C00499	0.101	0.998	0.006	0.008	NA	NA	NA	NA
Citrate Isocitrate	C00158; C00311	0.108	0.998	0.003	0.015	NA	NA	NA	NA
Creatinine	C00791	0.108	0.998	0.001	0.011	NA	NA	NA	NA
Xylose	C00181	0.108	0.998	0.002	0.004	NA	NA	NA	NA
Creatine	C00300	0.132	0.998	0.002	0.003	0.056	NA	NA	NA
Allantoin	C01551	0.135	0.998	0.002	0.007	NA	NA	NA	NA
1-Methyladenosine	C02494	0.138	0.998	0.015	NA	0.020	0.049	0.042	NA
Homocysteine	C00155	0.138	0.998	0.002	0.019	NA	NA	NA	NA

Table 4 continued

Metabolite	KEGG ID[1]	False Discovery Rate							
		Serum E2[2] at GnRH2[3] (pg/ml)	Follicle diameter at GnRH2 (mm)	FF[4] P4[5] at FA[6] (ng/ml)	Weight (kg)	Hours GnRH2 to FA	BCS[7]	FF E2 at FA (ng/ml)	Days Postpartum
Kynurenine	C00328	0.138	0.998	0.009	0.004	NA	NA	NA	NA
Uridine	C00299	0.139	0.998	0.004	0.017	NA	NA	NA	NA
N-Acetyl-β-Alanine	C01073	0.139	0.998	0.013	0.010	NA	NA	NA	NA
Glutamine	C00064	0.140	0.998	0.001	0.004	NA	NA	NA	NA
Homocitrulline	C02427	0.140	0.998	0.015	0.024	NA	NA	NA	NA
Succinate/Methylmalonate	C00042; C02170	0.140	0.998	0.023	0.039	NA	NA	NA	NA
Methionine	C00073	0.141	0.998	0.006	0.034	NA	NA	NA	NA
Phosphoenolpyruvate	C00074	0.141	0.998	NA	0.0276	0.056	NA	NA	NA
Hydroxyproline	C01157	0.152	0.998	0.0002	0.002	NA	NA	NA	NA
Xylitol	C00379	0.152	0.998	0.013	0.070	NA	NA	NA	NA
Deoxycytidine	C00881	0.164	0.998	0.004	0.011	NA	NA	NA	NA
Tryptophan	C00078	0.183	0.998	0.015	0.031	NA	NA	NA	NA
Aconitate	C00417	0.198	0.998	0.003	0.031	NA	NA	NA	NA
Phenylalanine	C00079	0.198	0.998	0.023	0.025	0.406	NA	NA	NA
Pyroglutamic Acid	C01879	0.198	0.998	0.005	0.007	NA	NA	NA	NA
Tyrosine	C00082	0.198	0.998	0.006	0.019	NA	NA	NA	NA
N-Carbamoyl-L-Aspartate	C00438	0.200	0.739	0.006	NA	NA	NA	NA	NA
Valine/Betaine	C00183; C00719	0.200	0.998	0.006	0.013	NA	NA	NA	NA
D-Gluconate	C00257	0.201	0.998	0.004	0.004	NA	NA	NA	NA
Sulfolactate	C11537	0.209	0.998	NA	0.031	NA	NA	NA	NA
Thiamine	C00378	0.215	0.998	0.003	0.008	NA	NA	NA	NA
Aminocaproic Acid	C02378	0.228	0.998	0.007	0.010	NA	NA	NA	NA
Glutamate	C00025	0.228	0.998	0.014	0.036	NA	NA	NA	NA
Leucine/Isoleucine	C00123; C00407	0.228	0.998	0.011	0.010	NA	NA	NA	NA
SN-Glycerol-3-Phosphate	C00093	0.239	0.998	NA	NA	NA	NA	NA	NA
2-Oxo-4-Methylthiobutanoate	C01180	0.271	0.998	0.029	NA	NA	NA	NA	NA
Uracil	C00106	0.271	0.998	NA	0.029	NA	NA	NA	NA
Ophthalmate	C21016	0.278	0.998	NA	0.029	NA	NA	NA	NA
Arginine	C00062	0.309	0.998	0.001	0.003	NA	NA	NA	NA
Deoxyuridine	C00526	0.321	0.998	0.008	NA	NA	NA	NA	NA
Ornithine	C00077	0.321	0.998	0.001	0.004	NA	NA	NA	NA

Table 4 continued

Metabolite	KEGG ID[1]	False Discovery Rate							
		Serum E2[2] at GnRH2[3] (pg/ml)	Follicle diameter at GnRH2 (mm)	FF[4] P4[5] at FA[6] (ng/ml)	Weight (kg)	Hours GnRH2 to FA	BCS[7]	FF E2 at FA (ng/ml)	Days Postpartum
Cystathionine	C02291	0.324	0.998	0.011	NA	NA	NA	NA	NA
6-Phospho-D-Gluconate	C00345	0.335	0.998	NA	NA	NA	NA	NA	NA
Citrulline	C00327	0.350	0.998	0.001	0.004	NA	NA	NA	NA
Cysteine	C00097	0.380	0.998	NA	NA	NA	NA	NA	NA
Guanidoacetic Acid	C00581	0.430	0.998	0.006	NA	NA	NA	NA	NA
Taurine	C00245	0.432	0.998	NA	NA	NA	NA	NA	NA
Uric Acid	C00366	0.432	0.998	0.011	0.008	NA	NA	NA	NA
Trehalose Sucrose	C01083; C00089	0.472	0.998	NA	NA	NA	NA	NA	NA
Methionine Sulfoxide	C02989	0.505	0.998	0.003	0.007	NA	NA	NA	NA
Hydroxyphenylacetate	C05852	0.516	0.998	0.046	NA	NA	0.037	NA	NA
Cholesterol Sulfate	C18043	0.523	0.998	NA	0.008	0.0163	NA	NA	NA
Orotate	C00295	0.545	0.998	NA	0.037	NA	NA	NA	NA
Octulose Bisphosphate	---	0.588	0.998	NA	NA	NA	NA	NA	NA
2-3-Dihydroxybenzoate	C00230	0.598	0.998	NA	NA	NA	0.042	NA	NA
N-Acetylglucosamine-1-6-Phosphate	C00357	0.663	0.998	NA	NA	NA	NA	NA	NA
Cystine	C00491	0.706	0.998	0.0138	0.031	NA	NA	NA	NA
s-Methyl-5-Thioadenosine	C00170	0.706	0.998	NA	NA	NA	0.042	NA	0.007
GMP	C00144	0.716	0.998	NA	NA	NA	NA	NA	NA
Biotin	C00120	0.742	0.998	0.019	NA	NA	NA	NA	NA
Lactate	C00186	0.742	0.998	NA	NA	NA	NA	NA	NA
Myo-Inositol	C00137	0.742	0.998	NA	NA	NA	NA	NA	NA
Phosphorylethanolamine	C00346	0.742	0.998	NA	NA	NA	NA	NA	NA
Quinolinate	C03722	0.742	0.998	NA	NA	NA	NA	NA	NA
Aspartate	C00049	0.755	0.998	NA	NA	NA	NA	NA	NA
Xanthurenic Acid	C02470	0.794	0.998	NA	NA	NA	NA	NA	NA
Phenyllactic Acid	C01479	0.823	0.998	NA	NA	NA	NA	NA	NA
Jasmonate	C08491	0.968	0.998	NA	NA	NA	NA	NA	NA
Citraconate	C02226	0.992	0.998	NA	NA	0.016	NA	NA	NA

[1] KEGG = Kyoto Encyclopedia of Genes and Genomes
[2] E2 = Estradiol
[3] GnRH2 = Gonadotropin releasing hormone administration to induce the pre-ovulatory gonadotropin surge
[4] FF = Follicular fluid
[5] P4 = Progesterone
[6] FA = Follicle aspiration
[7] BCS = Body condition score
[8] Pubmed chem ID

Metabolites that were significantly associated with serum estradiol concentration at GnRH2, follicular fluid progesterone concentration at follicle aspiration, and/or weight were primarily involved in proteinogenesis, the citric acid cycle, and pyrimidine metabolism. Follicular fluid composition fluctuates throughout the estrous cycle and can be influenced by multiple extraovarian factors including ovarian stimulation protocols (Fortune and Hansel, 1985; Assey et al., 1994; Ambrose et al., 2006; Leroy et al., 2006; Bender et al., 2010; Von Wald et al., 2010; Wonnacott et al., 2010; Zachut et al., 2010; Leroy et al., 2011; Liu et al., 2012; Alves et al., 2014; O'Doherty et al., 2014; Palini et al., 2014; Moreno et al., 2015; Forde et al., 2016; Takeo et al., 2017). Inducing the pre-ovulatory gonadotropin surge in physiologically immature dominant follicles prior to the onset of estrus could result in decreased levels of metabolites involved in proteinogenesis and the citric acid cycle. This is consistent with our previous study that reported decreased abundance of metabolites enriched the KEGG pathway 'aminoacyl tRNA biosynthesis' as well as multiple pathways associated with the production of citric acid cycle intermediates in pre-follicles with decreased diameter (Read et al., 2021b). The positive relationship between serum estradiol concentration at GnRH2 administration and metabolites involved in proteinogenesis or the citric acid cycle suggests altered protein production and metabolism throughout the time period of oocyte maturation in less physiologically mature follicles near the time of the pre-ovulatory gonadotropin surge.

Follicular fluid collected from ovulatory follicles contains proteins that are important for luteinization, maturation of the oocyte, and expansion of the cumulus cells (Krisher, 2013; Brown et al., 2017; Ferrazza et al., 2017). Bovine ovulatory follicles have increased

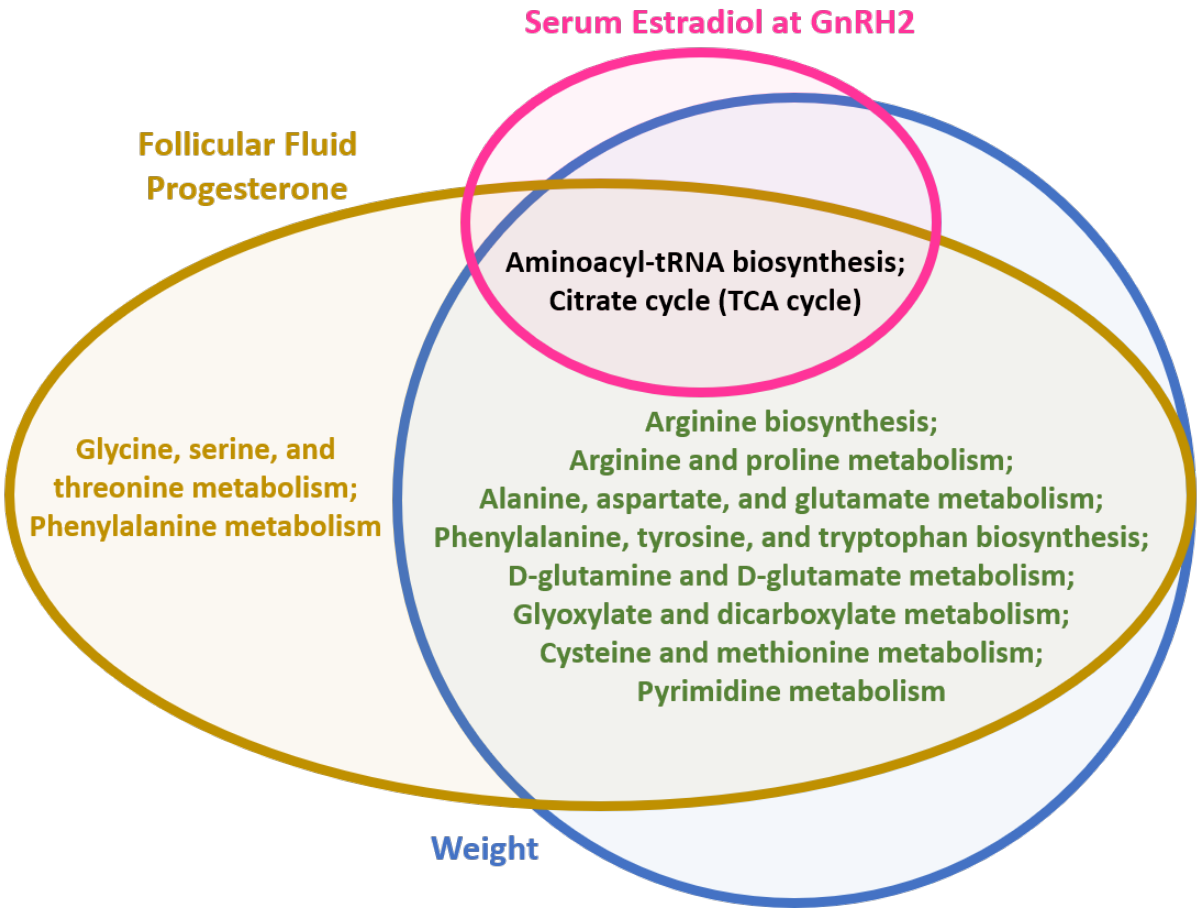

Figure 12. Venn diagram listing the KEGG pathways significantly enriched with follicular fluid metabolites related to serum estradiol concentration at GnRH2 (pg/ml), follicular fluid progesterone concentration at follicle aspiration (ng/ml), and cow weight (kg). GnRH2 = gonadotropin releasing hormone administration to induce the pre-ovulatory gonadotropin surge.

Table 5: KEGG pathways significantly enriched with metabolites that were significantly correlated with serum estradiol concentration at GnRH2.

Pathway	Pathway Name	Match Status[1]	FDR [2]	Differentially Abundant Metabolites in Pathway[3]
bta00970	Aminoacyl-tRNA biosynthesis	5 of 48	0.018259	L-Asparagine (C00152), L-Histidine (C00135), Glycine (C00037), L-Lysine (C00047), L-Proline (C00148)
bta00020	Citrate cycle (TCA cycle)	3 of 20	0.070452	α-ketoglutarate (C00026), S-Malate (C00149), Pyruvate (C00022)

[1] Number of differentially abundant metabolites in pathway/total number of metabolites in pathway

[2] FDR = False Discovery Rate

[3] Displayed as Name (KEGG identifier number); KEGG = Kyoto Encyclopedia of Genes and Genomes

Table 6: KEGG pathways significantly enriched with metabolites that were significantly correlated with follicular fluid progesterone concentration at follicle aspiration.

Pathway	Pathway Name	Match Status [1]	FDR [2]	Differentially Abundant Metabolites in Pathway [3]
bta00970	Aminoacyl-tRNA biosynthesis	12 of 48	< 0.001	L-Asparagine (C00152), L-Histidine (C00135), L-Phenylalanine (C00079), L-Arginine (C00062), L-Glutamine (C00064), Glycine (C00135), L-Methionine (C00073), Glycine (C00047), Tryptophan (C00078), L-Tyrosine (C00082), Glycine (C00148), L-Glutamate (C00025)
bta00220	Arginine biosynthesis	7 of 14	< 0.001	L-Glutamate (C00025), L-Arginine (C00062), N-Acetylornithine (C00437), L-Citrulline (C00327), L-Ornithine (C00077), L-Glutamine (C00064), α-ketoglutarate (C00026)
bta00330	Arginine and proline metabolism	8 of 38	0.001	L-Arginine (C00062), Guanidinoacetate (C00581), Creatine (C00300), Hydroxyproline (C01157), Glycine (C00148), L-Glutamate (C00025), L-Ornithine (C00077), Pyruvate (C00022)
bta00250	Alanine, aspartate and glutamate metabolism	6 of 28	0.008	L-Asparagine (C00152), L-Glutamate (C00025), L-Glutamine (C00064), Pyruvate (C00149), N-Carbamoyl-L-aspartate (C00438), α-ketoglutarate (C00026)
bta00471	D-Glutamine and D-glutamate metabolism	3 of 5	0.008	L-Glutamate (C00025), L-Glutamine (C00064), α-ketoglutarate (C00026)
bta00630	Glyoxylate and dicarboxylate metabolism	6 of 32	0.012	cis-Aconitate (C00417), S-Malate (C00149), Glycine (C00135), L-Glutamate (C00025), Pyruvate (C00149), L-Glutamine (C00064)
bta00270	Cysteine and methionine metabolism	6 of 33	0.012	4-Methylthio-2-oxobutanoic acid (C01180), L-Cystathionine (C02291), L-Homocysteine (C00155), L-Methionine (C00073), L-Cystine (C00491), Pyruvate (C00149)
bta00240	Pyrimidine metabolism	6 of 38	0.023	L-Glutamine (C00064), Uridine (C00299), Cytidine (C00475), Deoxycitidine (C00881), Deoxyuridine (C00299), N-Carbamoyl-L-aspartate (C00438)
bta00020	Citrate cycle (TCA cycle)	4 of 20	0.049	α-ketoglutarate (C00026), S-Malate (C00149), cis-Aconitate (C00417), Pyruvate (C00149)
bta00260	Glycine, serine and threonine metabolism	5 of 34	0.058	Guanidinoacetate (C00581), L-Cystathionine (C02291), Glycine (C00135), Creatine (C00300), Pyruvate (C00149)
bta00400	Phenylalanine, tyrosine, and tryptophan biosynthesis	2 of 4	0.058	L-Phenylalanine (C00079), L-Tyrosine (C00082)
bta00360	Phenylalanine metabolism	3 of 12	0.058	L-Phenylalanine (C00079), 2-Hydroxyphenylacetate (C05852), L-Tyrosine (C00082)

[1] Number of differentially abundant metabolites in pathway/total number of metabolites in pathway

[2] FDR = False Discovery Rate

[3] Displayed as Name (KEGG identifier number); KEGG = Kyoto Encyclopedia of Genes and Genomes

Table 7: KEGG pathways significantly enriched with metabolites that were significantly correlated with animal weight.

Pathway	Pathway Name	Match Status [1]	FDR [2]	Differentially Abundant Metabolites in Pathway [3]
bta00220	Arginine biosynthesis	7 of 14	< 0.001	L-Glutamate (C00025); L-Arginine (C00062); N-Acetylornithine (C00437), L-Citrulline (C00327), L-Ornithine (C00077), L-Glutamine (C00064); α-ketoglutarate (C00026)
bta00970	Aminoacyl-tRNA biosynthesis	11 of 48	< 0.001	L-Asparagine (C00152), L-Phenylalanine (C00079); L-Arginine (C00062); L-Glutamine (C00064), Glycine (C00037), L-Methionine (C00073), L-Lycine (C00047), L-Tryptophan (C00078), L-Tyrosine (C00082); L-Proline (C00148); L-Glutamate (C00025)
bta00330	Arginine and proline metabolism	7 of 38	0.007	L-Arginine (C00062), Creatine (C00300), Hydroxyproline (C00148); L-Proline (C00148), L-Glutamate (C00025), L-Ornithine (C00077), Pyruvate (C00022)
bta00471	D-Glutamine and D-Glutamate metabolism	3 of 5	0.008	L-Glutamate (C00025); L-Glutamine (C00064); α-ketoglutarate (C00026)
bta00020	Citrate cycle (TCA cycle)	5 of 20	0.008	α-ketoglutarate (C00026), S-Malate (C00149); cis-Aconitate (C00417), Pyruvate (C00022), Phosphoenolpyruvate (C00074)
bta00630	Glyoxylate and dicarboxylate metabolism	6 of 32	0.009	cis-Aconitate (C00417), S-Malate (C00149), Glycine (C00037), L-Glutamate (C00025), Pyruvate (C00022), L-Glutamine (C00064)
bta00240	Pyrimidine metabolism	6 of 38	0.019	L-Glutamine (C00064), Uridine (C00299), Cytidine (C00475), Deoxycytidine (C00475), Orotate (C00295); Uracil (C00106)
bta00250	Alanine, aspartate and glutamate metabolism	5 of 28	0.024	Asparagine (C00152), L-Glutamate (C00025), L-Glutamine (C00064), Pyruvate (C00022), α-ketoglutarate (C00026)
bta00270	Cysteine and methionine metabolism	5 of 33	0.046	L-Homocysteine (C00155); L-Methionine (C00073), L-Cystine (C00491), Pyruvate (C00022), Ophthalmate
bta00400	Phenylalanine, tyrosine, and tryptophan biosynthesis	2 of 4	0.058	L-Phenylalanine (C00079); L-Tyrosine (C00082)

[1] Number of differentially abundant metabolites in pathway/total number of metabolites in pathway

[2] FDR = False Discovery Rate

[3] Displayed as Name (KEGG identifier number); KEGG = Kyoto Encyclopedia of Genes and Genomes

expression of proteins involved in inflammatory, nitric oxide synthase (NOS), and reactive oxygen species (ROS) pathways compared to follicular fluid obtained from follicles prior to the LH surge (Ferrazza et al., 2017). Free amino acids in the follicular fluid are important to support the increased protein production occurring during the peri-ovulatory time period. In fact, aberrant follicular fluid protein expression is associated with reduced fertility in dairy cattle (Zachut et al., 2016). Amino acids can also be converted to substrates for the citric acid cycle (Guda et al., 2007; Martínez-Reyes and Chandel, 2020). The citric acid cycle generates ATP for cellular energy and NADH/$FADH_2$ that are used during oxidative phosphorylation to generate additional energy (Fernie et al., 2004; Martínez-Reyes and Chandel, 2020). Increased levels of the metabolic substrates utilized by the citric acid cycle indicates increased citric acid cycle activity of the follicular cells. This aligns with previous studies demonstrating that cumulus cells have high glycolytic activity and NADH production (Biggers et al., 1967; Sutton-McDowall et al., 2010; Cinco et al., 2016; Richani et al., 2021).

The metabolites within the numerous pathways that were significantly associated with follicular fluid progesterone or weight are primarily involved in the citric acid cycle. They are either components of the citric acid cycle (pyruvate, malate, and α-ketoglutarate, cis-aconitate) or are amino acids that can be converted into cycle intermediates (tyrosine, phenylalanine, asparagine, glycine, cysteine, tryptophan, arginine, histidine, glutamine, glutamate, methionine). There may be a direct effect of follicular fluid progesterone concentration at the time of follicle aspiration on both COC metabolism and follicular fluid metabolites. Both bovine cumulus cells and oocytes express progesterone receptors

(Aparicio et al., 2011). In somatic cells, progesterone increases oxidative phosphorylation and beta oxidation (Behera et al., 2009; Dai et al., 2019; Dai et al., 2020; Lee et al., 2021). During oocyte meiotic maturation, energy production via oxidative phosphorylation increases (Biggers et al., 1967; Babayev and Seli, 2015; Coticchio et al., 2015; Brown et al., 2017). Beta oxidation of fatty acids also increases and is used to generate substrates for use in the citric acid cycle (Hyttel et al., 1986; Sturmey et al., 2009; Paczkowski et al., 2013; Dunning et al., 2014; Dalbies-Tran et al., 2020). The citric acid cycle produces ATP as well as the NADH and $FADH_2$ that are required for oxidative phosphorylation (Martínez-Reyes and Chandel, 2020). Based on this information, the increased presence of citric acid cycle components in follicular fluid with increased progesterone concentration could be directly due to progesterone receptor signaling to increase oxidative phosphorylation and beta oxidation within the oocyte and/or cumulus cells. Progesterone receptor signaling also induces the expression of genes involved with ovulation in granulosa cells (Robker et al., 2009).

Once false discovery rate was applied to account for testing multiple hypotheses, we did not detect a significant relationship between any follicular fluid metabolites and oocyte ATP level (FDR >0.10, Table 3). This preliminary experiment may have been performed too late in oocyte maturation to detect significant relationships among follicular fluid metabolites and oocyte ATP. Samples in the present study were collected near ovulation and the completion of oocyte maturation when the oocytes have decoupled from their surrounding cumulus cells. Collection of samples earlier or at the time of the pre-ovulatory gonadotropin surge, may have better represented the metabolic environment

available to the COC before or early in maturation when a higher level of active transfer of metabolites from the cumulus cells to the oocyte was present. Potential influences of granulosa cell metabolism on the follicular fluid metabolome may have also overshadowed potential relationships between the follicular fluid metabolome and oocyte ATP at ~19 hours after GnRH2 administration. We are optimistic to further explore relationships between the follicular fluid milieu and oocyte metabolic competency in future studies.

Conclusions

The results of the present study provided an essential advancement to our knowledge of the relationship between pre-ovulatory follicle physiological status near the time of an induced gonadotropin surge on oocyte developmental and metabolic competency. We identified a positive relationship between serum estradiol concentration at GnRH2 and time from GnRH2 to follicle aspiration on the availability of ATP within the oocyte after ~17 hours of maturation. Pre-ovulatory serum estradiol concentration's positive association with total ATP levels and ATP produced per mtDNA copy number in oocytes may be both correlative due to estradiol's relationship with follicle maturity at the time of GnRH2 and causative due to estradiol's upregulation of gap junction transfer of metabolites between the cumulus cells and oocyte. Oocyte meiotic maturation and early embryo development are energy-demanding processes, and the decreased developmental competence of oocytes following premature induction of the pre-ovulatory gonadotropin surge in physiologically immature pre-ovulatory follicle is likely due to decreased metabolic capacity of the oocyte. Additionally, we found a positive relationship between the follicle's physiological status before and after exposure to the pre-ovulatory

gonadotropin surge on the metabolome of the follicular fluid. Premature exposure of the follicle to the LH surge coupled with reduced follicular fluid progesterone production post surge resulted in an altered follicular environment that could have implications for oocyte developmental competence related to metabolism and areas beyond what was measured in this study. Future studies will seek to further elucidate the effects of premature induction of ovulation on oocyte developmental competence.

CONCLUSION

Previous studies have reported decreased pregnancy rate, embryo quality, and fertilization rate in cattle induced to ovulate prior to estrus during a FTAI protocol. A subsequent study reported decreased expression of transcripts involved with cumulus cell glycolysis and oocyte oxidative phosphorylation in cumulus-oocyte-complexes retrieved from smaller pre-ovulatory follicles exposed to an exogenous GnRH surge prior to estrus. The overall objective of the studies included in this dissertation was to examine the relationship between follicle physiological status at GnRH administration to induce the pre-ovulatory gonadotropin surge (GnRH2) and oocyte metabolic capacity and the follicular fluid metabolome. An initial study revealed eighteen out of thirty-eight metabolites in follicular fluid 19.59±0.34 hours after GnRH administration were positively correlated with follicle diameter at the time of GnRH administration. KEGG pathway analysis of the significantly correlated metabolites revealed significant enrichment in glucose metabolism, energy production, and proteinogenesis. The composition of the follicular fluid provides the cumulus-oocyte complex with nutrients and metabolic substrates that are important for the acquisition of oocyte developmental competence. Decreased availability of metabolites and proteinogenic components to cumulus-oocyte-complexes from smaller pre-ovulatory follicles may contribute to the reduced oocyte developmental competence and lower pregnancy rates observed when beef cows are induced to ovulate a smaller pre-ovulatory follicle. A method was developed to quantify intraoocyte ATP levels and mtDNA copy number within individual oocytes. This allowed us to determine the metabolic capacity of individual oocyte samples and relate it to the

physiological status of the corresponding follicle. We utilized these methods and identified a significant, positive relationship between oocyte ATP and serum estradiol concentration at GnRH2 as well as hours between GnRH2 and follicle aspiration. Reduced availability of ATP within the oocytes collected from pre-ovulatory follicles with decreased estradiol levels suggest an importance of completion of the oocyte capacitation phase on the metabolic capacity of the oocyte. The positive relationship between serum estradiol concentration and oocyte metabolic capacity could be due to estradiol's relationship with follicle maturity or because of the increase in functional gap junctions available to transport metabolic substrates between the cumulus cells and the oocyte. The positive relationship between oocyte ATP levels and time from GnRH2 administration to follicle aspiration is likely due to the increase in intraoocyte ATP levels observed as oocytes progress through meiotic maturation. We also identified a significant positive relationship between the physiological status of the follicle before and after exposure to the exogenous pre-ovulatory gonadotropin surge and follicular fluid metabolome profiles. Lower serum estradiol concentrations at the time of GnRH injection and reduced follicular fluid progesterone production by ~19 hours post surge was associated with alterations in 22 and 63 metabolites, respectively, that were enriched in KEGG pathways primarily related to proteinogenesis and the TCA cycle. Follicular fluid composition is susceptible to multiple extraovarian factors. Changes in the follicular fluid proteinogenic and TCA cycle components as a result of premature induction of ovulation are indicative of altered metabolism of the cells within the follicle. Future studies will seek to further elucidate the

importance of the pre-ovulatory follicular environment and the oocyte capacitation phase on oocyte metabolic capacity and developmental competence.

REFERENCES

Aardema, H., B. A. Roelen, H. T. van Tol, C. H. Oei, B. M. Gadella, and P. L. Vos. 2013. Follicular 17β-estradiol and progesterone concentrations and degree of cumulus cell expansion as predictors of in vivo-matured oocyte developmental competence in superstimulated heifers. Theriogenology. 80(6):576-583. doi: 10.1016/j.theriogenology.2013.05.025.

Abel, J. M., B. E. Bishop, J. M. Thomas, M. R. Ellersieck, S. E. Poock, M. F. Smith, and D. J. Patterson. 2017. Comparing strategies to synchronize estrus before fixed-time artificial insemination in primiparous 2-year-old beef cows. Theriogenology. 87:306-315. doi: 10.1016/j.theriogenology.2016.09.010.

Aerts, J. M., and P. E. Bols. 2010. Ovarian follicular dynamics. A review with emphasis on the bovine species. Part II: Antral development, exogenous influence and future prospects. Reproduction in domestic animals. Zuchthygiene. 45(1):180-187. doi: 10.1111/j.1439-0531.2008.01298x.

Aerts, J. M., and P. E. Bols. 2010. Ovarian follicular dynamics: a review with emphasis on the bovine species. Part I: Folliculogenesis and pre-antral follicle development. Reproduction in domestic animals. Zuchthygiene. 45(1):171-179. doi: 10.1111/j.1439-0531.2008.01302x.

Aguila, L., F. Treulen, J. Therrien, R. Felmer, M. Valdivia, and L. C. Smith. 2020. Oocyte selection for in vitro embryo production in bovine species: noninvasive approaches for new challenges of oocyte competence. Animals (Basel). 10(12):2196. doi: 10.3390/ani10122196.

Allrich, R. D. 1994. Endocrine and neural control of estrus in dairy cows. J. Dairy Sci. 77(9):2738-2744. doi: 10.3168/jds.S0022-0302(94)77216-7.

Alvarez, P., L. J. Spicer, C. C. Chase, Jr., M. E. Payton, T. D. Hamilton, R. E. Stewart, A. C. Hammond, T. A. Olson, and R. P. Wettemann. 2000. Ovarian and endocrine characteristics during an estrous cycle in Angus, Brahman, and Senepol cows in a subtropical environment. J. Anim. Sci. 78(5):1291-1302. doi: 10.2527/2000.7851291x.

Alves, B. G., K. A. Alves, M. C. Martins, L. S. Braga, T. H. Silva, B. G. Alves, R. M. Santos, T. V. Silva, M. A. Viu, M. E. Beletti, J. O. Jacomini, and M. L. Gambarini. 2014. Metabolic profile of serum and follicular fluid from postpartum dairy cows during summer and winter. Reprod. Fertil. Dev. 26(6):866-874. doi: 10.1071/rd13102.

Ambrose, D. J., J. P. Kastelic, R. Corbett, P. A. Pitney, H. V. Petit, J. A. Small, and P. Zalkovic. 2006. Lower pregnancy losses in lactating dairy cows fed a diet enriched in alpha-linolenic acid. J. Dairy. Sci. 89(8):3066-3074. doi: 10.3168/jds.S0022-0302(06)72581-4.

Aparicio, I. M., M. Garcia-Herreros, L. C. O'Shea, C. Hensey, P. Lonergan, and T. Fair. 2011. Expression, regulation, and function of progesterone receptors in bovine cumulus oocyte complexes during in vitro maturation. Biol. Reprod. 84(5):910-921. doi: 10.1095/biolreprod.110.087411.

Archer, S. L. 2013. Mitochondrial dynamics—mitochondrial fission and fusion in human diseases. N. Engl. J. Med. 369(23):2236-2251. doi: 10.1056/NEJMra1215233.

Arlotto, T., J. L. Schwartz, N. L. First, and M. L. Leibfried-Rutledge. 1996. Aspects of follicle and oocyte stage that affect in vitro maturation and development of bovine oocytes. Theriogenology. 45(5):943-956. doi: 10.1016/0093-691x(96)00024-6.

Assey, R. J., P. Hyttel, J. F. Roche, and M. Boland. 1994. Oocyte structure and follicular steroid concentrations in superovulated versus unstimulated heifers. Mol. Reprod. Dev. 39(1):8-16. doi: 10.1002/mrd.1080390103.

Atkins, J. A., M. F. Smith, M. D. MacNeil, E. M. Jinks, F. M. Abreu, L. J. Alexander, and T. W. Geary. 2013. Pregnancy establishment and maintenance in cattle. J. Anim. Sci. 91(2):722-733. doi: 10.2527/jas.2012-5368.

Atkins, J. A., M. F. Smith, K. J. Wells, and T. W. Geary. 2010. Factors affecting preovulatory follicle diameter and ovulation rate after gonadotropin-releasing hormone in postpartum beef cows. Part I: cycling cows. J. Anim. Sci. 88(7):2300-2310. doi: 10.2527/jas.2009-2531.

Atkins, J. A., M. F. Smith, K. J. Wells, and T. W. Geary. 2010. Factors affecting preovulatory follicle diameter and ovulation rate after gonadotropin-releasing hormone in postpartum beef cows. Part II: anestrous cows. J. Anim. Sci. 88(7):2311-2320. doi: 10.2527/jas.2009-2532.

ATP molarity was calculated using the GraphPad QuickCalcs Web site: https://www.graphpad.com/quickcalcs/molarityform/ (accessed June 2021).

Babayev, E., and E. Seli. 2015. Oocyte mitochondrial function and reproduction. Curr. Opin. Obstet. 27(3):175-181. doi: 10.1097/gco.0000000000000164.

Baka, S., and A. Malamitsi-Puchner. 2006. Novel follicular fluid factors influencing oocyte developmental potential in IVF: a review. Reprod. Biomed. Online. 12(4):500-506. doi: 10.1016/s1472-6483(10)62005-6.

Baruselli, P. S., R. M. Ferreira, M. F. Filho, and G. A. Bó. 2018. Review: using artificial insemination v. natural service in beef herds. Animal. 12(1):45-52. doi: 10.1017/s175173111800054x.

Bazer, F. W., T. E. Spencer, G. A. Johnson, and R. C. Burghardt. 2011. Uterine receptivity to implantation of blastocysts in mammals. Front. Biosci. 3:745-767. doi: 10.2741/s184.

Behera, M. A., Q. Dai, R. Garde, C. Saner, E. Jungheim, and T. M. Price. 2009. Progesterone stimulates mitochondrial activity with subsequent inhibition of apoptosis in MCF-10A benign breast epithelial cells. Am. J. Physiol. Endocrinol. Metab. 297(5):1089-1096. doi: 10.1152/ajpendo.00209.2009

Bender, K., S. Walsh, A. C. Evans, T. Fair, and L. Brennan. 2010. Metabolite concentrations in follicular fluid may explain differences in fertility between heifers and lactating cows. Reproduction. 139(6):1047-1055. doi: 10.1530/rep-10-0068.

Bernabé, B. P., I. Thiele, E. Galdones, A. Siletz, S. Chandrasekaran, T. K. Woodruff, L. J. Broadbelt, and L. D. Shea. 2019. Dynamic genome-scale cell-specific metabolic models reveal novel inter-cellular and intra-cellular metabolic communications during ovarian follicle development. BMC Bioinform. 20(1):1-16. doi: 10.1186/s12859-019-2825-2.

Berry, D. P., P. R. Amer, R. D. Evans, T. Byrne, A. R. Cromie, and F. Hely. 2019. A breeding index to rank beef bulls for use on dairy females to maximize profit. J. Dairy. Sci. 102(11):10056-10072. doi: 10.3168/jds.2019-16912.

Bertoldo, M. J., L. Nadal-Desbarats, N. Gérard, A. Dubois, P. K. Holyoake, and C. G. Grupen. 2013. Differences in the metabolomic signatures of porcine follicular fluid collected from environments associated with good and poor oocyte quality. Reproduction. 146(3):221-231. doi: 10.1530/rep-13-0142.

Biggers, J., D. Whittingham, and R. Donahue. 1967. The pattern of energy metabolism in the mouse oocyte and zygote. Proc. Natl. Acad. Sci. U.S.A. 58(2):560-567. doi: 10.1073/pnas.58.2.560.

Bilodeau-Goeseels, S. 2006. Effects of culture media and energy sources on the inhibition of nuclear maturation in bovine oocytes. Theriogenology. 66(2):297-306. doi: https://doi.org/10.1016/j.theriogenology.2005.11.014.

Bisinotto, R. S., and J. E. Santos. 2011. The use of endocrine treatments to improve pregnancy rates in cattle. Reprod. Fertil. Dev. 24(1):258-266. doi: 10.1071/rd11916.

Blaschka, C., G. Schuler, A. Sánchez-Guijo, B. Zimmer, S. Feller, F. Kotarski, S. A. Wudy, and C. Wrenzycki. 2018. Occurrence of sulfonated steroids and ovarian expression of steroid sulfatase and SULT1E1 in cyclic cows. J. Steroid. Biochem. Mol. Biol. 179:79-87. doi: 10.1016/j.jsbmb.2017.12.010.

Blondin, P., K. Coenen, L. A. Guilbault, and M. A. Sirard. 1996. Superovulation can reduce the developmental competence of bovine embryos. Theriogenology. 46(7):1191-1203. doi: 10.1016/s0093-691x(96)00290-7.

Blondin, P., and M. A. Sirard. 1995. Oocyte and follicular morphology as determining characteristics for developmental competence in bovine oocytes. Mol. Reprod. Dev. 41(1):54-62. doi: 10.1002/mrd.1080410109.

Bodensteiner, K. J., M. C. Wiltbank, D. R. Bergfelt, and O. J. Ginther. 1996. Alterations in follicular estradiol and gonadotropin receptors during development of bovine antral follicles. Theriogenology. 45(2):499-512. doi: https://doi.org/10.1016/0093-691X(95)00386-M.

Bódis, J., E. Sulyok, M. Koppán, V. Prémusz, K. Gödöny, W. Rascher, and M. Rauh. 2020. Tryptophan catabolism to serotonin and kynurenine in women undergoing in-vitro fertilization. Physiol. Res. 69(6):1113-1124. doi: 10.33549/physiolres.934435.

Bonacker, R. C., K. R. Gray, C. A. Breiner, J. M. Anderson, D. J. Patterson, C. M. Spinka, and J. M. Thomas. 2020. Comparison of the 7 & 7 Synch protocol and the 7-day CO-Synch + CIDR protocol among recipient beef cows in an embryo transfer program. Theriogenology. 158:490-496. doi: 10.1016/j.theriogenology.2020.09.033.

Boni, R. 2012. Origins and effects of oocyte quality in cattle. Anim. Reprod. 9(3):333-340.

Bou Nemer, L., H. Shi, B. R. Carr, R. A. Word, and O. Bukulmez. 2019. Effect of body weight on metabolic hormones and fatty acid metabolism in follicular fluid of women undergoing in vitro fertilization: a pilot study. Reprod. Sci. 26(3):404-411. doi: 10.1177/1933719118776787.

Boyer, C.N., A. P. Griffith, and K. L. DeLong. 2020. Reproductive failure and long-term profitability of spring- and fall-calving beef cows. J. Agric. Resour. 45(1):78-91. doi: 10.22004/ag.econ.298435.

Breuel, K. F., P. E. Lewis, F. N. Schrick, A. W. Lishman, E. K. Inskeep, and R. L. Butcher. 1993. Factors affecting fertility in the postpartum cow: role of the oocyte and follicle in conception rate. Biol. Reprod. 48(3):655-661. doi: 10.1095/biolreprod48.3.655.

Bridges, G. A., S. L. Lake, S. G. Kruse, S. L. Bird, B. J. Funnell, R. Arias, J. A. Walker, J. K. Grant, and G. A. Perry. 2014. Comparison of three CIDR-based fixed-time AI protocols in beef heifers. J. Anim. Sci. 92(7):3127-3133. doi: 10.2527/jas.2013-7404.

Brown, H. M., K. R. Dunning, M. Sutton-McDowall, R. B. Gilchrist, J. G. Thompson, and D. L. Russell. 2017. Failure to launch: aberrant cumulus gene expression during oocyte in vitro maturation. Reproduction. 153(3):109-120. doi: 10.1530/REP-16-0426

Bucher, A., R. Kasimanickam, J. B. Hall, J. M. DeJarnette, W. D. Whittier, W. Kähn, and Z. Xu. 2009. Fixed-time AI pregnancy rate following insemination with frozen-thawed or fresh-extended semen in progesterone supplemented CO-Synch protocol in beef cows. Theriogenology. 71(7):1180-1185. doi: https://doi.org/10.1016/j.theriogenology.2008.12.009.

Busch, D. C., J. A. Atkins, J. F. Bader, D. J. Schafer, D. J. Patterson, T. W. Geary, and M. F. Smith. 2008. Effect of ovulatory follicle size and expression of estrus on progesterone secretion in beef cows. J. Anim. Sci. 86(3):553-563. doi: 10.2527/jas.2007-0570.

Calarco, P. G. 1995. Polarization of mitochondria in the unfertilized mouse oocyte. Dev. Genet. 16(1):36-43. doi: 10.1002/dvg.1020160108.

Cao, L., H. Shitara, T. Horii, Y. Nagao, H. Imai, K. Abe, T. Hara, J.-I. Hayashi, and H. Yonekawa. 2007. The mitochondrial bottleneck occurs without reduction of mtDNA content in female mouse germ cells. Nat. Genet. 39(3):386-390. doi: 10.1038/ng1970.

Carter, F., N. Forde, P. Duffy, M. Wade, T. Fair, M. A. Crowe, A. C. Evans, D. A. Kenny, J. F. Roche, P. Lonergan. 2008. Effect of increasing progesterone concentration from Day 3 of pregnancy on subsequent embryo survival and development in beef heifers. Reprod. Fertil. Dev. 20(3):368-375. doi: 10.1071/rd07204.

Casas, E., and L. V. Cundiff. 2003. Maternal grandsire, granddam, and sire breed effects on growth and carcass traits of crossbred cattle. J. Anim. Sci. 81(4):904-911. doi: 10.2527/2003.814904x.

Cassano, E., L. Tosto, M. Balestrieri, L. Zicarelli, and P. Abrescia. 1999. Antioxidant defense in the follicular fluid of water buffalo. Cell. Physiol. Biochem. 9(2):106-116. doi: 10.1159/000016307.

Cetica, P., L. Pintos, G. Dalvit, and M. Beconi. 2002. Activity of key enzymes involved in glucose and triglyceride catabolism during bovine oocyte maturation in vitro. Reproduction. 124(5):675-681. doi: 10.1530/rep.0.1240675.

Chambers, M. C., B. Maclean, R. Burke, D. Amodei, D. L. Ruderman, S. Neumann, L. Gatto, B. Fischer, B. Pratt, J. Egertson, K. Hoff, D. Kessner, N. Tasman, N. Shulman, B. Frewen, T. A. Baker, M. Y. Brusniak, C. Paulse, D. Creasy, L. Flashner, K. Kani, C. Moulding, S. L. Seymour, L. M. Nuwaysir, B. Lefebvre, F. Kuhlmann, J. Roark, P. Rainer, S. Detlev, T. Hemenway, A. Huhmer, J. Langridge, B. Connolly, T. Chadick, K. Holly, J. Eckels, E. W. Deutsch, R. L. Moritz, J. E. Katz, D. B. Agus, M. MacCoss, D. L. Tabb, and P. Mallick. 2012. A cross-platform toolkit for mass spectrometry and proteomics. Nat. Biotechnol. 30(10):918-920. doi: 10.1038/nbt.2377.

Chang, S. C., J. D. Jones, R. D. Ellefson, and R. J. Ryan. 1976. The porcine ovarian follicle: I. Selected chemical analysis of follicular fluid at different developmental stages. Biol. Reprod. 15(3):321-328. doi: 10.1095/biolreprod15.3.321.

Chappel, S. 2013. The role of mitochondria from mature oocyte to viable blastocyst. Obstet. Gynecol. Int. 2013:183024. doi: 10.1155/2013/183024.

Chiaratti, M. R., F. F. Bressan, C. R. Ferreira, A. R. Caetano, L. C. Smith, A. E. Vercesi, and F. V. Meirelles. 2010. Embryo mitochondrial DNA depletion is reversed during early embryogenesis in cattle. Biol. Reprod. 82:76-85. doi: 10.1095/biolreprod.109.077776.

Christian, C. A., and S. M. Moenter. 2010. The neurobiology of preovulatory and estradiol-induced gonadotropin-releasing hormone surges. Endocr. Rev. 31(4): 544-577. doi: 10.1210/er.2009-0023.

Ciernia, L. A., G. A. Perry, M. F. Smith, J. J. Rich, E. J. Northrop, S. D. Perkins, J. A. Green, A. L. Zezeski, and T. W. Geary. 2021. Effect of estradiol preceding and progesterone subsequent to ovulation on proportion of postpartum beef cows pregnant. Anim. Reprod. Sci. 227:106-723. doi:10.1016/j.anireprosci.2021.106723.

Cinco, R., M. A. Digman, E. Gratton, and U. Luderer. 2016. Spatial Characterization of Bioenergetics and Metabolism of Primordial to Preovulatory Follicles in Whole Ex Vivo Murine Ovary. Biol. Reprod. 95(6):129. doi: 10.1095/biolreprod.116.142141

Clarke, H. G., S. A. Hope, S. Byers, and R. J. Rodgers. 2006. Formation of ovarian follicular fluid may be due to the osmotic potential of large glycosaminoglycans and proteoglycans J. Reprod. 132:119-131. doi: 10.1530/rep.1.00960.

Clasquin, M. F., E. Melamud, and J. D. Rabinowitz. 2012. LC-MS data processing with MAVEN: a metabolomic analysis and visualization engine. Curr. Protoc. Bioinformatics 14(14):11. doi: 10.1002/0471250953.bi1411s37.

Colazo, M. G., and R. J. Mapletoft. 2014. A review of current timed-AI (TAI) programs for beef and dairy cattle. Can. Vet. J. 55(8): 772-780.

Colazo, M. G., P. Whittaker, K. Macmillan, D. Bignell, G. Boender, R. de Carvalho Guimaraes, and R. J. Mapletoft. 2018. Evaluation of a modified GnRH-based timed-AI protocol associated with estrus detection in beef heifers inseminated with sex-selected or conventional semen. Theriogenology. 118:90-95. doi: 10.1016/j.theriogenology.2018.05.037.

Colonna, R., and F. Mangia. 1983. Mechanisms of amino acid uptake in cumulus-enclosed mouse oocytes. Biol. Reprod. 28:797-803. doi: 10.1095/biolreprod28.4.797.

Conti, M., and F. Franciosi. 2018. Acquisition of oocyte competence to develop as an embryo: integrated nuclear and cytoplasmic events. Hum Reprod Update 24:245-266. doi: 10.1093/humupd/dmx040.

Conti, M., M. Hsieh, A. M. Zamah, and J. S. Oh. 2012. Novel signaling mechanisms in the ovary during oocyte maturation and ovulation. Mol. Cell. 356(1-2):65-73. doi: 10.1016/j.mce.2011.11.002

Contreras-Solís, I., M. Catalá, S. Soto-Heras, M. Roura, M. T. Paramio, and D. Izquierdo. 2021. Effect of follicle size on hormonal status of follicular fluid, oocyte ATP content, and in vitro embryo production in prepubertal sheep. Domest Anim Endocrinol 75:106582. doi: 10.1016/j.domaniend.2020.106582

Cooke, R. F., K. G. Pohler, J. L. M. Vasconcelos, and R. L. A. Cerri. 2019. Estrous expression during a fixed-time artificial insemination protocol enhances development and interferon-tau messenger RNA expression in conceptuses from Bos indicus beef cows. Animal : an international journal of animal bioscience 13(11):2569-2575. doi: 10.1017/s1751731119000636

Coticchio, G., M. Dal Canto, M. Mignini Renzini, M. C. Guglielmo, F. Brambillasca, D. Turchi, P. V. Novara, and R. Fadini. 2015. Oocyte maturation: gamete-somatic cells interactions, meiotic resumption, cytoskeletal dynamics and cytoplasmic reorganization. Hum. Reprod. Update 21:427-454. doi:10.1093/humupd/dmv011.

Crews, D. 2002. The relationship between beef sire carcass EPD and progeny phenotype. Can. J. Anim. Sci. 82:503-506. doi: 10.4141/A02-037.

Crites, B. R., R. Vishwanath, A. M. Arnett, P. J. Bridges, W. R. Burris, K. R. McLeod, and L. H. Anderson. 2018. Conception risk of beef cattle after fixed-time artificial insemination using either SexedUltra™ 4M sex-sorted semen or conventional semen. Theriogenology 118:126-129. doi:10.1016/j.theriogenology.2018.05.003.

Cunningham, B. E., W. T. Magee, and H. D. Ritchie. 1987. Effects of using sires selected for yearling weight and crossbreeding with beef and dairy breeds: birth and weaning traits. J. Anim. Sci. 6:1591-1600. doi: 10.2527/jas1987.6461591x.

Cushman, R. A., M. F. Allan, R. M. Thallman, and L. V. Cundiff. 2007. Characterization of biological types of cattle (Cycle VII): Influence of postpartum interval and estrous cycle length on fertility12. J. Anim. Sci. 85:2156-2162. doi: 10.2527/jas.2007-0136.

Cushman, R. A., L. K. Kill, R. N. Funston, E. M. Mousel, and G. A. Perry. 2013. Heifer calving date positively influences calf weaning weights through six parturitions1. J. Anim. Sci. 91:4486-4491. doi: 10.2527/jas.2013-6465.

D'Aniello, G., N. Grieco, M. A. Di Filippo, F. Cappiello, E. Topo, E. D'Aniello, and S. Ronsini. 2007. Reproductive implication of D-aspartic acid in human pre-ovulatory follicular fluid. Hum. Reprod. 22:3178-3183. doi: 10.1093/humrep/dem328.

Da Broi, M. G., V. S. I. Giorgi, F. Wang, D. L. Keefe, D. Albertini, and P. A. Navarro. 2018. Influence of follicular fluid and cumulus cells on oocyte quality: clinical implications. J. Assist. Reprod. Genet. 35:735-751. doi: 10.1007/s10815-018-1143-3.

Dadarwal, D., F. C. F. Dias, G. P. Adams, and J. Singh. 2017. Effect of follicular aging on ATP content and mitochondria distribution in bovine oocytes. Theriogenology 89:348-358. doi: 10.1016/j.theriogenology.2016.09.039.

Dai, Q., C. E. Likes, A. L. Luz, L. Mao, J. S. Yeh, Z. Wei, M. Kuchibhatla, O. R. Ilkayeva, T. R. Koves, and T. M. Price. 2019. A Mitochondrial Progesterone Receptor Increases Cardiac Beta-Oxidation and Remodeling. JES. 3(2):446-467. doi: 10.1210/js.2018-00219

Dai, Q., M. P. Provost, D. J. Raburn, and T. M. Price. 2020. Progesterone Increases Mitochondria Membrane Potential in Non-human Primate Oocytes and Embryos. Reprod. Sci. 27(5):1206-1214. doi: 10.1007/s43032-019-00132-2

Dalbies-Tran, R., V. Cadoret, A. Desmarchais, S. Elis, V. Maillard, P. Monget, D. Monniaux, K. Reynaud, M. Saint-Dizier, and S. Uzbekova. 2020. A comparative analysis of oocyte development in mammals. Cells. 9(4). doi: 10.3390/cells9041002.

Dalton, C. M., G. Szabadkai, and J. Carroll. 2014. Measurement of ATP in single oocytes: Impact of maturation and cumulus cells on levels and consumption. J. Cell. Physiol. 229:353-361. doi: 10.1002/jcp.24457.

Damiran, D., K. A. Larson, L. T. Pearce, N. E. Erickson, and B. H. A. Lardner. 2018. Effect of calving period on beef cow longevity and lifetime productivity in western Canada. Transl. Anim. Sci. 2(1):61-65. doi: 10.1093/tas/txy020.

de Lima, M. A., F. Morotti, B. M. Bayeux, R. G. de Rezende, R. C. Botigelli, T. H. C. De Bem, P. K. Fontes, M. F. G. Nogueira, F. V. Meirelles, P. S. Baruselli, J. C. da Silveira, F. Perecin, and M. M. Seneda. 2020. Ovarian follicular dynamics, progesterone concentrations, pregnancy rates and transcriptional patterns in Bos indicus females with a high or low antral follicle count. Sci. Rep. 10:19557. doi: 10.1038/s41598-020-76601-5.

de Loos, F. A. M., M. M. Bevers, S. J. Dieleman, and T. A. M. Kruip. 1991. Morphology of preovulatory bovine follicles as related to oocyte maturation. Theriogenology 35:527-535. doi: https://doi.org/10.1016/0093-691X(91)90449-N.

De los Reyes, M., M. L. Villagrán, R. Cepeda, M. Duchens, V. Parraguez, and B. Urquieta. 2006. Histological characteristics and steroid concentration of ovarian follicles at different stages of development in pregnant and non-pregnant dairy cows. Vet. Res. Commun. 30:161-173. doi: 10.1007/s11259-006-3100-3.

Dickinson, S., T. Geary, J. Monnig, K. Pohler, J. Green, and M. Smith. 2016. Effect of preovulatory follicle maturity on pregnancy establishment in cattle: the role of oocyte competence and the maternal environment. Anim. Reprod. Sci. 13:209-216. doi: 10.21451/1984-3143-AR879.

Dieleman, S. J., M. M. Bevers, J. Poortman, and H. T. van Tol. 1983. Steroid and pituitary hormone concentrations in the fluid of preovulatory bovine follicles relative to the peak of LH in the peripheral blood. J. Reprod. Fertil. 69:641-649. doi: 10.1530/jrf.0.0690641.

Dieleman, S. J., P. J. Hendriksen, D. Viuff, P. D. Thomsen, P. Hyttel, H. M. Knijn, C. Wrenzycki, T. A. Kruip, H. Niemann, B. M. Gadella, M. M. Bevers, and P. L. Vos. 2002. Effects of in vivo prematuration and in vivo final maturation on

developmental capacity and quality of pre-implantation embryos. Theriogenology 57:5-20. doi: 10.1016/s0093-691x(01)00655-0.
Diskin, M. G., and J. M. Sreenan. 1980. Fertilization and embryonic mortality rates in beef heifers after artificial insemination. J. Reprod Fertil. 59:463-468. doi: 10.1530/jrf.0.0590463.
Downs, S. M., and E. D. Hudson. 2000. Energy substrates and the completion of spontaneous meiotic maturation. Zygote. 8:339-351. doi: 10.1017/s0967199400001131.
Dumesic, D. A., D. R. Meldrum, M. G. Katz-Jaffe, R. L. Krisher, and W. B. Schoolcraft. 2015. Oocyte environment: follicular fluid and cumulus cells are critical for oocyte health. Fertil. Steril. 103:303-316. doi:10.1016/j.fertnstert.2014.11.015.
Dumollard, R., J. Carroll, M. R. Duchen, K. Campbell, and K. Swann. 2009. Mitochondrial function and redox state in mammalian embryos. Semin. Cell Devel. Biol. 20:346-353. doi: 10.1016/j.semcdb.2008.12.013.
Dumollard, R., M. Duchen, and J. Carroll. 2007. The role of mitochondrial function in the oocyte and embryo. Curr. Top. Dev. Biol. 21-49. doi: 10.1016/S0070-2153(06)77002-8
Dunning, K. R., D. L. Russell, and R. L. Robker. 2014. Lipids and oocyte developmental competence: the role of fatty acids and β-oxidation. J. Reprod. 148:R15-R27. doi: 10.1530/rep-13-0251.
Ealy, A. D. 2020. Pregnancy losses in livestock: An overview of the physiology and endocrinology symposium for the 2020 ASAS-CSAS-WSASAS Virtual Meeting. J. Anim. Sci. 98. doi: 10.1093/jas/skaa277.
Edson, M. A., A. K. Nagaraja, and M. M. Matzuk. 2009. The mammalian ovary from genesis to revelation. Endocr. Rev. 30:624-712. doi: 10.1210/er.2009-0012.
Edwards, R. G. 1974. Follicular fluid. J. Reprod. Fertil. 37:189-219. doi: 10.1530/jrf.0.0370189.
Emori, C., and K. Sugiura. 2014. Role of oocyte-derived paracrine factors in follicular development. J. Anim. Sci. 85:627-633. doi: 10.1111/asj.12200.
Eriksson, S., P. Ask-Gullstrand, W. F. Fikse, E. Jonsson, J.-Å. Eriksson, H. Stålhammar, A. Wallenbeck, and A. Hessle. 2020. Different beef breed sires used for crossbreeding with Swedish dairy cows - effects on calving performance and carcass traits. Lives. Sc. 232:103-902. doi: 10.1016/j.livsci.2019.103902.
Fahiminiya, S., and N. Gérard. 2010. Le liquide folliculaire chez les mammifères. Gynecol. Obstet. Fertil. 38:402-404. doi: 10.1016/j.gyobfe.2010.04.010.
Fair, T. 2003. Follicular oocyte growth and acquisition of developmental competence. Anim. Reprod. Sci. 78:203-216. doi: 10.1016/s0378-4320(03)00091-5.
Fair, T., S. C. J. Hulshof, P. Hyttel, T. Greve, and M. Boland. 1997. Oocyte ultrastructure in bovine primordial to early tertiary follicles. J. Anat. Embryol. 195:327-336. doi: 10.1007/s004290050052.
Fair, T., P. Hyttel, and T. Greve. 1995. Bovine oocyte diameter in relation to maturational competence and transcriptional activity. 42:437-442. doi: 10.1002/mrd.1080420410.

Fair, T., and P. Lonergan. 2012. The role of progesterone in oocyte acquisition of developmental competence. Reprod. Dom. Anim. 4:142-147. doi: 10.1111/j.1439-0531.2012.02068.x.

Fernie, A. R., F. Carrari, and L. J. Sweetlove. 2004. Respiratory metabolism: glycolysis, the TCA cycle and mitochondrial electron transport. Curr. Opin. Plant Biol. 7(3):254-261. doi: 10.1016/j.pbi.2004.03.007

Ferrazza, R. d. A., H. D. M. Garcia, E. M. d. S. Schmidt, M. Mihm Carmichael, F. F. d. Souza, R. Burchmore, R. Sartori, P. D. Eckersall, and J. C. P. Ferreira. 2017. Quantitative proteomic profiling of bovine follicular fluid during follicle development†. J. Biol. Reprod. 97:835-849. doi: 10.1093/biolre/iox148.

Ferré, L. B., M. E. Kjelland, L. B. Strøbech, P. Hyttel, P. Mermillod, and P. J. Ross. 2020. Review: Recent advances in bovine in vitro embryo production: reproductive biotechnology history and methods. Intern. J. Anim. Bios.14:991-1004. doi: 10.1017/S1751731119002775.

Fields, S. D., K. L. Gebhart, B. L. Perry, M. G. Gonda, C. L. Wright, R. C. Bott, and G. A. Perry. 2012. Influence of standing estrus before an injection of GnRH during a beef cattle fixed-time AI protocol on LH release, subsequent concentrations of progesterone, and steriodogenic enzyme expression. Dom. Anim. Endocrinol. 42:11-19. doi: 10.1016/j.domaniend.2011.08.002.

Firestone, G. L., and B. J. Kapadia. 2012. Minireview: regulation of gap junction dynamics by nuclear hormone receptors and their ligands. J. Mol. Endocrinol. 26:1798-1807. doi: 10.1210/me.2012-1065.

Forde, N., A. O'Gorman, H. Whelan, P. Duffy, L. O'Hara, A. K. Kelly, V. Havlicek, U. Besenfelder, L. Brennan, and P. Lonergan. 2016. Lactation-induced changes in metabolic status and follicular-fluid metabolomic profile in postpartum dairy cows. Reprod. Fertil. Dev. 28(12):1882-1892. doi: https://doi.org/10.1071/RD14348.

Fortune, J. E. 1993. Follicular dynamics during the bovine estrous cycle: a limiting factor in improvement of fertility? Anim. Reprod. Sci. 33(1):111-125. doi: https://doi.org/10.1016/0378-4320(93)90110-D.

Fortune, J. E., and W. Hansel. 1985. Concentrations of steroids and gonadotropins in follicular fluid from normal heifers and heifers primed for superovulation. Biol. Reprod. 32(5):1069-1079. doi: 10.1095/biolreprod32.5.1069.

Fortune, J. E., G. M. Rivera, and M. Y. Yang. 2004. Follicular development: the role of the follicular microenvironment in selection of the dominant follicle. Anim. Reprod. Sci. 82-83:109-126. doi: 10.1016/j.anireprosci.2004.04.031.

Funston, R. N., J. A. Musgrave, T. L. Meyer, and D. M. Larson. 2012. Effect of calving distribution on beef cattle progeny performance. J. Anim. Sci. 90(13):5118-5121. doi: 10.2527/jas.2012-5263.

Garrett, J. E., R. D. Geisert, M. T. Zavy, and G. L. Morgan. 1988. Evidence for maternal regulation of early conceptus growth and development in beef cattle. J. Reprod. Infertil. 84(2):437-446. doi: 10.1530/jrf.0.0840437.

Ge, H. S., X. H. Li, F. Zhang, H. Chen, H. T. Xi, J. Y. Huang, C. F. Zhu, and J. Q. Lv. 2013. Suppression of mitochondrial oxidative phosphorylation on in vitro

maturation, fertilization and developmental competence of oocytes. Journal of Peking University. Health sciences 45(6):864-868.
Geary, T. W., J. C. Whittier, D. M. Hallford, and M. D. MacNeil. 2001. Calf removal improves conception rates to the Ovsynch and CO-Synch protocols. J. Anim. Sci. 79(1):1-4. doi: 10.2527/2001.7911.
Gérard, N., S. Loiseau, G. Duchamp, and F. Seguin. 2002. Analysis of the variations of follicular fluid composition during follicular growth and maturation in the mare using proton nuclear magnetic resonance (1H NMR). Reproduction. 124(2):241-248. doi: 10.1530/rep.0.1240241.
Ginther, O. J., M. A. Beg, D. R. Bergfelt, F. X. Donadeu, and K. Kot. 2001. Follicle selection in monovular species. Biol. Reprod. 65(3):638-647. doi: 10.1095/biolreprod65.3.638.
Ginther, O. J., D. R. Bergfelt, L. J. Kulick, and K. Kot. 2000. Selection of the dominant follicle in cattle: role of estradiol. Biol. Reprod. 63(2):383-389. doi: 10.1095/biolreprod63.2.383.
Ginther, O. J., K. Kot, L. J. Kulick, and M. C. Wiltbank. 1997. Emergence and deviation of follicles during the development of follicular waves in cattle. Theriogenology. 48(1):75-87. doi: 10.1016/s0093-691x(97)00192-1.
Giordano, J. O., P. M. Fricke, J. N. Guenther, G. Lopes, M. M. Herlihy, A. B. Nascimento, and M. C. Wiltbank. 2012. Effect of progesterone on magnitude of the luteinizing hormone surge induced by two different doses of gonadotropin-releasing hormone in lactating dairy cows. J. of Dairy Sci. 95(7):3781-3793. doi: https://doi.org/10.3168/jds.2011-5155
Gjorret J.O., H.M. Knijn, S.J. Dieleman, B. Avery, L.I. Larsson,P. Hyttel. 2003. Chronology of Apoptosis in Bovine Embryos Produced in vivo and in vitro. Biol. Reprod. 69:1193-1200.
Gosden, R. G. 2002. Oogenesis as a foundation for embryogenesis. Mol. Cell. Endoncrinol. 186(2):149-153. doi: 10.1016/s0303-7207(01)00683-9.
Gosden, R. G., R. H. Hunter, E. Telfer, C. Torrance, and N. Brown. 1988. Physiological factors underlying the formation of ovarian follicular fluid. J. Reprod. Infertil. 82(2):813-825. doi: 10.1530/jrf.0.0820813.
Gougeon, A. 2010. Human ovarian follicular development: from activation of resting follicles to preovulatory maturation. Annales d'endocrinologie. 71(3):132-143. doi: 10.1016/j.ando.2010.02.021
Graf, A., S. Krebs, M. Heininen-Brown, V. Zakhartchenko, H. Blum, and E. Wolf. 2014. Genome activation in bovine embryos: review of the literature and new insights from RNA sequencing experiments. Anim. Reprod. Sci. 149(1-2):46-58. doi: 10.1016/j.anireprosci.2014.05.016.
Granot, I., and N. Dekel. 2002. The ovarian gap junction protein connexin43: regulation by gonadotropins. Trends Endocrinol. Metab. 13(7):310-313. doi: 10.1016/s1043-2760(02)00623-9.
Greene, E., R. Cauble, A. E. Dhamad, M. T. Kidd, B. Kong, S. M. Howard, H. F. Castro, S. R. Campagna, M. Bedford, and S. Dridi. 2020. Muscle metabolome profiles in

woody breast-(un)affected broilers: effects of quantum blue phytase-enriched diet. Front. Vet. Sci. 7:458-458. doi: 10.3389/fvets.2020.00458.
Grimek, H. J., M. E. Bellin, and R. L. Ax. 1984. Characteristics of proteoglycans isolated from small and large bovine ovarian follicles. Biol. Reprod. 30(2):397-409. doi: 10.1095/biolreprod30.2.397.
Guerreiro, T. M., R. F. Gonçalves, C. Melo, D. N. de Oliveira, E. O. Lima, J. A. Visintin, M. A. de Achilles, and R. R. Catharino. 2018. A metabolomic overview of follicular fluid in cows. Front. Vet. Sci. 5:10. doi: 10.3389/fvets.2018.00010.
Guo, X., X. Wang, R. Di, Q. Liu, W. Hu, X. He, J. Yu, X. Zhang, J. Zhang, K. Broniowska, W. Chen, C. Wu, and M. Chu. 2018. Metabolic effects of FecB gene on follicular fluid and ovarian vein serum in sheep (Ovis aries). Int. J. Mol. Sci. 19(2):539. doi: 10.3390/ijms19020539.
Hagemann, L. J. 1999. Influence of the dominant follicle on oocytes from subordinate follicles. Theriogenology. 51(2):449-459. doi: 10.1016/s0093-691x(98)00239-8
Hagemann, L. J., S. E. Beaumont, M. Berg, M. J. Donnison, A. Ledgard, A. J. Peterson, A. Schurmann, and H. R. Tervit. 1999. Development during single IVP of bovine oocytes from dissected follicles: interactive effects of estrous cycle stage, follicle size and atresia. Mol. Reprod. Dev. 53(4):451-458. doi: 10.1002/(sici)1098-2795(199908)53:4<451::Aid-mrd11>3.0.Co;2-3.
Harris, S. E., I. Adriaens, H. J. Leese, R. G. Gosden, and H. M. Picton. 2007. Carbohydrate metabolism by murine ovarian follicles and oocytes grown in vitro. Reproduction. 134(3):415-424. doi: 10.1530/rep-07-0061.
Hashimoto, S., M. Yamanaka, T. Yamochi, H. Iwata, R. Kawahara-Miki, M. Inoue, and Y. Morimoto. 2019. Mitochondrial function in immature bovine oocytes is improved by an increase of cellular cyclic AMP. Sci. Rep. 9(1):5167. doi: 10.1038/s41598-019-41610-6.
Hazra, A., and N. Gogtay. 2016. Biostatistics series module 6: correlation and linear regression. Indian J. Dermatol. 61(6):593-601. doi: 10.4103/0019-5154.193662.
He, M., T. Zhang, Y. Yang, and C. Wang. 2021. Mechanisms of Oocyte Maturation and Related Epigenetic Regulation. Front. Cell. Dev. Biol. 9(Review) doi: 10.3389/fcell.2021.654028.
Hendriksen, P. J., P. L. Vos, W. N. Steenweg, M. M. Bevers, and S. J. Dieleman. 2000. Bovine follicular development and its effect on the in vitro competence of oocytes. Theriogenology. 53(1):11-20. doi: 10.1016/s0093-691x(99)00236-8.
Hendriksen, P. J., B. M. Gadella, P. L. Vos, E. Mullaart, T. A. Kruip, and S. J. Dieleman. 2003. Follicular dynamics around the recruitment of the first follicular wave in the cow. Biol. Reprod. 69(6):2036-2044. doi: 10.1095/biolreprod.103.019828.
Hennet, M. L., and C. M. Combelles. 2012. The antral follicle: a microenvironment for oocyte differentiation. Int. J. Dev. Biol. 56(10-12):819-831. doi: 10.1387/ijdb.120133cc.
Hill, S. L., G. A. Perry, V. R. Mercadante, G. C. Lamb, J. R. Jaeger, K. C. Olson, and J. S. Stevenson. 2014. Altered progesterone concentrations by hormonal manipulations before a fixed-time artificial insemination CO-Synch + CIDR program in suckled

beef cows. Theriogenology. 82(1):104-113. doi: 10.1016/j.theriogenology.2014.03.008.
Hou, E., Y. Zhao, J. Hang, and J. Qiao. 2021. Metabolomics and correlation network analysis of follicular fluid reveals associations between l-tryptophan, l-tyrosine and polycystic ovary syndrome. Biomed. Chromatogr. 35(3):4993. doi: https://doi.org/10.1002/bmc.4993.
Humblot, P., P. Holm, P. Lonergan, C. Wrenzycki, A. S. Lequarré, C. G. Joly, D. Herrmann, A. Lopes, D. Rizos, H. Niemann, and H. Callesen. 2005. Effect of stage of follicular growth during superovulation on developmental competence of bovine oocytes. Theriogenology. 63(4):1149-1166. doi: 10.1016/j.theriogenology.2004.06.002.
Hyttel, P., H. Callesen, and T. Greve. 1986. Ultrastructural features of preovulatory oocyte maturation in superovulated cattle. J. Reprod. Fertil. 76(2):645-656. doi: 10.1530/jrf.0.0760645.
Hyttel, P., T. Fair, H. Callesen, and T. Greve. 1997. Oocyte growth, capacitation and final maturation in cattle. Theriogenology. 47(1):23-32. doi: https://doi.org/10.1016/S0093-691X(96)00336-6.
Hyttel, P., T. Greve, and H. Callesen. 1989. Ultrastructural aspects of oocyte maturation and fertilization in cattle. J. Reprod. Fertil. Suppl. 38:35-47.
Iwata, H., H. Goto, H. Tanaka, Y. Sakaguchi, K. Kimura, T. Kuwayama, and Y. Monji. 2011. Effect of maternal age on mitochondrial DNA copy number, ATP content and IVF outcome of bovine oocytes. Reprod. Fertil. Dev. 23(3):424-432. doi: 10.1071/rd10133.
Iwata, H., S. Hashimoto, M. Ohota, K. Kimura, K. Shibano, and M. Miyake. 2004. Effects of follicle size and electrolytes and glucose in maturation medium on nuclear maturation and developmental competence of bovine oocytes. Reproduction. 127(2):159-164. doi: 10.1530/rep.1.00084.
Jaiswal, R. S., J. Singh, and G. P. Adams. 2004. Developmental pattern of small antral follicles in the bovine ovary. Biol. Reprod. 71(4):1244-1251. doi: 10.1095/biolreprod.104.030726.
Jeng, J. Y., T. S. Yeh, J. W. Lee, S. H. Lin, T. H. Fong, and R. H. Hsieh. 2008. Maintenance of mitochondrial DNA copy number and expression are essential for preservation of mitochondrial function and cell growth. J. Cell. Biochem. 103(2):347-357. doi: 10.1002/jcb.21625.
Jeong, W. J., S. J. Cho, H. S. Lee, G. K. Deb, Y. S. Lee, T. H. Kwon, and I. K. Kong. 2009. Effect of cytoplasmic lipid content on in vitro developmental efficiency of bovine IVP embryos. Theriogenology. 72(4):584-589. doi: 10.1016/j.theriogenology.2009.04.015.
Jiao, F., J. B. Yan, X. Y. Yang, H. Li, Q. Wang, S. Z. Huang, F. Zeng, and Y. T. Zeng. 2007. Effect of oocyte mitochondrial DNA haplotype on bovine somatic cell nuclear transfer efficiency. Mol. Reprod. Dev. 74(10):1278-1286. doi: 10.1002/mrd.20698.
Jinks, E. M., M. F. Smith, J. A. Atkins, K. G. Pohler, G. A. Perry, M. D. MacNeil, A. J. Roberts, R. C. Waterman, L. J. Alexander, and T. W. Geary. 2013. Preovulatory

estradiol and the establishment and maintenance of pregnancy in suckled beef cows. J. Anim. Sci. 91(3):1176-1185. doi: 10.2527/jas.2012-5611.
Johnson, M. T., E. A. Freeman, D. K. Gardner, and P. A. Hunt. 2007. Oxidative metabolism of pyruvate is required for meiotic maturation of murine oocytes in vivo. Biol. Reprod. 77(1):2-8. doi: 10.1095/biolreprod.106.059899.
Jóźwik, M., M. Jóźwik, A. J. Milewska, F. C. Battaglia, and M. Jóźwik. 2017. Competitive inhibition of amino acid transport in human preovulatory ovarian follicles. Syst. Biol. Reprod. Med. 63(5):311-317. doi: 10.1080/19396368.2017.1341962.
Kafi, M., M. Azari, O. Chashnigir, S. Gharibzadeh, Z. Aghabozorgi, A. Asaadi, and M. R. Divar. 2017. Inherent inferior quality of follicular fluid in repeat breeder heifers as evidenced by low rates of in vitro production of bovine embryos. Theriogenology. 102:29-34. doi: 10.1016/j.theriogenology.2017.07.011.
Kand'ár, R., P. Záková, and V. Muzáková. 2006. Monitoring of antioxidant properties of uric acid in humans for a consideration measuring of levels of allantoin in plasma by liquid chromatography. Clin. Chim. Acta. 365(1-2):249-256. doi: 10.1016/j.cca.2005.09.002.
Kasimanickam, R., M. L. Day, J. S. Rudolph, J. B. Hall, and W. D. Whittier. 2009. Two doses of prostaglandin improve pregnancy rates to timed-AI in a 5-day progesterone-based synchronization protocol in beef cows. Theriogenology. 71(5):762-767. doi: 10.1016/j.theriogenology.2008.09.049.
Kidder, G. M., and B. C. Vanderhyden. 2010. Bidirectional communication between oocytes and follicle cells: ensuring oocyte developmental competence. Can. J. Physio. Pharmacol. 88(4):399-413. doi: 10.1139/y10-009.
Kimble, K. M., S. E. Dickinson, and F. H. Biase. 2018. Extraction of total RNA from single-oocytes and single-cell mRNA sequencing of swine oocytes. BMC Res. Notes. 11(1):155. doi: 10.1186/s13104-018-3264-2.
Knijn, H. M., C. Wrenzycki, P. J. Hendriksen, P. L. Vos, D. Herrmann, G. C. van der Weijden, H. Niemann, and S. J. Dieleman. 2002. Effects of oocyte maturation regimen on the relative abundance of gene transcripts in bovine blastocysts derived in vitro or in vivo. Reproduction. 124(3):365-375.
Komar, C. M., A. K. Berndtson, A. C. Evans, and J. E. Fortune. 2001. Decline in circulating estradiol during the periovulatory period is correlated with decreases in estradiol and androgen, and in messenger RNA for p450 aromatase and p450 17alpha-hydroxylase, in bovine preovulatory follicles. Biol. Reprod. 64(6):1797-1805. doi: 10.1095/biolreprod64.6.1797.
Krisher, R. L. 2013. In vivo and in vitro environmental effects on mammalian oocyte quality. Annu. Rev. Anim. Biosci. 1:393-417. doi: 10.1146/annurev-animal-031412-103647.
Kruip, T. A., and S. J. Dieleman. 1982. Macroscopic classification of bovine follicles and its validation by micromorphological and steroid biochemical procedures. Reprod. Nutr. Dev. 22(3):465-473. doi: 10.1051/rnd:19820403.
Labrecque, R., E. Fournier, and M. A. Sirard. 2016. Transcriptome analysis of bovine oocytes from distinct follicle sizes: Insights from correlation network analysis. Mol. Reprod. Dev. 83(6):558-569. doi: 10.1002/mrd.22651

Lamb, G. C., and V. R. Mercadante. 2016. Synchronization and artificial insemination strategies in beef cattle. Vet. Clin. North. Am. Food Anim. Pract. 32(2):335-347. doi: 10.1016/j.cvfa.2016.01.006.

Lamb, G. C., M. F. Smith, G. A. Perry, J. A. Atkins, M. E. Risley, D. C. Busch, and D. J. Patterson. 2010. Reproductive endocrinology and hormonal control of the estrous cycle. Bov. Pract. 44(1):18-26. doi: 10.21423/bovine-vol44no1p18-26.

Lamb, G. C., J. S. Stevenson, D. J. Kesler, H. A. Garverick, D. R. Brown, and B. E. Salfen. 2001. Inclusion of an intravaginal progesterone insert plus GnRH and prostaglandin F2α for ovulation control in postpartum suckled beef cows. J. Anim. Sci. 79(9):2253-2259. doi: 10.2527/2001.7992253x.

Landim-Alvarenga, F. C. and Maziero R.D. 2014. Control of oocyte maturation. J. Anim. Reprod. 11:150-158.

Lee, S. R., J. H. Heo, S. L. Jo, G. Kim, S. J. Kim, H. J. Yoo, K.P. Lee, H.J. Kwun, H.J. Shin, I.J. Baek, and E.J. Hong. 2021. Progesterone receptor membrane component 1 reduces cardiac steatosis and lipotoxicity via activation of fatty acid oxidation and mitochondrial respiration. Sci. Rep. 11(1):8781. doi: 10.1038/s41598-021-88251-2

Leese, H. J. 2012. Metabolism of the preimplantation embryo: 40 years on. Reproduction. 143(4):417-427. doi: 10.1530/rep-11-0484.

Lequarre, A.-S., C. Vigneron, F. Ribaucour, P. Holm, I. Donnay, R. Dalbiès-Tran, H. Callesen, and P. Mermillod. 2005. Influence of antral follicle size on oocyte characteristics and embryo development in the bovine. Theriogenology. 63(3):841-859. doi: https://doi.org/10.1016/j.theriogenology.2004.05.015.

Leroy, J. L., D. Rizos, R. Sturmey, P. Bossaert, A. Gutierrez-Adan, V. Van Hoeck, S. Valckx, and P. E. Bols. 2011. Intrafollicular conditions as a major link between maternal metabolism and oocyte quality: a focus on dairy cow fertility. Reprod. Fertil. Dev. 24(1):1-12. doi: 10.1071/rd11901.

Leroy, J. L., T. Vanholder, J. R. Delanghe, G. Opsomer, A. Van Soom, P. E. Bols, J. Dewulf, and A. de Kruif. 2004. Metabolic changes in follicular fluid of the dominant follicle in high-yielding dairy cows early post partum. Theriogenology. 62(6):1131-1143. doi: 10.1016/j.theriogenology.2003.12.017.

Leroy, J. L., T. Vanholder, B. Mateusen, A. Christophe, G. Opsomer, A. de Kruif, G. Genicot, and A. Van Soom. 2005. Non-esterified fatty acids in follicular fluid of dairy cows and their effect on developmental capacity of bovine oocytes in vitro. Reproduction. 130(4):485-495. doi: 10.1530/rep.1.00735.

Leroy, J. L., T. Vanholder, G. Opsomer, A. Van Soom, and A. de Kruif. 2006. The in vitro development of bovine oocytes after maturation in glucose and beta-hydroxybutyrate concentrations associated with negative energy balance in dairy cows. Reprod. Domest. Anim. 41(2):119-123. doi: 10.1111/j.1439-0531.2006.00650.x.

Lesmeister, J. L., P. J. Burfening, and R. L. Blackwell. 1973. Date of first calving in beef cows and subsequent calf production. J. Anim. Sci. 36:1-6. doi: 10.2527/jas1973.3611.

Lima, F., A. De Vries, C. Risco, J. Santos, and W. J. J. Thatcher. 2010. Economic comparison of natural service and timed artificial insemination breeding programs in dairy cattle. J. Dairy. Sci. 93:4404-4413. doi: 10.3168/jds.2009-2789

Liu, N., Y. Ma, R. Li, H. Jin, M. Li, X. Huang, H. L. Feng, and J. Qiao. 2012. Comparison of follicular fluid amphiregulin and EGF concentrations in patients undergoing IVF with different stimulation protocols. Endocrine 42:708-716. doi: 10.1007/s12020-012-9706-z.

Liu, S., L. He, and K. Yao. 2018. The antioxidative function of alpha-ketoglutarate and its applications. Biomed. Res. Int. 2018:3408467. doi: 10.1155/2018/3408467.

Liu, W., Q. Xin, X. Wang, S. Wang, H. Wang, W. Zhang, Y. Yang, Y. Zhang, Z. Zhang, C. Wang, Y. Xu, E. Duan, and G. Xia. 2017. Estrogen receptors in granulosa cells govern meiotic resumption of pre-ovulatory oocytes in mammals. Cell death Dis. 8:e2662-e2662. doi: 10.1038/cddis.2017.82.

Lonergan, P., P. Monaghan, D. Rizos, M. P. Boland, and I. Gordon. 1994. Effect of follicle size on bovine oocyte quality and developmental competence following maturation, fertilization, and culture in vitro. Mol. Reprod. Dev. 37:48-53. doi: 10.1002/mrd.1080370107.

Lonergan, P., D. Rizos, A. Gutierrez-Adan, T. Fair, and M. P. Boland. 2003. Oocyte and embryo quality: effect of origin, culture conditions and gene expression patterns. Reprod. Dom. Anim. 38:259-267. doi: 10.1046/j.1439-0531.2003.00437.x.

Lonergan, P., D. Rizos, F. Ward, and M. P. J. R. N. D. Boland. 2001. Factors influencing oocyte and embryo quality in cattle. Reprod. Nutri. Dev. 41(5):427-437. doi: 10.1051/rnd:2001142

Lu, W., M. F. Clasquin, E. Melamud, D. Amador-Noguez, A. A. Caudy, and J. D. Rabinowitz. 2010. Metabolomic analysis via reversed-phase ion-pairing liquid chromatography coupled to a stand alone orbitrap mass spectrometer. Anal. Chem. 82:3212-3221. doi: 10.1021/ac902837x.

Luciano, A. M., V. Lodde, F. Franciosi, F. Ceciliani, and J. J. Peluso. 2010. Progesterone receptor membrane component 1 expression and putative function in bovine oocyte maturation, fertilization, and early embryonic development. Reprod. 140:663-672. doi: 10.1530/rep-10-0218.

Lucy, M. C., J. D. Savio, L. Badinga, R. L. De La Sota, and W. W. Thatcher. 1992. Factors that affect ovarian follicular dynamics in cattle. J. Anim. Sci. 70:3615-3626. doi: 10.2527/1992.70113615x.

Luti, S., T. Fiaschi, F. Magherini, P. A. Modesti, P. Piomboni, L. Governini, A. Luddi, A. Amoresano, A. Illiano, G. Pinto, A. Modesti, and T. Gamberi. 2020. Relationship between the metabolic and lipid profile in follicular fluid of women undergoing in vitro fertilization. Mol. Reprod. Devel. 87:986-997. doi:10.1002/mrd.23415.

MacNeil, M. D., T. W. Geary, G. A. Perry, A. J. Roberts, and L. J. Alexander. 2006. Genetic partitioning of variation in ovulatory follicle size and probability of pregnancy in beef cattle. J. Anim. Sci. 84:1646-1650. doi: 10.2527/jas.2005-698.

Madureira, A. M. L., T. A. Burnett, S. Borchardt, W. Heuwieser, C. F. Baes, J. L. M. Vasconcelos, and R. L. A. Cerri. 2021. Plasma concentrations of progesterone in the preceding estrous cycle are associated with the intensity of estrus and fertility

of Holstein cows. PLOS ONE. 16(8):e0248453. doi: 10.1371/journal.pone.0248453

Mao, J., K. M. Whitworth, L. D. Spate, E. M. Walters, J. Zhao, and R. S. Prather. 2012. Regulation of oocyte mitochondrial DNA copy number by follicular fluid, EGF, and neuregulin 1 during in vitro maturation affects embryo development in pigs. Theriogenology 78:887-897. doi: 10.1016/j.theriogenology.2012.04.002.

Martens, L., M. Chambers, M. Sturm, D. Kessner, F. Levander, J. Shofstahl, W. H. Tang, A. Römpp, S. Neumann, A. D. Pizarro, L. Montecchi-Palazzi, N. Tasman, M. Coleman, F. Reisinger, P. Souda, H. Hermjakob, P. A. Binz, and E. W. Deutsch. 2011. mzML--a community standard for mass spectrometry data. Mol. Cell Proteomics. 10:R110.000133. doi: 10.1074/mcp.R110.000133.

Martín, N., N. Schreurs, S. Morris, N. López-Villalobos, J. McDade, and R. Hickson. 2020. Sire effects on post-weaning growth of beef-cross-dairy cattle: A case study in New Zealand. Animals (Basel) 10:2313. doi: 10.3390/ani10122313.

Martín, N., N. Schreurs, S. Morris, N. López-Villalobos, J. McDade, and R. Hickson. 2021. Sire effects on carcass of beef-cross-dairy cattle: A case study in New Zealand. Animals (Basel) 11:636. doi: 10.3390/ani11030636.

Martin, N. T., J. M. Thomas, J. M. Nash, D. A. Mallory, M. R. Ellersieck, S. E. Poock, M. F. Smith, and D. J. Patterson. 2014. Comparison of a 16- versus a 19-day interval between controlled internal drug release removal and prostaglandin F2α following a 14-day controlled internal drug releasetreatment and fixed-time artificial insemination in postpartum beef cows. J. Anim. Sci. 92:1759-1767. doi: 10.2527/jas.2013-7045.

Martínez-Reyes, I. and N. S. Chandel. 2020. Mitochondrial TCA cycle metabolites control physiology and disease. Nat. Common. 11(1):102. doi: 10.1038/s41467-019-13668-3

Mathews, K.H. 2001. The beef cow replacement decision. J. Agribus. 19:191-211.

Matoba, S., K. Bender, A. G. Fahey, S. Mamo, L. Brennan, P. Lonergan, and T. Fair. 2014. Predictive value of bovine follicular components as markers of oocyte developmental potential. Reprod. Fertil. Dev. 26:337-345. doi: 10.1071/rd13007.

May-Panloup, P., M. Boguenet, H. E. Hachem, P.-E. Bouet, and P. Reynier. 2021. Embryo and its mitochondria. Antioxidants (Basel) 10:139. doi: 10.3390/antiox10020139.

May-Panloup, P., M. F. Chretien, Y. Malthiery, and P. Reynier. 2007. Mitochondrial DNA in the oocyte and the developing embryo. Curr. Top. Dev. Biol. 77:51-83. doi: 10.1016/s0070-2153(06)77003-x.

Melamud, E., L. Vastag, and J. D. Rabinowitz. 2010. Metabolomic analysis and visualization engine for LC-MS data. Anal. Chem. 82:9818-9826. doi: 10.1021/ac1021166.

Mermillod, P., B. Oussaid, and Y. Cognié. 1999. Aspects of follicular and oocyte maturation that affect the developmental potential of embryos. J. Reprod. Fertil. Suppl. 54:449-460.

Merton, J. S., A. P. de Roos, E. Mullaart, L. de Ruigh, L. Kaal, P. L. Vos, and S. J. Dieleman. 2003. Factors affecting oocyte quality and quantity in commercial

application of embryo technologies in the cattle breeding industry. Theriogenology. 59(2):651-674. doi: 10.1016/s0093-691x(02)01246-3

Michaels, G. S., W. W. Hauswirth, and P. J. Laipis. 1982. Mitochondrial DNA copy number in bovine oocytes and somatic cells. Dev. Biol. 94:246-251. doi: https://doi.org/10.1016/0012-1606(82)90088-4.

Mihm, M., A. Baguisi, M. P. Boland, and J. F. Roche. 1994. Association between the duration of dominance of the ovulatory follicle and pregnancy rate in beef heifers. J. Reprod. Fertil. 102:123-130. doi: 10.1530/jrf.0.1020123.

Miura, R. 2019. Physiological characteristics and effects on fertility of the first follicular wave dominant follicle in cattle. J. Reprod. Dev. 65:289-295. doi: 10.1262/jrd.2019-027.

Mo, J., L. Sun, J. Cheng, Y. Lu, Y. Wei, G. Qin, J. Liang, and G. Lan. 2021. Non-targeted metabolomics reveals metabolic characteristics of porcine atretic follicles. Front. Vet. Sci. 8:679947-679947. doi: 10.3389/fvets.2021.679947.

Monnot, S., D. C. Samuels, L. Hesters, N. Frydman, N. Gigarel, P. Burlet, V. Kerbrat, F. Lamazou, R. Frydman, A. Benachi, J. Feingold, A. Rotig, A. Munnich, J. P. Bonnefont, and J. Steffann. 2013. Mutation dependance of the mitochondrial DNA copy number in the first stages of human embryogenesis. Hum. Mol. Genet. 22:1867-1872. doi: 10.1093/hmg/ddt040.

Moorey, S. E., J. M. Monnig, M. F. Smith, M. S. Ortega, J. A. Green, K. G. Pohler, G. A. Bridges, S. K. Behura, and T. W. Geary. 2021. Differential transcript profiles in cumulus-oocyte complexes originating from pre-ovulatory follicles of varied physiological maturity in beef cows. Genes. 12:893.

Moreno, J. M., M. J. Núñez, A. Quiñonero, S. Martínez, M. de la Orden, C. Simón, A. Pellicer, C. Díaz-García, and F. Domínguez. 2015. Follicular fluid and mural granulosa cells microRNA profiles vary in in vitro fertilization patients depending on their age and oocyte maturation stage. Fertil. Steril. 104:1037-1046.e1031. doi: 10.1016/j.fertnstert.2015.07.001.

Motta, P. M., S. A. Nottola, S. Makabe, and R. Heyn. 2000. Mitochondrial morphology in human fetal and adult female germ cells. Hum. Reprod. 15(2):129-147. doi: 10.1093/humrep/15.suppl_2.129.

Mu, Y.-M., T. Yanase, Y. Nishi, A. Tanaka, M. Saito, C.-H. Jin, C. Mukasa, T. Okabe, M. Nomura, K. Goto, and H. Nawata. 2001. Saturated FFAs, palmitic acid and stearic acid, induce apoptosis in human granulosa cells. J. Endocrinology 142:3590-3597. doi: 10.1210/endo.142.8.8293.

Nagano, M. 2019. Acquisition of developmental competence and in vitro growth culture of bovine oocytes. J. Reprod. Dev. 65:195-201. doi: 10.1262/jrd.2019-022.

Nagy, R. A., A. P. A. van Montfoort, A. Dikkers, J. van Echten-Arends, I. Homminga, J. A. Land, A. Hoek, and U. J. F. Tietge. 2015. Presence of bile acids in human follicular fluid and their relation with embryo development in modified natural cycle IVF. Hum. Reprod. 30:1102-1109. doi: 10.1093/humrep/dev034.

Nandi, S., V. G. Kumar, B. M. Manjunatha, and P. S. P. Gupta. 2007. Biochemical composition of ovine follicular fluid in relation to follicle size. Dev. Growth Differ. 49:61-66. doi: 10.1111/j.1440-169X.2007.00901.x.

Nash, J. M., D. A. Mallory, M. R. Ellersieck, S. E. Poock, M. F. Smith, and D. J. Patterson. 2012. Comparison of long- versus short-term CIDR-based protocols to synchronize estrus prior to fixed-time AI in postpartum beef cows. Anim. Reprod. Sci. 132:11-16. doi: 10.1016/j.anireprosci.2012.03.013.

O'Doherty, A. M., A. O'Gorman, A. al Naib, L. Brennan, E. Daly, P. Duffy, and T. Fair. 2014. Negative energy balance affects imprint stability in oocytes recovered from postpartum dairy cows. Genom. 104:177-185. doi: 10.1016/j.ygeno.2014.07.006.

Ockerman, H. W., D. Jaworek, B. VanStavern, N. Parrett, and C. J. Pierson. 1984. Castration and sire effects on carcass traits, meat palatability and muscle fiber characteristics in Angus cattle. J. Anim. Sci. 59:981-990. doi: 10.2527/jas1984.594981x.

Opsomer, G., and A. de Kruif. 1999. Postpartum anestrus in dairy cattle a review. Tierarztliche Praxis. Ausgabe G, Grosstiere/Nutztiere 27:30-35.

Orsi, N. M., N. Gopichandran, H. J. Leese, H. M. Picton, and S. E. Harris. 2005a. Fluctuations in bovine ovarian follicular fluid composition throughout the oestrous cycle. Reprod. 129:219-288. doi: 10.1530/rep.1.00460.

Otoi, T., K. Yamamoto, N. Koyama, S. Tachikawa, and T. Suzuki. 1997. Bovine oocyte diameter in relation to developmental competence. Theriogenology. 48(5):769-774. doi: 10.1016/s0093-691x(97)00300-2.

Paczkowski, M., E. Silva, W. B. Schoolcraft, and R. L. Krisher. 2013. Comparative importance of fatty acid beta-oxidation to nuclear maturation, gene expression, and glucose metabolism in mouse, bovine, and porcine cumulus oocyte complexes. Biol. Reprod. 88(5):1-11. doi: 10.1095/biolreprod.113.108548.

Palini, S., S. Benedetti, M. C. Tagliamonte, S. De Stefani, M. Primiterra, V. Polli, P. Rocchi, S. Catalani, S. Battistelli, F. Canestrari, and C. Bulletti. 2014. Influence of ovarian stimulation for IVF/ICSI on the antioxidant defence system and relationship to outcome. Reprod. Biomed. Online. 29(1):65-71. doi: 10.1016/j.rbmo.2014.03.010.

Pang, Z., J. Chong, G. Zhou, D. A. de Lima Morais, L. Chang, M. Barrette, C. Gauthier, P. Jacques, S. Li, and J. Xia. 2021. MetaboAnalyst 5.0: narrowing the gap between raw spectra and functional insights. Nucleic Acids Res. 49(1):388-396. doi: 10.1093/nar/gkab382.

Pavlok, A., A. Lucas-Hahn, and H. Niemann. 1992. Fertilization and developmental competence of bovine oocytes derived from different categories of antral follicles. Mol. Reprod. Dev. 31(1):63-67. doi: https://doi.org/10.1002/mrd.1080310111

Payton, R. R., L. A. Rispoli, K. A. Nagle, C. Gondro, A. M. Saxton, B. H. Voy, and J. L. Edwards. 2018. Mitochondrial-related consequences of heat stress exposure during bovine oocyte maturation persist in early embryo development. J. Reprod. Dev. 64(3):243-251. doi: 10.1262/jrd.2017-160.

Perez, G. I., A. M. Trbovich, R. G. Gosden, and J. L. Tilly. 2000. Mitochondria and the death of oocytes. Nature. 403(6769):500-501. doi: 10.1038/35000651.

Perry, G. A., M. F. Smith, M. C. Lucy, J. A. Green, T. E. Parks, M. D. MacNeil, A. J. Roberts, and T. W. Geary. 2005. Relationship between follicle size at insemination

and pregnancy success. Proc. Natl. Acad. Sci. U.S.A. 102(14):5268-5273. doi: 10.1073/pnas.0501700102.
Perry, G. A., M. F. Smith, A. J. Roberts, M. D. MacNeil, and T. W. Geary. 2007. Relationship between size of the ovulatory follicle and pregnancy success in beef heifers. J. Anim. Sci. 85(3):684-689. doi: 10.2527/jas.2006-519.
Perry, G. A., O. L. Swanson, E. L. Larimore, B. L. Perry, G. D. Djira, and R. A. Cushman. 2014. Relationship of follicle size and concentrations of estradiol among cows exhibiting or not exhibiting estrus during a fixed-time AI protocol. Domest. Anim. Endocrinol. 48:15-20. doi: 10.1016/j.domaniend.2014.02.001.
Peterson, A. J., and R. S. Lee. 2003. Improving successful pregnancies after embryo transfer. Theriogenology. 59(2):687-697. doi: 10.1016/s0093-691x(02)01248-7.
Pikó, L., and K. D. Taylor. 1987. Amounts of mitochondrial DNA and abundance of some mitochondrial gene transcripts in early mouse embryos. Dev. Biol. 123(2):364-374. doi: 10.1016/0012-1606(87)90395-2.
Piñero-Sagredo, E., S. Nunes, M. J. de los Santos, B. Celda, and V. Esteve. 2010. NMR metabolic profile of human follicular fluid. NMR Biomed. 23(5):485-495. doi: 10.1002/nbm.1488.Pohler, K. G., M. H. C. Pereira, F. R. Lopes, J. C. Lawrence, D. H. Keisler, M. F. Smith, J. L. M. Vasconcelos, and J. A. Green. 2016. Circulating concentrations of bovine pregnancy-associated glycoproteins and late embryonic mortality in lactating dairy herds. Journal of dairy science 99(2):1584-1594. doi: 10.3168/jds.2015-10192
Pulley, S. L., D. H. Keisler, and J. S. Stevenson. 2015. Concentrations of luteinizing hormone and ovulatory responses in dairy cows before timed artificial insemination. J. Dairy Sci. 98(9):6188-6201. doi: 10.3168/jds.2015-9473
Pursley, J. R., M. C. Wiltbank, J. S. Stevenson, J. S. Ottobre, H. A. Garverick, and L. L. Anderson. 1997. Pregnancy rates per artificial insemination for cows and heifers inseminated at a synchronized ovulation or synchronized estrus. J. Dairy Sci. 80(2):295-300. doi: 10.3168/jds.S0022-0302(97)75937-X.
Quinn, P., and R. G. Wales. 1973. The relationships between the ATP content of preimplantation mouse embryos and their development in vitro during culture. J. Reprod. Infertil. 35(2):301-309. doi: 10.1530/jrf.0.0350301.
R Core Team (2020). R: A language and environment for statistical computing. Foundation for Statistical Computing, Vienna, Austria. URL https://www.R-project.org/.
Rathod, P. K., and J. H. Fellman. 1985. Regulation of mammalian aspartate-4-decarboxylase: its possible role in oxaloacetate and energy metabolism. Arch. Biochem. Biophys. 238(2):447-451. doi: 10.1016/0003-9861(85)90185-7.
Read, C. C., G. Willhelm, and P. W. Dyce. 2018. Connexin 43 coupling in bovine cumulus cells, during the follicular growth phase, and its relationship to in vitro embryo outcomes. Mol. Reprod. Dev. 85(7):579-589. doi: 10.1002/mrd.22993.
Reader, K. L., J.-A. L. Stanton, and J. L. Juengel. 2017. The role of oocyte organelles in determining developmental competence. Biology. 6(3):35. doi: 10.3390/biology6030035.

Reese, S. T., G. A. Franco, R. K. Poole, R. Hood, L. F. Montero, R. V. Filho, R. F. Cooke, and K. G. Pohler. 2020. Pregnancy loss in beef cattle: a meta-analysis. Anim. Reprod. Sci. 212:106251. doi: 10.1016/j.anireprosci.2019.106251.

Renaville, B., N. Bacciu, A. Comin, M. Motta, I. Poli, G. Vanini, and A. Prandi. 2010. Plasma and follicular fluid fatty acid profiles in dairy cows. Reprod. Domest. Anim. 45(1):118-121. doi: 10.1111/j.1439-0531.2008.01264.x.

Revelli, A., L. Delle Piane, S. Casano, E. Molinari, M. Massobrio, and P. Rinaudo. 2009. Follicular fluid content and oocyte quality: from single biochemical markers to metabolomics. Reprod. Biol. Endocrinol. 7:40. doi: 10.1186/1477-7827-7-40.

Reynier, P., P. May-Panloup, M. F. Chrétien, C. J. Morgan, M. Jean, F. Savagner, P. Barrière, and Y. Malthièry. 2001. Mitochondrial DNA content affects the fertilizability of human oocytes. Mol. Hum. Reprod. 7(5):425-429. doi: 10.1093/molehr/7.5.425.

Richani, D., K. R. Dunning, J. G. Thompson, and R. B. Gilchrist. 2021. Metabolic co-dependence of the oocyte and cumulus cells: essential role in determining oocyte developmental competence. Hum. Reprod. Update. 27(1):27-47. doi: 10.1093/humupd/dmaa043.

Richards, J. S., D. L. Russell, R. L. Robker, M. Dajee, and T. N. Alliston. 1998. Molecular mechanisms of ovulation and luteinization. Mol. Cell. Endoncrinol. 145(1):47-54. doi: https://doi.org/10.1016/S0303-7207(98)00168-3.

Richardson, B. N., S. L. Hill, J. S. Stevenson, G. D. Djira, and G. A. Perry. 2016. Expression of estrus before fixed-time AI affects conception rates and factors that impact expression of estrus and the repeatability of expression of estrus in sequential breeding seasons. Anim. Reprod. Sci. 166:133-140. doi: 10.1016/j.anireprosci.2016.01.013.

Rieger, D., and N. M. Loskutoff. 1994. Changes in the metabolism of glucose, pyruvate, glutamine and glycine during maturation of cattle oocytes in vitro. J. Reprod. Fertil. 100(1):257-262. doi: 10.1530/jrf.0.1000257.

Rispoli, L. A., J. L. Edwards, K. G. Pohler, S. Russell, R. I. Somiari, R. R. Payton, and F. N. Schrick. 2020. Heat-induced hyperthermia impacts the follicular fluid proteome of the periovulatory follicle in lactating dairy cows. PLOS ONE. 14(12):e0227095. doi: 10.1371/journal.pone.0227095

Roberts, R., S. Franks, and K. Hardy. 2002. Culture environment modulates maturation and metabolism of human oocytes. Hum. Reprod. 17(11):2950-2956. doi: 10.1093/humrep/17.11.2950.

Robker, R. L., L. K. Akison, and D. L. Russell. 2009. Control of oocyte release by progesterone receptor-regulated gene expression. Nucl. Recept. Signaling. 7:e012. doi: 10.1621/nrs.07012

Roche, J. F., M. P. Bolandl, and T. A. McGeady. 1981. Reproductive wastage following artificial insemination of heifers. Vet. Rec. 109(18):401-404. doi: 10.1136/vr.109.18.401.

Roche, J. F., E. J. Austin, M. Ryan, M. O'Rourke, M. Mihm, and M. G. Diskin. 1999. Regulation of follicle waves to maximize fertility in cattle. J. Reprod. Fertil. Suppl. 54:61-71.

Rodgers, J. C., S. L. Bird, J. E. Larson, N. Dilorenzo, C. R. Dahlen, A. Dicostanzo, and G. C. Lamb. 2012. An economic evaluation of estrous synchronization and timed artificial insemination in suckled beef cows. J. Anim. Sci. 90(11):4055-4062. doi: 10.2527/jas.2011-4836.

Rodgers, R. J., and H. F. Irving-Rodgers. 2010. Formation of the ovarian follicular antrum and follicular fluid. Biol. Reprod. 82(6):1021-1029. doi: 10.1095/biolreprod.109.082941.

Rodrigues, A. D., R. F. Cooke, R. S. Cipriano, L. G. Silva, R. L. Cerri, L. H. Cruppe, M. Meneghetti, K. G. Pohler, and J. L. Vasconcelos. 2018. Impacts of estrus expression and intensity during a timed-AI protocol on variables associated with fertility and pregnancy success in Bos indicus-influenced beef cows. J. Anim. Sci. 96(1):236-249. doi: 10.1093/jas/skx043.

Rose-Hellekant, T. A., E. A. Libersky-Williamson, and B. D. Bavister. 1998. Energy substrates and amino acids provided during in vitro maturation of bovine oocytes alter acquisition of developmental competence. Zygote. 6(4):285-294. doi: 10.1017/s0967199498000239.

Roth, Z. 2018. Symposium review: reduction in oocyte developmental competence by stress is associated with alterations in mitochondrial function. J. Dairy Sci. 101(4):3642-3654. doi: 10.3168/jds.2017-13389.

Sá Filho, M. F., A. M. Crespilho, J. E. Santos, G. A. Perry, and P. S. Baruselli. 2010. Ovarian follicle diameter at timed insemination and estrous response influence likelihood of ovulation and pregnancy after estrous synchronization with progesterone or progestin-based protocols in suckled Bos indicus cows. Anim. Reprod. Sci. 120(1):23-30. doi: 10.1016/j.anireprosci.2010.03.007.

Sá Filho, M.F., L. Penteado, E. L. Reis, T. A. Reis, K. N. Galvão, and P. S. Baruselli. 2013. Timed artificial insemination early in the breeding season improves the reproductive performance of suckled beef cows. Theriogenology 79:625-632. doi: 10.1016/j.theriogenology.2012.11.016.

Sarwar, Z., M. Saad, M. Saleem, A. Husnain, A. Riaz, and N. Ahmad. 2020. Effect of follicle size on oocytes recovery rate, quality, and in-vitro developmental competence in Bos indicus cows. Anim. Reprod. 17(3):e20200011. doi: 10.1590/1984-3143-AR2020-0011.

Scantland, S., I. Tessaro, C. H. Macabelli, A. D. Macaulay, G. Cagnone, É. Fournier, A. M. Luciano, and C. Robert. 2014. The adenosine salvage pathway as an alternative to mitochondrial production of ATP in maturing mammalian oocytes. Biol. Reprod. 91(3):75:1-11. doi: 10.1095/biolreprod.114.120931.

Seibel, M. M., D. Smith, A. M. Dlugi, and L. Levesque. 1989. Periovulatory follicular fluid hormone levels in spontaneous human cycles. J. Clin. Endocrinol. Metab. 68(6):1073-1077. doi: 10.1210/jcem-68-6-1073.

Seli, E., E. Babayev, S. C. Collins, G. Nemeth, and T. L. Horvath. 2014. Minireview: metabolism of female reproduction: regulatory mechanisms and clinical implications. Mol. Endocrinol. 28(6):790-804. doi: 10.1210/me.2013-1413.

Sendžikaitė, G., and G. Kelsey. 2019. The role and mechanisms of DNA methylation in the oocyte. Essays Biochem. 63(6):691-705. doi: 10.1042/ebc20190043.

Short, R. E., R. A. Bellows, R. B. Staigmiller, J. G. Berardinelli, and E. E. Custer. 1990. Physiological mechanisms controlling anestrus and infertility in postpartum beef cattle. J. Anim. Sci. 68(3):799-816. doi: 10.2527/1990.683799x.

Sinchak, K., and E. J. Wagner. 2012. Estradiol signaling in the regulation of reproduction and energy balance. Front. Neuroendocrinol. 33(4): 342-363. doi: 10.1016/j.yfrne.2012.08.004.

Sinclair, K. D., L. A. Lunn, W. Y. Kwong, K. Wonnacott, R. S. Linforth, and J. Craigon. 2008. Amino acid and fatty acid composition of follicular fluid as predictors of in-vitro embryo development. Reprod. Biomed. Online. 16(6):859-868. doi: 10.1016/s1472-6483(10)60153-8.

Sirard, M. A. 2011. Follicle environment and quality of in vitro matured oocytes. J. Assist. Reprod. Genet. 28(6):483-488. doi: 10.1007/s10815-011-9554-4.

Sirard, M. A., H. M. Florman, M. L. Leibfried-Rutledge, F. L. Barnes, M. L. Sims, and N. L. First. 1989. Timing of nuclear progression and protein synthesis necessary for meiotic maturation of bovine oocytes. Biol. Reprod. 40(6):1257-1263. doi: 10.1095/biolreprod40.6.1257

Sirard, M. A., F. Richard, P. Blondin, and C. Robert. 2006. Contribution of the oocyte to embryo quality. Theriogenology. 65(1):126-136. doi: 10.1016/j.theriogenology.2005.09.020.

Skarzynski, D. J., K. K. Piotrowska-Tomala, K. Lukasik, A. Galvão, S. Farberov, Y. Zalman, and R. Meidan. 2013. Growth and regression in bovine corpora lutea: regulation by local survival and death pathways. Reprod. Domest. Anim. 48(1):25-37. doi: 10.1111/rda.12203.

Skinner, D. C., N. P. Evans, B. Delaleu, R. L. Goodman, P. Bouchard, and A. Caraty. 1998. The negative feedback actions of progesterone on gonadotropin-releasing hormone secretion are transduced by the classical progesterone receptor. Proc. Natl. Acad. Sci. U.S.A. 95(18):10978-10983. doi: 10.1073/pnas.95.18.10978.

Smith, G. M. 1976. Sire breed effects on economic efficiency of a terminal-cross beef production system. J. Anim. Sci. 43(6):1163-1170. doi: https://doi.org/10.2527/jas1976.4361163x.

Smith, L. C., and A. A. Alcivar. 1993. Cytoplasmic inheritance and its effects on development and performance. J. Reprod. Fertil. Suppl. 48:31-43.

Smith, M. F., K. J. Nix, D. C. Kraemer, M. S. Amoss, M. A. Herron, and J. N. Wiltbank. 1982. Fertilization rate and early embryonic loss in Brahman crossbred heifers. J. Anim. Sci. 54(5):1005-1011. doi: 10.2527/jas1982.5451005x.

Sohel, M. M., M. Hoelker, S. S. Noferesti, D. Salilew-Wondim, E. Tholen, C. Looft, F. Rings, M. J. Uddin, T. E. Spencer, K. Schellander, and D. Tesfaye. 2013. Exosomal and non-exosomal transport of extra-cellular microRNAs in follicular fluid: implications for bovine oocyte developmental competence. PLoS One. 8(11):e78505. doi: 10.1371/journal.pone.0078505.

Song, J.-Y., S. Xiang, Y. Yang, and Z. Sun. 2019. Assessment of follicular fluid metabolomics of polycystic ovary syndrome in kidney yang deficiency syndrome. Eur. J. Integr. Med. 30:100944. doi: 10.1016/j.eujim.2019.100944.

Song, Y. X., P. Hu, Y. L. Bai, C. Zhao, C. Xia, and C. Xu. 2019b. Plasma metabolic characterisation of dairy cows with inactive ovaries and oestrus during the peak of lactation. J. Vet. Res. 63(3):359-367. doi: 10.2478/jvetres-2019-0047.

Spicer, L. J., and S. E. Echternkamp. 1986. Ovarian follicular growth, function and turnover in cattle: a review. J. Anim. Sci. 62(2):428-451. doi: 10.2527/jas1986.622428x.

Spikings, E. C., J. Alderson, and J. C. St. John. 2006. Transmission of mitochondrial DNA following assisted reproduction and nuclear transfer. Hum. Reprod. Update. 12(4):401-415. doi: 10.1093/humupd/dml011.

Spitzer, J. C., G. D. Niswender, G. E. Seidel Jr., and J. N. Wiltbank. 1978. Fertilization and blood levels of progesterone and LH in beef heifers on a restricted energy diet. J. Anim. Sci. 46(4):1071-1077. doi: 10.2527/jas1978.4641071x.

Srirattana, K., and J. C. St. John. 2018. Additional mitochondrial DNA influences the interactions between the nuclear and mitochondrial genomes in a bovine embryo model of nuclear transfer. Sci. Rep. 8(1):7246. doi: 10.1038/s41598-018-25516-3.

St. John, J. 2014. The control of mtDNA replication during differentiation and development. Biochim. Biophys. Acta. 1840(4):1345-1354. doi: 10.1016/j.bbagen.2013.10.036.

Stock, A. E., and J. E. Fortune. 1993. Ovarian follicular dominance in cattle: relationship between prolonged growth of the ovulatory follicle and endocrine parameters. Endocrinology. 132(3):1108-1114. doi: 10.1210/endo.132.3.8440173.

Stojkovic, M., S. A. Machado, P. Stojkovic, V. Zakhartchenko, P. Hutzler, P. B. Gonçalves, and E. Wolf. 2001. Mitochondrial distribution and adenosine triphosphate content of bovine oocytes before and after in vitro maturation: correlation with morphological criteria and developmental capacity after in vitro fertilization and culture. Biol. Reprod. 64(3):904-909. doi: 10.1095/biolreprod64.3.904.

Stumpf, T. T., M. L. Day, M. W. Wolfe, A.C. Clutter, J. A. Stotts, P.L. Wolfe, R. J. Kittok, and J.E. Kinder. 1989. Effect of estradiol on secretion of luteinizing hormone during the follicular phase of the bovine estrous cycle. Biol. Reprod. 41(1):91-97. doi: 10.1095/biolreprod41.1.91.

Sturmey, R. G., A. Reis, H. J. Leese, and T. G. McEvoy. 2009. Role of fatty acids in energy provision during oocyte maturation and early embryo development. Reprod. Domest. Anim. 44(3):50-58. doi: 10.1111/j.1439-0531.2009.01402.x.

Sutton-McDowall, M. L., R. B. Gilchrist, and J. G. Thompson. 2004. Cumulus expansion and glucose utilisation by bovine cumulus–oocyte complexes during in vitro maturation: the influence of glucosamine and follicle-stimulating hormone. Reproduction. 128(3):313-319. doi: 10.1530/rep.1.00225.

Sutton-McDowall, M. L., R. B. Gilchrist, and J. G. Thompson. 2010. The pivotal role of glucose metabolism in determining oocyte developmental competence. Reproduction. 139(4):685-695. doi: 10.1530/REP-09-0345.

Sutton, M. L., R. B. Gilchrist, and J. G. Thompson. 2003. Effects of in-vivo and in-vitro environments on the metabolism of the cumulus-oocyte complex and its influence

on oocyte developmental capacity. Hum. Reprod. Update. 9(1):35-48. doi: 10.1093/humupd/dmg009.

Svec, D., A. Tichopad, V. Novosadova, M. W. Pfaffl, and M. Kubista. 2015. How good is a PCR efficiency estimate: recommendations for precise and robust qPCR efficiency assessments. Biomol. Detect. Quantif. 3:9-16. doi: 10.1016/j.bdq.2015.01.005.

Swain, J. E., and T. B. Pool. 2008. ART failure: oocyte contributions to unsuccessful fertilization. Hum. Reprod. Update. 14(5):431-446. doi: 10.1093/humupd/dmn025.

Tabatabaei, S., M. Mamoei, and A. Aghaei. 2011. Dynamics of ovarian follicular fluid in cattle. Comp. Clin. Path. 20(6):591-595. doi: 10.1007/s00580-010-1038-x.

Takeo, S., K. Kimura, K. Shirasuna, T. Kuwayama, and H. Iwata. 2017. Age-associated deterioration in follicular fluid induces a decline in bovine oocyte quality. Reprod. Fertil. Dev. 29(4):759-767. doi: 10.1071/rd15228.

Tamassia, M., F. Nuttinck, P. May-Panloup, P. Reynier, Y. Heyman, G. Charpigny, M. Stojkovic, S. Hiendleder, J. P. Renard, and S. Chastant-Maillard. 2004. In vitro embryo production efficiency in cattle and its association with oocyte adenosine triphosphate content, quantity of mitochondrial DNA, and mitochondrial DNA haplogroup. Biol. Reprod. 71(2):697-704. doi: 10.1095/biolreprod.103.026104.

Tang, Z. R., R. Zhang, Z. X. Lian, S. L. Deng, and K. Yu. 2019. Estrogen-Receptor Expression and Function in Female Reproductive Disease. Cells 8(10):1123. doi: 10.3390/cells8101123

Taponen, J. 2009. Fixed-time artificial insemination in beef cattle. Acta. Vet. Scand. 51(1):48. doi: 10.1186/1751-0147-51-48.

Taylor, C., and R. Rajamahendran. 1991. Follicular dynamics, corpus luteum growth and regression in lactating dairy cattle. Can. J. Anim. Sci. 71(1):61-68. doi: 10.4141/cjas91-007.

Tenhagen, B. A., E. Birkelbach, and W. Heuwieser. 2000. Serum progesterone levels in post-partum dairy cows after repeated application of the prostaglandin F2 alpha analogue D - cloprostenol sodium. J. Vet. Med. 47(4):213-220. doi: 10.1046/j.1439-0442.2000.00281.x

Thompson, J. G., M. Lane, and R. B. Gilchrist. 2007. Metabolism of the bovine cumulus-oocyte complex and influence on subsequent developmental competence. Soc. Reprod. Fertil. Suppl. 64:179-190. doi: 10.5661/rdr-vi-179.

Thompson, J. G., R. B. Gilchrist, M. L. Sutton-McDowall. 2014. The metabolism of the ruminant cumulus-oocyte complex revisted. Reprod. Domest. Ruminants 8:311-326.

Trebichalská, Z., D. Kyjovská, S. Kloudová, P. Otevřel, A. Hampl, and Z. Holubcová. 2020. Cytoplasmic maturation in human oocytes: an ultrastructural study. Biol. Reprod. 104(1):106-116. doi: 10.1093/biolre/ioaa174.

Uhde, K., H. T. van Tol, T. A. Stout, and B. A. Roelen. 2018. Metabolomic profiles of bovine cumulus cells and cumulus-oocyte-complex-conditioned medium during maturation in vitro. Sci. Rep. 8(1):9477 doi: 10.1038/s41598-018-27829-9.

Van Blerkom, J. 2004. Mitochondria in human oogenesis and preimplantation embryogenesis: engines of metabolism, ionic regulation and developmental competence. Reproduction. 128(3):269-280. doi: 10.1530/rep.1.00240.

Van Blerkom, J. 2011. Mitochondrial function in the human oocyte and embryo and their role in developmental competence. Mitochondrion. 11(5):797-813. doi: 10.1016/j.mito.2010.09.012.

Van Blerkom, J., P. Davis, and S. Alexander. 2000. Differential mitochondrial distribution in human pronuclear embryos leads to disproportionate inheritance between blastomeres: relationship to microtubular organization, ATP content and competence. Hum. Reprod. 15(12):2621-2633. doi: 10.1093/humrep/15.12.2621.

Van Blerkom, J., J. Sinclair, and P. Davis. 1998. Mitochondrial transfer between oocytes: potential applications of mitochondrial donation and the issue of heteroplasmy. Hum. Reprod. 13(1):2857-2868. doi: 10.1093/humrep/13.10.2857.

van de Leemput, E. E., P. L. Vos, E. C. Zeinstra, M. M. Severs, G. C. van der Weijden, and S. J. Dieleman. 1999. Improved in vitro embryo development using in vivo matured oocytes from heifers superovulated with a controlled preovulatory LH surge. Theriogenology. 52(2):335-349. doi: 10.1016/s0093-691x(99)00133-8.

Vasconcelos, J. L., R. Sartori, H. N. Oliveira, J. G. Guenther, and M. C. Wiltbank. 2001. Reduction in size of the ovulatory follicle reduces subsequent luteal size and pregnancy rate. Theriogenology. 56(2):307-314. doi: 10.1016/s0093-691x(01)00565-9.

Von Wald, T., Y. Monisova, M. R. Hacker, S. W. Yoo, A. S. Penzias, R. R. Reindollar, and A. Usheva. 2010. Age-related variations in follicular apolipoproteins may influence human oocyte maturation and fertility potential. Fertil. Steril. 93(7):2354-2361. doi: 10.1016/j.fertnstert.2008.12.129.

Wai, T., A. Ao, X. Zhang, D. Cyr, D. Dufort, and E. A. Shoubridge. 2010. The role of mitochondrial DNA copy number in mammalian fertility. Biol. Reprod. 83(1):52-62. doi: 10.1095/biolreprod.109.080887

Wai, T., D. Teoli, and E. A. Shoubridge. 2008. The mitochondrial DNA genetic bottleneck results from replication of a subpopulation of genomes. Nat. Genet. 40(12):1484-1488. doi: 10.1038/ng.258.

Wang, T. Y., L. Wang, J. H. Zhang, and W. H. Dong. 2011. A simplified universal genomic DNA extraction protocol suitable for PCR. Genet. Mol. Res. 10(1):519-525. doi: 10.4238/vol10-1gmr1055.

Warzych, E., and P. Lipinska. 2020. Energy metabolism of follicular environment during oocyte growth and maturation. J. Reprod. Dev. 66(1):1-7. doi: 10.1262/jrd.2019-102.

Watson, A. J. 2007. Oocyte cytoplasmic maturation: a key mediator of oocyte and embryo developmental competence. J. Anim. Sci. 85(13):E1-3. doi: 10.2527/jas.2006-432.

Wettemann, R. P., H. D. Hafs, L. A. Edgerton, and L. V. Swanson. 1972. Estradiol and progesterone in blood serum during the bovine estrous cycle. J. Anim. Sci. 34(6):1020-1024. doi: 10.2527/jas1972.3461020x.

Whitman, R. W. 1975. Weight change, body condition and beef-cow reproduction, Colorado State University, Fort Collins, Co.

Whittier, W. D., J. F. Currin, H. Schramm, S. Holland, and R. K. Kasimanickam. 2013. Fertility in Angus cross beef cows following 5-day CO-Synch+ CIDR or 7-day CO-Synch+ CIDR estrus synchronization and timed artificial insemination. Theriogenology. 80(9):963-969. doi: 10.1016/j.theriogenology.2013.07.019.

Wiltbank, M. C., A. H. Souza, P. D. Carvalho, R. W. Bender, and A. B. Nascimento. 2011. Improving fertility to timed artificial insemination by manipulation of circulating progesterone concentrations in lactating dairy cattle. Reprod. Fertil. Dev. 24(1):238-243. doi: 10.1071/rd11913.

Winterhager, E., and G. M. Kidder. 2015. Gap junction connexins in female reproductive organs: implications for women's reproductive health. Hum. Reprod. Update. 21(3):340-352. doi: 10.1093/humupd/dmv007.

Wonnacott, K. E., W. Y. Kwong, J. Hughes, A. M. Salter, R. G. Lea, P. C. Garnsworthy, and K. D. Sinclair. 2010. Dietary omega-3 and -6 polyunsaturated fatty acids affect the composition and development of sheep granulosa cells, oocytes and embryos. Reproduction. 139(1):57-69. doi: 10.1530/rep-09-0219.

Xia, L., X. Zhao, Y. Sun, Y. Hong, Y. Gao, and S. Hu. 2014. Metabolomic profiling of human follicular fluid from patients with repeated failure of in vitro fertilization using gas chromatography/mass spectrometry. Int. J. Clin. Exp. Pathol. 7(10):7220-7229.

Zachut, M., I. Dekel, H. Lehrer, A. Arieli, A. Arav, L. Livshitz, S. Yakoby, and U. Moallem. 2010. Effects of dietary fats differing in n-6:n-3 ratio fed to high-yielding dairy cows on fatty acid composition of ovarian compartments, follicular status, and oocyte quality. J. Dairy Sci. 93(2):529-545. doi: 10.3168/jds.2009-2167.

Zachut, M., P. Sood, Y. Levin, and U. Moallem. 2016. Proteomic analysis of preovulatory follicular fluid reveals differentially abundant proteins in less fertile dairy cows. Journal of proteomics 139:122-129. doi: 10.1016/j.jprot.2016.03.027

Zeilmaker, G. H., and C. M. Verhamme. 1974. Observations on rat oocyte maturation in vitro: morphology and energy requirements. Biol. Reprod. 11(2):145-152. doi: 10.1095/biolreprod11.2.145.

Zhang, D., D. Keilty, Z. F. Zhang, and R. C. Chian. 2017. Mitochondria in oocyte aging: current understanding. Facts Views Vis. Obgyn. 9(1):29-38.

Zhang, K., and G. W. Smith. 2015. Maternal control of early embryogenesis in mammals. Reprod. Fertil. Dev. 27(6):880-896. doi: 10.1071/RD14441.

Zhang, M., Y.-Q. Su, K. Sugiura, G. Xia, and J. J. Eppig. 2010. Granulosa cell ligand NPPC and its receptor NPR2 maintain meiotic arrest in mouse oocytes. Science. 330(6002):366-369. doi: 10.1126/science.1193573.

Zhang, N. 2018. Role of methionine on epigenetic modification of DNA methylation and gene expression in animals. Anim. Nutr. 4(1):11-16. doi: 10.1016/j.aninu.2017.08.009.

Zhang, Z., C. He, Y. Gao, L. Zhang, Y. Song, T. Zhu, K. Zhu, D. Lv, J. Wang, X. Tian, T. Ma, P. Ji, W. Cui, and G. Liu. 2021. α-ketoglutarate delays age-related fertility decline in mammals. Aging Cell. 20(2):e13291. doi: https://doi.org/10.1111/acel.13291

Zhao, H., Y. Zhao, T. Li, M. Li, J. Li, R. Li, P. Liu, Y. Yu, and J. Qiao. 2015. Metabolism alteration in follicular niche: the nexus among intermediary metabolism, mitochondrial function, and classic polycystic ovary syndrome. Free Radic. Biol. Med. 86:295-307. doi: 10.1016/j.freeradbiomed.2015.05.013.

VITA

Casey Christine Read was born in 1994 in Denver, NC. She received her B.S. in Animal Sciences and M.Sc. in Reproductive Physiology from Auburn University in 2016 and 2018. She then attended the University of Tennessee – Knoxville where she married her wonderful husband and received her PhD in Reproductive Physiology.